Iron Efflux Mechanisms in the Central and Peripheral Nervous System

Katrin Schulz

Centre for Research in Neuroscience
The Research Institute of the McGill University Health Centre
Department of Neurology and Neurosurgery
McGill University, Montreal, Canada
August 2011

A thesis submitted to the Faculty of Medicine and Graduate and Postdoctoral Studies
in partial fulfillment of the requirements of the degree of Doctor of Philosophy

TABLE OF CONTENTS

Abstract

Iron is an essential metal that is required for various biological processes. However, excessive, unshielded iron is toxic because of its ability to promote free radical formation. Consequently, to prevent iron-induced cellular damage, iron homeostasis has to be tightly regulated. Disturbances of iron homeostasis in the central nervous system (CNS) are associated with several pathological conditions. While iron overload can lead to neurodegeneration, iron deficiency has been linked to defects in brain development. One key mechanism of regulating iron homeostasis is iron efflux, which occurs via the ubiquitously expressed iron exporter ferroportin (Fpn) facilitated by the activity of a ferroxidase. Iron export might not only be important for maintaining stable intracellular iron levels, but may also play a role in the delivery of iron between cells. The overall aim of my Ph.D. thesis work was to investigate iron efflux mechanisms in the central and peripheral nervous system with a focus on how iron efflux is involved in the transport of iron from one cell to another.

In the CNS, iron efflux from astrocytes via Fpn is mediated by a GPI-anchored form of the ferroxidase ceruloplasmin (Cp), which is only expressed by astrocytes in the CNS. I investigated in chapter 2 how other CNS cells export iron. To do this, I assessed the expression and role of Hephaestin (Heph), a ferroxidase first identified in the gut. My results show that Heph is expressed by mature oligodendrocytes and plays a role in iron efflux from these cells. I also found that mice with a mutation in the Heph gene (sex-linked anemia [sla] mice) show iron accumulation in oligodendrocytes in the grey but not white matter, and exhibit motor deficits. In addition, my work revealed that the sparing of iron accumulation in white matter oligodendrocytes in sla mice is due to compensatory

upregulation of Cp, suggesting that grey and white matter oligodendrocytes utilize different ferroxidases to efflux iron.

In chapter 3, I hypothesized that the astrocytic perivascular endfeet surrounding capillaries in the CNS can take up iron from the circulation and deliver it to oligodendrocytes, their precursors and microglia/marcophages for remyelination. To address this, I generated astrocyte-specific Fpn knockout mice that lack iron efflux specifically from astrocytes, and induced focal demyelination in the spinal cord of these mice by lysophosphatidylcholine (LPC) injections. The results revealed impaired remyelination after LPC injections in the astrocyte-specific Fpn knockout mice. This was accompanied by reduced proliferation of oligodendrocyte precursor cells (OPCs). In addition, my *in vitro* work showed that iron-deficient microglia express reduced levels of TNF-α and IL-1β, two cytokines implicated in remyelination either directly or by stimulating astrocytes to produce growth factors involved in OPC proliferation and differentiation. These results suggest that iron efflux from astrocytes is required for remyelination by either direct effects on OPCs or indirectly by affecting microglial activation.

In chapter 4, I examined the role of iron efflux from Schwann cells in providing iron to axons in peripheral nerves. Since axonal growth cones in particular show a high concentration of mitochondria, which require iron for their proper function, iron supply might be especially important for axonal growth. First, I showed using an iron chelator that iron is required for neurite outgrowth from dorsal root ganglia neurons in culture, likely by ensuring proper mitochondrial function. I then assessed the role of Schwann cells in delivering iron to regenerating axons after peripheral nerve injury. My results

demonstrate that Schwann cells express Fpn and Cp, two molecules essential for iron efflux. I also found increased Fpn expression after sciatic nerve crush injury, indicating an increased need of iron efflux during regeneration. In addition, I showed that sciatic nerve crush injury in Cp knockout mice that lack iron efflux from Schwann cells resulted in impaired axonal regeneration and motor recovery. These findings suggest a role for iron efflux from Schwann cells in peripheral axon regeneration, likely by ensuring proper mitochondrial function.

Together these results demonstrate the importance of iron efflux mechanisms from cells in the nervous system in maintaining proper intracellular iron levels and in delivering iron to surrounding cells for their physiological functions.

Résumé

Le fer est un métal essentiel requis dans plusieurs processus biologiques. Cependant, un excès de fer est toxique puisqu'il permet la formation de radicaux libres. En conséquence, pour prévenir les dommages cellulaires induits par la présence de fer, l'homéostasie doit être minutieusement régularisée. Des perturbations dans l'homéostasie du fer dans le système nerveux central (SNC) sont associées à plusieurs conditions pathologiques. Un excès en fer peut entraîner une neurodégénération, alors qu'une carence est généralement associée à des défectuosités lors du développement du cerveau. Un mécanisme clé de la régulation de l'homéostasie du fer est l'efflux ferrique, qui se produit via le transporteur ubiquiste ferroportine (Fpn) activé par la présence de ferroxidase. L'exportation de fer n'est pas seulement important pour la stabilité et le maintien intracellulaire ferrique mais pourrait jouer également un rôle dans la distribution du fer entre les cellules. Le but de ma thèse de doctorat est d'étudier les mécanismes des efflux ferriques dans le système nerveux central et le système nerveux périphérique, en mettant l'emphase sur le fonctionnement de ces efflux ferriques dans le transport du fer entre les cellules.

Dans le SNC, l'efflux ferrique provenant des astrocytes via Fpn est concilié par céruloplasmine (Cp), une ferroxidase ayant une forme ancrée par GPI qui est seulement exprimée par les astrocytes du SNC. Le chapitre 2 comprend une étude sur comment les autres cellules du SCN exportent le fer. Pour ce faire, j'ai étudié l'expression et le rôle de héphaestine (Heph), une ferroxidase identifiée dans le système digestif. Mes résultats montrent que Heph est exprimé par les oligodendrocytes matures et joue un rôle dans l'efflux ferrique provenant de ces cellules. De plus, les souris ayant une mutation du gène Heph (souris anémique lié au sexe [sla]) montrent une accumulation de fer seulement

dans les oligodendrocytes de la matière grise, et présentent des déficits moteurs. De plus, ce chapitre démontre que l'absence de l'accumulation du fer dans les oligodendrocytes de la matière blanche chez les souris sla a été attribuée à une régulation compensatoire à la hausse de Cp, ce qui suggère que les oligodendrocytes de la matière grise et ceux de la matière blanche utilisent différents ferroxidases pour les efflux ferriques.

Dans le chapitre 3, j'ai émis l'hypothèse que les terminaisons périvasculaires des astrocytes qui entourent les capillaires dans le SNC peuvent absorber le fer à partir de la circulation sanguine et le livrer aux oligodendrocytes, à leurs précurseurs et aux microglies/macrophages pour la remyélinisation. Pour tester cette hypothèse, j'ai généré des souris ayant une inactivation du gène de Fpn spécifiquement dans les astrocytes, donc aucun efflux ferrique ne provenait de ces astrocytes, et j'ai induit une démyélinisation à l'aide d'injections de lysophosphatidylcholine (LPC) dans la colonne vertébrale de ces souris. Mes résultats montrent que la remyélinisation a été perturbée suite à l'injection de LPC dans ces souris. Ceci est accompagné par une prolifération réduite de cellules précurseurs des oligodendrocytes (OPCs). De plus, mes expériences *in vitro* montrent que les microglies déficientes en fer montrent une réduction dans le niveau de TNF-α and IL-1β, deux cytokines impliquées dans la remyélinisation soit directement ou en stimulant chez les astrocytes la production de facteurs de croissance impliqués dans la prolifération et la différentiation des OPCs. Ces résultats suggèrent que l'efflux du fer provenant des astrocytes est requis pour de la remyélinisation soit par des effets directs sur les OPCs ou indirectement en affectant l'activation des microglies.

Dans le chapitre 4, j'ai examiné le rôle des efflux du fer des cellules de Schwann dans l'apport du fer aux axones des nerfs périphériques. Puisque les terminaisons des

axones croissantes en particulier montrent une grande concentration de mitochondries, ce qui requiert du fer pour leur propre fonction, l'apport en fer pourrait être particulièrement important pour la croissance de l'axone. Premièrement, en utilisant un chélateur, j'ai montré que le fer est requis pour la croissance de neurites des neurons du ganglion spinal, vraisemblablement pour assurer le bon fonctionnement des mitochondries. Par la suite, le rôle des cellules de Schwann dans la distribution du fer pour la régénération des axones après une blessure des nerfs périphériques a été étudié. Mes résultats démontrent que les cellules de Schwann expriment Fpn et Cp, deux molécules essentielles pour l'efflux ferrique. De plus, j'ai observé une augmentation de l'expression Fpn suite à un broyage du nerf sciatique, ce qui indique une nécessité de l'augmentation d'efflux en fer pendant la régénération. De plus, mes résultats montrent que les souris déficientes en Cp n'ayant pas d'efflux ferrique provenant des cellules de Schwann aboutissent à une déficience lors de la régénération axonale et lors de la récupération motrice. Ces résultats suggèrent un rôle des efflux ferriques provenant des cellules de Schwann pour la régénération des axones périphériques, vraisemblablement en s'assurant du bon fonctionnement des mitochondries.

L'ensemble de résultats mentionné précédemment démontre l'importance du mécanisme des efflux ferriques entre les cellules dans le système nerveux pour le maintien du niveau approprié en fer intracellulaire et dans la distribution du fer aux cellules avoisinantes pour leurs fonctions physiologiques.

Acknowledgements

I would like to acknowledge several people who helped me over the course of my PhD. First of all, I would like to acknowledge the support, guidance and encouragement that I received from my supervisor Dr. Samuel David. I am very grateful for all the helpful scientific discussions and the knowledge he taught me throughout these years.

I would also like to thank my committee members, Dr. Prem Ponka and Dr.Guillermina Almazan for their advice and thoughtful discussions over the course of my studies. I am also grateful to Dr. Yong Rao for serving as my mentor within the program.

I must also thank my collaborators Dr. Chris Vulpe, Dr. Leah Harris, Dr. Magdalena Götz and Dr. Nancy Andrews for providing animals and reagents that made this work possible. I am also grateful to Dr. Malorie Gélinas for translating my abstract into French.

I would like to thank all members of the David lab, past and present, for their help, support and friendship. In particular, I would like to thank Dr. Suh Young Jeong for the help and advice I got from her when I started working in the lab. I would also like to thank Dr. Khizr Rathore for many helpful discussions. I am particularly grateful for all the help and assistance I received from Hiba Kazak, Ourania Tsatas and Margaret Attiwell throughout the years.

Lastly, but very importantly, I would like to extend a very special thank you to my parents for their constant love and support over all these years. Without their encouragement, this work would not have been possible.

Contribution of authors

Chapter 2:

Schulz K, Vulpe CD, Harris ZL and David S (2011) "Iron Efflux from Oligodendrocytes is Differentially Regulated in Grey and White Matter" *J Neurosci.* 31(37):13301-1.

All the experimental work described in this manuscript and writing of the initial manuscript was done by me. Dr. Chris Vulpe provided the antibody for Hephaestin and Dr. Leah Harris provided the spinal cord tissue of some of the $Cp^{-/-}/Heph^{sla}$ double mutant mice that were generated in her laboratory. The experiments were planned and the manuscript edited jointly by me and my supervisor, Dr. Samuel David.

Chapter 3:

Schulz K, Andrews NC, Götz M and David S (2011) "Iron efflux from astrocytes is required for remyelination"

The work in this chapter has been submitted for publication. All experimental work and writing of the initial manuscript was done by me. Dr. Nancy Andrews provided the $Fpn^{flox/flox}$ mice and Dr. Magdalena Götz the GLAST::CreERT2 mice that were crossed to generate the astrocyte-specific Fpn knockout mice used in this study. The experiments were planned and the manuscript edited jointly by me and my supervisor, Dr. Samuel David.

Chapter 4:

Schulz K and David S (2011) "Iron plays a role in peripheral axon growth"

The work in this manuscript is being prepared for publication. All experimental work was planned by me and my supervisor, Dr. Samuel David and carried out by me. The initial manuscript was written by me and then edited jointly by me and Dr. Samuel David.

Publications

Publications based on Ph.D. thesis work

Schulz K, Vulpe CD, Harris ZL and David S (2011) "Iron Efflux from Oligodendrocytes is Differentially Regulated in Grey and White Matter" *J Neurosci.* 31(37):13301-1.

Schulz K, Andrews NC, Götz M and David S (2011) "Iron efflux from astrocytes is required for remyelination" (manuscript submitted).

Schulz K and David S (2011) "Iron plays a role in peripheral axon growth" (manuscript in preparation).

Publications based on collaborations on iron homeostasis

Jeong SY, Rathore KI, **Schulz K**, Ponka P, Arosio P, David S. (2009) "Dysregulation of iron homeostasis in the CNS contributes to disease progression in a mouse model of amyotrophic lateral sclerosis" *J Neurosci*. 29(3):610-619.

Gresle MM, **Schulz K**, Perreau V, Cipriani T, Jonas A, Doherty W, Field JS, Jokubaitis V, Cherny R, Volitakis I, David S, Kilpatrick TJ, Butzkueven H. (2011) "Ceruloplasmin gene deficient mice with experimental autoimmune encephalomyelitis show attenuated disease progression" (manuscript in preparation).

Claims of Originality

My Ph.D. thesis research generated the following original findings and observations.

1. The ferroxidase hephaestin (Heph) is expressed by oligodendrocytes and microglia, but not by astrocytes and neurons in the CNS.

2. Heph as well as the iron exporter ferroportin (Fpn) are only expressed by mature oligodendrocytes, but not by oligodendrocyte precursor cells (OPCs).

3. Heph mediates iron efflux from oligodendrocytes.

4. Sex-linked anemia (sla) mice that are Heph deficient show age-dependent iron accumulation in grey matter oligodendrocytes.

5. Sla mice exhibit deficits in motor function with age that likely result from alterations in the paranodal structure of myelinated fibres observed in these mice.

6. White matter oligodendrocytes in sla mice upregulate the ferroxidase ceruloplasmin (Cp) to compensate for the loss of Heph function, suggesting that white and grey matter oligodendrocytes regulate iron efflux differentially by utilizing different ferroxidases.

7. $Heph^{sla}/Cp^{-/-}$ double mutant mice show iron accumulation in grey and white matter oligodendrocytes, confirming a compensatory and protective role of Cp in white matter oligodendrocytes.

8. Remyelination after lysophosphatidylcholine (LPC)-induced demyelination is impaired in mice that lack iron efflux from astrocytes (astrocyte-specific Fpn knockout mice), suggesting that iron export from astrocytes plays a role in delivering iron to other CNS cells that require iron for the remyelination process.

9. The proliferation of OPCs is reduced in astrocyte-specific Fpn knockout mice after LPC injection, likely due to lack of iron supply from astrocytes.

10. The expression of the cytokines TNF-α and IL-1β by LPS-activated microglia is reduced under iron-deficient conditions. Both cytokines are known to promote

remyelination by either direct effects on OPCs or by indirectly stimulating astrocytes to produce growth factors involved in OPC proliferation and differentiation.

11. IL-1β stimulates astrocytes to produce FGF-2, which promotes OPC proliferation whereas TNF-α induces astrocytes to express IGF-1, which primarily enhances OPC differentiation. Reduced expression of IL-1β and TNF-α expression by iron-deficient microglia could therefore contribute to reduced proliferation and differentiation of OPCs.

12. IL-1β stimulates astrocytes to produce TGF-ß which is involved in the polarization of macrophages towards an 'alternatively activated' M2 phenotype thought to promote regeneration and repair processes. Reduced IL-1β expression by microglia could thus contribute to reduced repair/remyelination processes. High iron conditions in astrocytes (as would be expected in the astrocyte-specific Fpn knockout mice) leads to a reduction in TGF-β expression.

13. Iron chelation results in impaired initiation and elongation of neurite outgrowth from dorsal root ganglia (DRG) neurons in culture, suggesting that iron plays a role in neurite growth, possibly by ensuring proper mitochondrial function.

14. Mitochondria show increased cluster formation in DRG neurons treated with an iron chelator, which may indicate mitochondrial dysfunction.

15. Schwann cells do not only express Cp but also Fpn, and are thus equipped to export iron.

16. The mRNA expression of Fpn is increased after sciatic nerve crush injury, indicating an increased need for iron efflux for axonal regeneration after peripheral nerve injury.

17. Axonal regeneration and recovery of motor function after sciatic nerve crush injury are impaired in Cp knockout mice that would lack iron efflux from Schwann cells. These results suggest that iron efflux from Schwann cells might play a role in providing iron to axons in the peripheral nerve for axonal regeneration.

Abbreviations

Abc	ATP-binding cassette
ALS	amyotrophic lateral sclerosis
AMD	age-related macular degeneration
BBB	blood-brain barrier
BDNF	brain-derived neurotrophic factor
BFGF	basic fibroblast growth factor
BMP	bone morphogenic protein
Caspr	contactin-associated protein 1
CNS	central nervous system
CNPase	3'5'-cyclic nucleotide phosphohydrolase
COXVI	cytochrome C oxidase subunit VI
Cp	ceruloplasmin
CSF	cerebrospinal fluid
CTRL	control
DAB	diaminobenzidine
DAPI	4'-6-diamidino-2-phenylindole
DIG	digoxygenin
Dcytb	duodenal cytochrome b
DMEM	Dulbecco's modified Eagle's medium
DMT1	divalent metal transporter 1
DRG	dorsal root ganglia
EAE	experimental autoimmune encephalomyelitis
EGF	epidermal growth factor
ERK	extracellular signal-regulated kinase
FBS	fetal bovine serum
FGF-2	fibroblast growth factor 2
FLCVR	feline leukemia virus subgroup c receptor
FtMt	mitochondrial ferritin
Fpn	ferroportin

FBXL5	F-box and leucine-rich repeat protein 5
Gal-C	galactocerebroside
GAP-43	growth associated protein 43
GLAST	L-glutamate/L-aspartate
GPI	glycosylphosphatidylinositol
HEPC	hepcidin
Heph	hephaestin
HCP1	heme carrier protein 1
HJV	hemojuvelin
IGF-1	insulin-like growth factor 1
IL-1β	interleukin 1β
IRE	iron-responsive element
IRP	iron-regulatory protein
ISC	iron-sulfur cluster
JAK	janus kinase
LPC	lysophosphatidylcholine
LPS	lipopolysaccharide
LNA	locked nucleic acid
MAP-2	microtubule-associated protein 2
MBP	myelin basic protein and
MS	multiple sclerosis
NBIA	neurodegeneration with brain iron accumulation
NGF	nerve growth factor
Nogo A	reticulon-4
NPM	neurosphere growth medium
OPC	oligodendrocyte precursor cell
PANK2	pantothenate kinase 2
PDGF-α	platelet-derived growth factor α
PFA	paraformaldehyde
PKAN	pantothenate kinase-associated neurodegeneration
PLP	proteolipid protein

PNS	peripheral nervous system
RLS	restless leg syndrome
ROS	reactive oxygen species
Scara5	scavenger receptor member 5
SFI	sciatic functional index
SFM	serum- and transferrin-free oligodendrocyte medium
SIH	salicylaldehyde isonicotinoyl hydrazone
Sla	sex-linked anemia
SOD1	superoxide dismutase 1
SSC	saline-sodium citrate
STAT	signal transducer and activator of transcription
STEAP3	ferrireductase six-transmembrane epithelial antigen of the prostate 3
TAM	tamoxifen
TGF-β	transforming growth factor β
TNF-α	tumor necrosis factor α
TIM-2	T cell immunoglobulin-domain and mucin domain protein 2
TF	transferrin
TfR1	transferrin receptor 1
TfR2	transferrin receptor 2
TMPRSS6	transmembrane protease serine 6
USF2	upstream stimulatory factor 2
Veh	vehicle
WT	wildtype
ZIP14	zrt- and irt-like protein 14
Zp	zyklopen

Chapter 1

Literature review

1.1 Introduction

Iron is the most abundant transition metal in the human body. It is essential for life because it is required for many biological functions such as oxygen transport, DNA synthesis and oxidative phosphorylation (Andrews and Schmidt, 2007). Because of its ability to donate and accept electrons, iron is an important factor for the catalytic activity of various enzymes including heme and iron-sulfur cluster (ISC) enzymes. Lack of iron can therefore lead to loss of proper cellular function and viability. The main cause of low iron levels in the body is inadequate dietary intake. Iron deficiency is one of the world's most significant nutritional deficiencies. Iron deficiency during pregnancy or in infants can severely affect brain development. Although the uptake of dietary iron is tightly regulated to match systemic levels, too much iron in cells and tissues can also have significant clinical consequences due to its prooxidant nature. Iron can be harmful to cells because if unshielded it can catalyze the generation of highly reactive free radicals which can cause protein oxidation, DNA damage and lipid peroxidation. The central nervous system (CNS) is particularly vulnerable to oxidative stress because of its high oxygen consumption, low regenerative capacity and high lipid content (Halliwell, 2006). Therefore, cellular iron levels in the CNS have to be tightly regulated. The aim of this thesis is to explore the mechanisms involved in controlling cellular iron homeostasis in the CNS under physiological as well as pathophysiological conditions. The main focus will be to investigate iron efflux mechanism in CNS glial cells, and how iron is transported from cell to cell in the nervous system.

1.2 Free Radical Biology

Under physiological conditions, the production of reactive species including free radicals is balanced with cellular antioxidant defense systems. Disturbances of the prooxidant-antioxidant balance result in oxidative stress, which can cause cellular damage. As with many transition metals, iron is a strong prooxidant and has therefore the ability to catalyze the production of undesirable free radical reactions. The redox reactions underlying iron toxicity are the Fenton and the Haber-Weiss reaction, in which the reduced, ferrous form of iron (Fe^{2+}) converts hydrogen peroxide (H_2O_2) and superoxide anion (O^{2-}) leading to the formation of highly reactive hydroxyl radicals ($OH^{\cdot}$) (Halliwell and Gutteridge, 1990).

Fenton Reaction

$$Fe^{2+} + H_2O_2 \rightarrow Fe^{3+} + OH^- + {}^{\cdot}OH$$

Haber-Weiss Reaction

$$Fe^{2+} + O_2 \rightarrow Fe^{3+} + {}^{\cdot}O_2^-$$

$$2\ {}^{\cdot}O_2^- + 2\ H^+ \rightarrow O_2 + H_2O_2$$

$$Fe^{2+} + H_2O_2 \rightarrow Fe^{3+} + OH^- + {}^{\cdot}OH$$

Hydroxyl radicals have a very high reduction potential and can therefore cause especially high oxidative damage such as DNA damage, protein oxidation and lipid peroxidation (Gutteridge, 1994).

1.3 The role of iron in the CNS

Besides its general role in cellular metabolism, iron is required in the CNS for specific functions (Beard et al., 1993). For example, iron is involved in the synthesis of

neurotransmitters as an important cofactor for tyrosine hydroxylase and tryptophan hydroxylase, enzymes involved in the formation of catecholamines and 5-hydroxytryptamines, respectively (Youdim and Green, 1978). In addition, iron is essential for oligodendrocytes to generate and maintain myelin (Todorich et al., 2009). Oligodendrocytes are the cells with the highest iron levels in the CNS which is presumably linked to their highly metabolic needs associated with the process of myelination (LeVine and Macklin, 1990; Connor and Menzies, 1996). Iron is also directly required for myelin synthesis as a cofactor for enzymes involved in cholesterol and lipid synthesis such as HMG-CoA reductase or lipid saturase and desaturase enzymes (Lange and Que, 1998; Beard et al., 2003). Imbalances of iron homeostasis in the CNS can result in neuropathological conditions. Excessive iron levels have been associated with neurodegenerative diseases (Zecca et al., 2004; Molina-Holgado et al., 2007), whereas iron deficiency during development has been linked to cognitive impairment (Georgieff, 2008). Therefore, maintaining stable cellular iron levels in the CNS is very important.

1.4 Iron homeostatic proteins

To prevent iron toxicity but to also maintain adequate iron supply at the same time, iron homeostatic mechanisms have evolved to regulate iron levels. Several proteins have been shown to play a role in maintaining iron homeostasis by controlling the import, storage and export of iron. I will give a brief summary of the major iron homeostatic proteins involved in these processes in mammals.

1.4.1 Transferrin and Transferrin receptor 1

Transferrin (TF) is the major iron carrier protein in the plasma, primarily expressed and secreted by hepatocytes (Schade and Caroline, 1946). It is an 80 kDa glycoprotein with two iron-binding sites that can reversibly bind ferric iron. By binding ferric iron, TF keeps iron in its soluble, non-reactive form and delivers it to various tissues. TF-bound iron is taken up by cells via transferrin receptor 1 (TfR1), a homodimeric, disulfide bonded receptor that is expressed on the surface of many cells throughout the body. The binding affinity of TF to TfR1 depends on its iron status as well as on the pH of its environment (Dautry-Varsat et al., 1983). At neutral pH, diferric TF has a high affinity to TfR1 and forms therefore a complex with its receptor at the cell surface. TF/TfR1 complexes are then internalized via clathrin-mediated endocytosis (Figure 1). TF/TfR1-containing endosomes are acidified to a pH of 5.5 by the action of a proton pumping ATPase resulting in a conformational change of TF and TfR1 and consequent release of ferric iron (Dautry-Varsat et al., 1983; Watkins et al., 1992). Apo-TF remains bound to its receptor due to its high affinity to TfR1 at acid pH. The apo-TF/TfR1-complex is then recycled to the cell surface, where the apo-TF is released due to the neutral pH of the extracellular milieu (Dautry-Varsat, 1986). The ferric iron inside the endosomes is reduced into its ferrous form by the endosomal ferrireductase six-transmembrane epithelial antigen of the prostate 3 (STEAP3) (Ohgami et al., 2005) and transported by the divalent metal transporter 1 (DMT1) into the cytosol (Fleming et al., 1998).

Besides the classical TfR1, a second transferrin receptor TfR2 has been reported in mice and humans (Kawabata et al., 1999). In contrast to TfR1, which is ubiquitisouly expressed, TfR2 is predominantly expressed by hepatocytes. Since TfR2 has a 25-fold lower affinity to TF than TfR1, it is unlikely to be a major mediator of TF-bound iron

uptake. TfR2 has been suggested to play a role in the regulation of systemic iron homeostasis by controlling the expression of hepcidin in response to iron (see section 1.6) (Anderson et al., 2007).

In the CNS, TfR1 is expressed by neurons and immature oligodendrocytes (Connor and Fine, 1986; Giometto et al., 1990). TF has been shown to be expressed by the choroid plexus and oligodendrocytes (Bloch et al., 1985). However, oligodendrocytes express an alternatively spliced form of TF that is not secreted (de Arriba Zerpa et al., 2000). The function of intracellular TF in oligodendrocytes is unclear, but it appears to play an important role in myelination (Todorich et al., 2009). In the PNS, TF is expressed by Schwann cells during their maturation and after nerve injury (Salis et al., 2007). Also TfR1 expression has been found in Schwann cells and suggested to play a role in increased iron uptake after peripheral nerve injury (Raivich et al., 1991). TfR1 is also expressed on endothelial cells where it mediates the uptake of TF-bound iron from the circulation into the CNS parenchyma (Moos et al., 2007). However, unlike most cells outside the CNS, TfR1-mediated endocytosis does not appear to be a primary iron uptake system of cells within the CNS.

1.4.2 Divalent metal transporter 1

DMT1 (also known as DCT1 or Nramp2) is a transmembrane protein with 12 putative membrane-spanning domains that transports divalent metal cations including ferrous iron (Gunshin et al., 1997; Picard et al., 2000). Four isoforms of DMT1 have been identified that are encoded by a single gene, two of which contain IRE binding motives (see section 1.5.3) (Fleming et al., 1997; Gunshin et al., 1997; Hubert and Hentze, 2002). Besides its role in the endosomal transfer of iron in the TF cycle, DMT1 is an important plasma

membrane iron importer of non-TF bound iron. DMT1 is a symporter that requires the co-transport of protons to move Fe^{2+} across the membrane (Gunshin et al., 1997). It is highly expressed on the apical membranes of enterocytes in the duodenum where it functions in the non-heme iron uptake from the diet. Animals with spontaneous mutations in the DMT1 gene such as the microcytic anemia mice and Belgrade rats show severe defects in intestinal iron absorption and erythrocyte iron utilization resulting in severe anemia (Fleming et al., 1997; Fleming et al., 1998).

In the CNS, DMT1 is expressed on the cell surface of neurons, astrocytes and oligodendrocytes (Burdo et al., 2001; Jeong and David, 2003). In neurons, DMT1 expression has been shown to be upregulated in response to NMDA. In this study, high DMT1 levels and increased iron uptake have been suggested to contribute to NMDA toxicity (Cheah et al., 2006). DMT1 expression has also been shown to be upregulated in the substantia nigra of patients with Parkinson's disease and in a mouse model of this disease (Salazar et al., 2008). In addition, a recent study demonstrates that one of the DMT1 isoforms, DMT1b, is regulated by proteasomal degradation mediated by the E3 ubiquitin ligase parkin, a gene mutated in some forms of autosomal recessively inherited Parkinson's (Roth et al., 2010). Increased DMT1 expression was also seen in neurons in the mouse model of ALS (i.e., mice expressing the G37R mutant form of human SOD1) (Jeong et al., 2009). Thus, iron import via DMT1 might be an important iron uptake mechanism of cells in the CNS.

1.4.3 Ferrireductases

Ferrireductases reduce the ferric form of iron to its ferrous form. The transmembrane ferrireductase duodenal cytochrome b (Dcytb) has been identified in the duodenum where

it is highly expressed on the apical membranes of enterocytes (McKie et al., 2001). Dcytb is required to convert the dietary ferric iron to the ferrous form, which can then be transported via DMT1 into the cytosol of enterocytes. However, Dcytb null mice show no defects in intestinal iron absorption, suggesting that other ferrireductases exist that can also assist DMT1 (Gunshin et al., 2005; McKie, 2008).

As mentioned above, another ferrireductase that plays a role in the endosomal release of iron in the TF cycle is STEAP3. It reduces the ferric iron that is released from TF upon acidification in the endosomes to ferrous iron which can then be transported into the cytosol by DMT1 (McKie, 2005). STEAP3 is highly expressed in immature erythroid cells (Ohgami et al., 2005), but has been also found in non-erythroid tissue where it could play a similar role. Also other members of the STEAP family have been identified which might also function as endosomal ferrireductases, in particular in non-erythroid tissue (Ohgami et al., 2006) .

In the CNS, astrocytes have been shown to express Dcytb (Jeong and David, 2003). It is unclear whether other CNS cells also express Dcytb to reduce ferrous iron required for the uptake by DMT1. Recently, α-synuclein, a protein that is predominantly expressed in neurons, has also been shown to possess ferrireductase activity (Davies et al., 2011).

1.4.4 Ferritin

Ferritin is the major iron storage protein, first identified in horse spleen in 1937 (Laufberger, 1937). It is a heteropolymer composed of 24 subunits of H- (heavy or heart) and L- (light or liver) types which can store up to 4500 iron atoms (Harrison et al., 1967).

The ratio of H and L subunits varies from tissue to tissue (Arosio et al., 1976). The H-subunit contains ferroxidase activity, which is required for converting soluble Fe^{2+} into Fe^{3+} which is then deposited as ferric oxyhyroxide phosphate within the core of ferritin (Levi et al., 1988; Harrison and Arosio, 1996). The function of the L-subunit is to facilitate the incorporation of iron in the ferritin core (Levi et al., 1994). The major role of the ubiquitously expressed ferritin is to sequester and store iron, thereby preventing iron cytotoxicity. It is still unclear how iron is released from ferritin. Iron has been suggested to be released by at least two different ways of ferritin degradation: lysosomal-dependent and proteasome-dependent (De Domenico et al., 2006b; Kidane et al., 2006). Ferritin degradation and subsequent iron release has been suggested to be accelerated by reducing agents, oxidative damage and the induction of the cellular iron exporter ferroportin (Arosio and Levi, 2010). It is generally thought that iron is released from ferritin when needed. However, a recent study demonstrates that ferritin-iron cannot be utilized for heme synthesis in macrophages (Mikhael et al., 2010) which suggests that iron released from ferritin might not always be bioavailable for the cell. Regulation of ferritin expression occurs transcriptionally by various inflammatory cytokines and post-transcriptionally by cytosolic iron via the IRE/IRP system (Rouault, 2006) (see section 1.5.3). There is also low concentrations of circulating ferritin in the serum that is mainly composed of the L-subunit (Linder et al., 1996). Unlike cytosolic ferritin, serum ferritin is relatively poor in iron. Serum ferritin levels are increased in iron-overload diseases, inflammation (Rambod et al., 2008) and the rare human genetic disorder hyperferritinemia with cataracts (Hetet et al., 2003). Thus, serum ferritin is an indicator for body iron stores and is used in diagnostics for iron-related diseases. Serum ferritin has

been suggested to be produced and secreted by macrophages (Cohen et al., 2010). A minor portion of ferritin is also found in the nucleus that is translocated from the cytosol (Cai et al., 1997). It has been suggested to play a role in protecting DNA from iron-induced oxidative damage (Cai et al., 1998; Thompson et al., 2002; Cai et al., 2008).

Another member of the ferritin family that is localized to mitochondria is mitochondrial ferritin (MtFt) (Levi et al., 2001). The MtFt gene is an intronless gene, which is transcribed into a long precursor mRNA containing a mitochondrial localization sequence. The product of this gene is similar in size to cytosolic ferritin and shares 80% homology with H-Ferritin and 63% with L-Ferritin (Levi and Arosio, 2004). But unlike cytosolic ferritin, MtFt assembles as a homopolymer and is not expressed ubiquitously. In human, it has been found in testis, spermatozoa (Levi and Arosio, 2004) and sideroblasts of patients with sideroblasitc anemia (Cazzola et al., 2003). In mouse, it is expressed in tissues with high energy metabolism and oxygen consumption such as heart, kidney, pancreas and CNS (Santambrogio et al., 2007). MtFt also contains ferroxidase activity and is very efficient in oxidizing and storing iron. Its main function appears to be the control of ROS formation and oxidative damage by locally regulating iron availability which is particularly important in mitochondria considering that they produce especially high levels of ROS due to oxidative phosphorylation. However, in contrast to cytosolic ferritin, MtFt mRNA does not contain a functional IRE motif and is therefore not regulated by iron via the IRE/IRP system (see section 1.5.3).

In the CNS, the highest ferritin expression levels are in oligodendrocytes which express equal amounts of both H and L subunits (Connor et al., 1994). Microglia cells express ferritin enriched in L subunits whereas ferritin in neurons is mainly composed of

H subunits (Connor et al., 1994). Astrocytes express only very little ferritin under physiological conditions (Koeppen and Dentinger, 1988; Benkovic and Connor, 1993; Connor et al., 1994). However, in iron overload conditions, such as in ceruloplasmin deficient mice, astrocytes upregulate ferritin levels (Jeong and David, 2006).

Ferritin has been also suggested to mediate cellular iron uptake via ferritin receptors that have been identified more recently. The T cell immunoglobulin-domain and mucin-domain 2 (TIM-2) receptor has been shown to be expressed by B-lymphocytes and to bind and endocytose H-ferritin (Chen et al., 2005). In addition, a L-ferritin receptor, scavenger receptor member 5 (scara5), has been identified in the kidney (Li et al., 2009).

In the CNS, the TIM-2 receptor has been shown to be expressed in oligodendrocytes and to mediate H-ferritin-bound iron uptake in these cells (Todorich et al., 2008a) . Another study suggested a role for H-ferritin in mediating iron uptake into the CNS at the level of the BBB (Fisher et al., 2007). However, since the predominant ferritin subunit in the serum is L-ferritin, the physiological relevance of this iron uptake is still unclear.

1.4.5 Ferroportin

Ferroportin (Fpn; also known as MTP1, Ireg1, and SLC40A1) is the only known cellular iron exporter to date which was identified by three different labs simultaneously (Abboud and Haile, 2000; Donovan et al., 2000; McKie et al., 2000). Fpn is a 571-amino acid glycoprotein with 12 predicted transmembrane domains (Rice et al., 2009). It is highly expressed on the basolateral membrane of duodenal enterocytes, placental syncytiotrophoblasts, macrophages and hepatocytes, but also in various other cell types.

The importance of Fpn in iron export from these cells has been demonstrated by inactivation of the gene in mice and zebrafish (Donovan et al., 2005; Fraenkel et al., 2005). Mice that are globally deficient in Fpn are embryonically lethal, demonstrating an important role of Fpn in the maternal iron transfer to the embryo in the placenta. When Fpn was conditionally deleted in all tissues but the extraembryonic visceral endoderm and the placenta, the animals were born alive but developed severe anemia rapidly after birth, when the intestine becomes the only site of iron absorption (Donovan et al., 2005). These mice accumulate iron in duodenal enterocytes, macrophages and hepatocytes, indicating a critical role of Fpn in iron export from these cells. Fpn has also been inactivated selectively in postnatal intestinal enterocytes of mice resulting in intestinal iron accumulation and subsequent iron-deficient anemia confirming the requirement of Fpn for transfer of dietary iron from enterocytes into the circulation (Donovan et al., 2005).

Autosomal dominant mutations in the human Fpn gene result in a subtype of iron overload disease, hemochromatosis type IV, also called Ferroportin disease (Pietrangelo, 2004). The majority of these mutations causes loss of Fpn function leading to iron accumulation in macrophages, low saturation of plasma TF and only mild liver injury (Montosi et al., 2001; Njajou et al., 2001). A minor group of human Fpn mutations causes hepcidin resistance resulting in a more classical phenotype of hemochromatosis with parenchymal iron overload and high plasma TF saturation (De Domenico et al., 2006a). Fpn levels are regulated by at least three different mechanisms: transcriptional regulation, which controls mRNA levels (Marro et al., 2010) and splice variants (Zhang et al., 2009); translational control via an IRE motif in the 5′ untranslated region of its mRNA

(Lymboussaki et al., 2003); and systemic iron status, which regulates Fpn stability on the cell surface through interaction with the peptide hormone hepcidin (Nemeth et al., 2004). The binding of hepcidin to the extracellular loop domain on Fpn results in the internalization and lysosomal degradation of Fpn (Nemeth et al., 2004; De Domenico et al., 2007b). Recently, alterations in Fpn levels have been linked to breast cancer. The study reports reduced Fpn levels in malignant breast cell lines as well as in human breast cancer tissue which was accompanied by increased hepcidin levels (Pinnix et al., 2010). In addition, Fpn levels were correlated with the degree of anaplasia: the reduction of Fpn was higher in more aggressive breast cancer subtypes (Pinnix et al., 2010).

In the CNS, Fpn is expressed on the cell surface of neurons as well as glia cells including oligodendrocytes, astrocytes and microglia (Burdo et al., 2001; Wu et al., 2004; Moos and Rosengren Nielsen, 2006). Fpn expression is also found in the retinal pigment epithelium and retinal Müller cells (Hahn et al., 2004a). In addition, Fpn is expressed in ependymal cells of the choroid plexus and brain capillary endothelial cells where it might play a role in iron entry into the CNS (Wu et al., 2004). It has also been detected in presynaptic vesicles suggesting that iron might be transported via synaptic vesicles and released into the synaptic cleft upon vesicle fusion (Wu et al., 2004). In astrocytes, Fpn has been shown to be involved in iron export (Jeong and David, 2003). However, the role of Fpn in other CNS cells than astrocytes is less understood.

1.4.6 Ceruloplasmin

Ceruloplasmin (Cp) is a multi-copper ferroxidase that converts Fe^{2+} to Fe^{3+}. It is one of the most abundant proteins in plasma, first identified in 1948 by Holmberg and Laurell (Holmberg and Laurell, 1948). Cp is synthesized and secreted by the liver as a single

polypeptide chain composed of 1046 amino acids. The structure of this 132 kDa α2-glycoprotein has been analyzed by X-ray crystallography, revealing 6 β-barrel domains that are arranged in a triangular fashion (Zaitsev et al., 1999). Each of these domains consists of eight anti-parallel β strands. Due to its high copper content, Cp has been originally thought to play a role in copper metabolism (Meyer et al., 2001; Bielli and Calabrese, 2002). However, it is now known that copper is only important for its catalytic activity. Cp contains 6 copper atoms in three different types of binding sites (Bento et al., 2007). There are three mononuclear copper binding sites in domains 2, 4 and 6 and a trinuclear copper center located between domain 1 and 6. The trinuclear copper center is essential for its ferroxidase activity. The highest Cp levels in the body are found in the plasma, but Cp is also expressed by ependymal cells lining the ventricles and the choroid plexus (Klomp et al., 1996; Klomp and Gitlin, 1996). A membrane-bound glycosylphosphatidylinositol (GPI)-anchored form of Cp was first identified in astrocytes in the CNS (Patel and David, 1997). GPI-Cp is also found on the surface of leptomeningeal cells that cover the brain and the spinal cord (Mittal et al., 2003), Schwann cells in the PNS and Sertoli cells in the testes (Salzer et al., 1998). GPI-Cp is generated by alternative splicing (Patel et al., 2000). By oxidizing the highly reactive Fe^{2+} into the nonreactive Fe^{3+}, Cp plays an important detoxifying role. In addition, studies on humans with mutations in the Cp gene and mice lacking Cp has shown that Cp is involved in releasing iron from different tissues including the CNS (Harris et al., 1999; Patel et al., 2002; Xu et al., 2004; Jeong and David, 2006).

In the CNS specifically, GPI-Cp has been shown to facilitate iron efflux from astrocytes by partnering with the iron exporter Fpn (Jeong and David, 2003). Ferrous iron

that is transported through Fpn is immediately oxidized by Cp to ferric iron, which can then bind to the extracellular iron binding protein TF. This oxidation appears to be necessary for the iron efflux to occur, as astrocytes from Cp null mice are unable to efflux iron *in vitro* (Jeong and David, 2003). Moreover, GPI-Cp is required for the stability of Fpn on the cell surface, since Fpn is internalized and degraded in astrocytes lacking GPI-Cp (De Domenico et al., 2007a).

1.4.7 Hephaestin

Hephaestin (Heph) is another copper-dependent ferroxidase that shares 50% homology with Cp (Petrak and Vyoral, 2005). All copper-binding sites and key structural features that are essential for its function as a ferroxidase are conserved in Heph and Cp (Syed et al., 2002). But in contrast to Cp, Heph contains a predicted single transmembrane-spanning region at its C-terminus. It is comprised of 1185 amino acids and contains multiple sites for posttranslational modifications such as N-glycosylation (Nittis and Gitlin, 2004; Petrak and Vyoral, 2005). Heph has been identified as the defective gene in the sex-linked anemia (sla) mouse (Vulpe et al., 1999). These mice have a spontaneous deletion in the heph gene resulting in the expression of a truncated form of the Heph protein with only partial activity (Chen et al., 2004). The lack of Heph activity in the sla mutant mice leads to a block in intestinal iron absorption. They can absorb the iron from the diet, but are unable to release it into the circulation. Therefore, iron accumulates in the enterocytes and is lost by exfoliation resulting in iron deficiency and development of microcytic hypochromic anemia (Bannerman and Cooper, 1966). Thus, Heph has been suggested to be implicated in iron export from duodenal enterocytes, possibly by interacting with the iron exporter Fpn (Figure 2) (Wessling-Resnick, 2006). Consistent

with its important role in intestinal iron transport, the highest levels of Heph expression are found on the basolateral membrane of duodenal enterocytes. It has been also shown that Heph colocalizes with Fpn in human intestinal Caco-2 cells (Han and Kim, 2007), and that Heph and Fpn are able to co-immunoprecipitate (Yeh et al., 2009), suggesting that an interaction of Fpn and Heph might underlie the efflux mechanism. Heph function appears to be also important for other cells, since Heph is also expressed in various other tissues such as brain, spleen, kidney, lung and placenta (Vulpe et al., 1999; Frazer et al., 2001). In the retina, Heph as well as Cp have been shown to be expressed by Müller glia and the retinal pigment epithelium (Hahn et al., 2004b). Mice lacking both ferroxidases show retinal iron overload and retinal degeneration, and has been proposed as a model for age-related macular degeneration (AMD), a common cause of vision loss (Hahn et al., 2004b; Hadziahmetovic et al., 2008).

Since Heph mRNA does not contain an IRE sequence, its expression is not regulated by the IRE/IRP system (see section 1.5.3). However, Heph expression appears to be regulated by copper and iron levels. In the intestine, Heph expression is increased under iron-deficient conditions, whereas iron repletion causes downregulation of Heph expression (Frazer et al., 2001; Sakakibara and Aoyama, 2002; Chen et al., 2003). Similarly, in patients with the iron overload disease hemachromatosis duodenal Heph expression was decreased (Stuart et al., 2003), while an increased expression was observed in patients with iron-deficiency (Zoller et al., 2003). Also copper repletion has been shown to increase Heph expression (Han and Wessling-Resnick, 2002). Copper seems to be not only required for the synthesis and ferroxidase function of Heph but also

for its protein stability. In copper-depleted cells, Heph is ubiquitinated and quickly degraded by the proteasome (Nittis and Gitlin, 2004).

As mentioned above, Heph expression has been detected in the CNS including the retina. Other than the retina, its expression and function in different CNS cell types has not been studied. The analysis of the cell-type specific expression and function of Heph in cells of the CNS is part of this thesis (see chapter 2).

1.4.8 Other ferroxidases

Another multicopper ferroxidase called Zyklopen (Zp) was recently identified (Chen et al., 2010). This membrane-bound ferroxidase had been first detected in BeWo cells, a placental cell line, where it had been suggested to mediate iron efflux (Danzeisen et al., 2000; Danzeisen et al., 2002). The sequence of Zp is highly homologous to Heph and Cp (Chen et al., 2010). Molecular modeling also revealed similar putative iron-binding sites as well as copper-binding sites that are essential for its ferroxidase function (Chen et al., 2010). Zp is highly expressed in the placenta, but can be also found in the CNS, kidney, testes and mammary glands. Zp has been suggested to play an important role in the transfer of iron from the mother to the fetus in the placenta (Gambling et al., 2011).

In the CNS, Zp has been shown to be expressed in the retina, the choroid plexus, the dentate gyrus, and the CA1 region of the hippocampus (Chen et al., 2010). But nothing is known so far about the role of Zp in the CNS.

Recently, the amyloid precursor protein APP has been shown to possess ferroxidase activity and to mediate iron export from HEK293T cells and primary neurons (Duce et al., 2010). This study further demonstrated that the ferroxidase activity of APP

is inhibited by zinc, which accumulates in Aβ aggregates in brains of patients with Alzheimer's disease.

1.4.9 Hepcidin

Hepcidin (HEPC) is a small amino acid peptide with antimicrobial activity, first identified in human urine and plasma (Krause et al., 2000; Park et al., 2001; Pigeon et al., 2001). It is synthesized by hepatocytes and secreted into the circulation. The mature 25 amino acid peptide is generated from an 84 amino acid prepropeptide by furin cleavage. The functional role of HEPC was demonstrated in two different mouse models. Mice have two different HEPC genes, HEPC1 and HEPC2, whose expression is controlled by the transcription factor upstream stimulatory factor 2 (USF2). USF2 null mice that failed to express both HEPC showed a hemachromatosis phenotype with iron deposition in the liver and pancreas (Nicolas et al., 2001). In contrast, transgenic mice overexpressing HEPC1 developed severe iron deficiency (Nicolas et al., 2002). However, transgenic mice overexpressing HEPC2 showed no disturbances of iron metabolism indicating that HEPC1 is the main regulator of iron homeostasis in mice (Lou et al., 2004). In humans, HEPC mutations result in a rare but very severe "juvenile" form of hemachromatosis with early onset and prominent cardiac and endocrine involvement (Roetto et al., 2003). Thus, HEPC has been suggested to play a role in negatively regulating iron absorption, the details of which are described in section 1.6. In the CNS, HEPC is expressed by astrocytes and neurons (Zechel et al., 2006), but its role in the CNS is still unclear.

1.5 Cellular iron homeostasis

1.5.1 Iron import mechanisms

Iron can be taken up by cells in a TF-dependent and -independent way. Most mammalian cells acquire iron via TfR1-mediated endocytosis (Ponka, 1999). Immature erythroid cells, which have the highest iron requirements of all cells due to haemoglobin synthesis, take up iron almost entirely through the TF-TfR1 pathway (Wrighting and Andrews, 2008). Diferric TF has the highest affinity for TfR1 at physiological pH and is therefore the form that is most efficiently used by cells.

TF-independent iron uptake is primarily carried out by DMT1, which is expressed on the surface of several cell types. DMT1 is particularly high expressed on the apical membranes of enterocytes in the duodenum where it functions in the non-heme iron uptake from the diet. Dietary as well as extracellular iron is usually present in the ferric form. To be transported by DMT1, ferric iron has to be first converted into its ferrous form by the membrane-bound ferrireductase Dcytb.

Another potential transporter for TF-independent iron uptake is Zrt- and Irt-like protein 14 (Zip14), a member of the ZIP family of metal transporters that has been reported to transport zinc and iron in hepatocytes (Liuzzi et al., 2006).

In addition, ferritin-dependent iron uptake has been suggested to occur in B-lymphocytes via the TIM-2 receptor which binds and endocytoses H-ferritin (Chen et al., 2005). Recently, the TIM-2 receptor was also shown to play a role in H-ferritin uptake in oligodendrocytes in the CNS (Todorich et al., 2008b). Another ferritin receptor that was more recently identified is Scara5 which binds and internalizes L-Ferritin in the kidney

(Li et al., 2009). Scara5 is also expressed in several embryonic tissues and thus is likely to play a role in iron uptake during development.

As an alternate pathway, iron can also be taken up in form of heme (Krishnamurthy et al., 2007). Heme uptake has been suggested to play a role especially in duodenal enterocytes, since high amounts of dietary iron are present in form of heme. It is likely that once inside the enterocytes, heme is metabolized by heme oxygenase to release Fe^{2+}, and then enter a common pathway with dietary nonheme iron. Heme uptake at the intestinal brush border has been suggested to be mediated by the heme carrier protein 1 (HCP1) (Shayeghi et al., 2005). However, another study demonstrated that HCP1 transports folate more efficiently than heme, suggesting that HCP1 may not be the major intestinal heme transporter (Qiu et al., 2006).

1.5.2 Iron export mechanisms

The only known exporter of inorganic iron to date is Fpn, which is expressed in almost every cell type. To efflux iron, Fpn requires the action of a ferroxidase. In the liver, iron efflux through Fpn has been shown to be facilitated by the plasma ferroxidase Cp (Osaki and Johnson, 1969; Harris et al., 1999). Cp oxidizes the ferrous iron that is transported through Fpn into ferric iron, which allows it to bind to TF in the circulation. Such an oxidation might create a gradient of ferrous iron by removing ferrous iron from the cell membrane, and thus driving the transport of ferrous iron through Fpn. As a plasma protein, Cp is likely to mediate iron efflux from many different tissues. In addition, the GPI-anchored form of Cp has also been shown to partner with Fpn to efflux iron from astrocytes *in vitro* (Jeong and David, 2003). On the other hand, iron export from

duodenal enterocytes has been shown to be mediated by the Cp homologue Heph (Anderson et al., 2002). The ferroxidase Heph is likely to function in a similar way than Cp to drive iron release from enterocytes through the basolaterally expressed Fpn. In the placenta, iron transfer from the mother to the fetus is thought to be facilitated by the ferroxidase Zp (Chen et al., 2010).

Another way of iron export is heme export. Recently, the feline leukemia virus subgroup c receptor (FLCVR) has been identified as heme exporter and appears to play a role in reducing excess heme in erythroid cell precursors and in heme release from macrophages (Quigley et al., 2004; Keel et al., 2008). Another heme transporter is the ATP-binding cassette transporter g 2 (Abcg2) which may mediate heme efflux from immature erythroid cells (Krishnamurthy and Schuetz, 2006).

Iron export in the form of ferritin has also been suggested but is not well characterized. One study shows that erythrophagocytosing macrophages secrete ferritin (Sibille et al., 1988). Secretion of L-ferritin into the circulation by macrophages was shown to occur via a non-classical lysosomal secretory pathway (Cohen et al., 2010). However, since serum ferritin is poor in iron under physiological conditions, ferritin secretion is unlikely to be a major iron export mechanism normally. This is supported by a recent study demonstrating that ferritin secretion occurs when cellular ferritin is synthesized in the relative absence of free cytosolic iron (De Domenico et al., 2011).

1.5.3 Regulation of intracellular iron homeostasis

One essential control of cellular iron homeostasis is the regulation of iron homeostatic proteins by the iron-responsive element/iron-regulatory protein (IRE/IRP) system. IRPs

are cytosolic proteins that “sense” intracellular iron levels and post-transcriptionally regulate the expression of iron homeostatic proteins by binding to RNA stem loops, known as IREs, in their mRNAs (Figure 3) (Muckenthaler et al., 2008). There are two different IRPs, IRP1 and IRP2, that are regulated by different mechanisms in response to intracellular iron levels. However, both are inactive as IRE-binding proteins under high iron conditions. Under high iron conditions, IRP1 incorporates iron-sulfur [4Fe-4S] clusters, which results in switching its function to ‘cytosolic aconitase’, an enzyme that interconverts citrate and isocitrate (Rouault and Klausner, 1996). Absence of the iron-sulfur cluster in aconitase causes a conformational change to IRP1 that transforms the active site of IRP1 to a high affinity-binding motif for IREs. In contrast, IRP2 is ubiquitinated and degraded by the proteasome under iron-replete conditions (Guo et al., 1995). This degradation is mediated by the adaptor protein F-box and leucine-rich repeat protein 5 (FBXL5). FBXL5 acts as an iron sensor, since iron-binding stabilizes it. When iron levels are high, FBXL5 interacts with IRP2 and recruits an E3 ubiquitin ligase complex, promoting ubiquitination of IRP2 and subsequent proteasomal degradation (Salahudeen et al., 2009; Vashisht et al., 2009). In iron-deficient cells, less FBXL5-dependent degradation occurs. IRPs can either negatively or positively regulate the expression of iron-homeostatic proteins depending on the location and the number of the IRE motives in their mRNA. IRP-binding to IREs in the 5’untranslated regions (UTR) of mRNAs leads to inhibition of translation of several iron homeostatic proteins such as ferritin, aminolevulinic acid synthase2, aconitase2, Fpn and hypoxia-inducible factor 2α, whereas IRP-binding to the multiple IREs in the 3’UTR of the TFR1 mRNA results in stabilization of the mRNA and consequent increased translation (Koeller et al., 1991;

Muckenthaler et al., 2008). IRPs also positively regulate DMT1 mRNA expression via a single 3'UTR IRE motif, but the exact molecular mechanism is still unknown (Gunshin et al., 2001).

IRPs can also respond to non-iron signals. IRP1 can be activated by ROS, which cause the disassembly of the Fe/S cluster (Pantopoulos and Hentze, 1998). Hypoxia has also been shown to inactivate IRP1, while stabilizing IRP2 (Meyron-Holtz et al., 2004a). In addition, phosphorylation by different kinases can regulate IRP activity (Rouault and Klausner, 1996; Eisenstein, 2000).

Mice with inactivation of both IRPs are embryonically lethal (Smith et al., 2006; Galy et al., 2008). By contrast, mice lacking either of the two proteins are viable. IRP1 deficient mice are asymptomatic (Meyron-Holtz et al., 2004b), whereas IRP2 deficient mice develop mild microcytic anemia and altered body iron distribution (LaVaute et al., 2001; Galy et al., 2005). One group also reported iron accumulation in different regions of the CNS in the IRP2 null mice, which was accompanied by neurodegeneration (LaVaute et al., 2001). However, such neuropathology was not detected by another group in another line of IRP2 deficient mice (Galy et al., 2005), which might be due to different deletion techniques or different genetic backgrounds of the mice.

1.6 Systemic iron homeostasis

The adult human male contains about 4 g of iron, most of which is bound within hemoglobin in erythrocytes (65-70%). About 3 mg of iron are bound to plasma TF which delivers iron to tissues throughout the body (Anderson et al., 2007). A great portion is transported to the bone marrow for erythropoiesis, but other tissues also require iron for

various metabolic processes. Excessive iron that is not immediately utilized by the body is stored by the liver (about 1 g) and can be released upon demand.

Iron is taken up by the body at the level of the gut (1-2 mg/day). Dietary iron is absorbed by the proximal duodenum in form of inorganic iron or heme (Anderson et al., 2007). Since the body has no means of actively excreting iron, absorption of dietary iron is tightly regulated. However, the major source of body iron does not result from dietary absorption, but rather from iron recycling in the reticulo-endothelial system, consisting of specialized macrophages present mainly in the spleen, liver (Kupffer cells), and bone marrow (Kaplan et al., 2011). Macrophages phagocytose and lyse senescent or damaged erythrocytes to recover the iron from these cells and subsequently release it back into the circulation. This internal turnover of iron is essential to meet the requirements of erythropoiesis (20-30 mg/day). In order to maintain stable plasma iron levels, the release of iron from reticulo-endothelial macrophages as well as intestinal iron absorption are tightly controlled. The major regulator of iron concentrations in the plasma is hepcidin (HEPC), an antimicrobial peptide hormone, produced and secreted by the liver (Park et al., 2001). HEPC negatively regulates systemic iron levels by preventing the release of iron from duodenal enterocytes, reticulo-endothelial macrophages and iron-storing hepatocytes. During pregnancy, fetal HEPC controls the placental transfer of iron from maternal plasma to the fetal circulation (Nemeth et al., 2004). HEPC acts by binding to the iron exporter Fpn, which is then internalized and degraded by the lysosome (Nemeth et al., 2004). Loss of Fpn on the cell surface results in decreased iron release into the circulation. When body iron requirements are low due to high plasma iron levels or inflammation, HEPC is upregulated resulting in decreased intestinal iron absorption and

increased iron sequestration in macrophages and hepatocytes. Conversely, HEPC expression is decreased in conditions requiring increased cellular iron release, such as iron deficiency and increased erythropoeisis. Decreased HEPC levels lead to increased Fpn on the cell surface and thus increased release of iron from cells into the circulation. HEPC itself is regulated by body iron levels, erythropoietic requirements, hypoxia and inflammation (Ganz, 2003). The regulation of HEPC by iron levels is independent of the IRE/IRP system, since HEPC mRNA does not contain any IRE motives. Regulation of HEPC expression appears to occur at the level of transcription (Flanagan et al., 2007). Human mutations and transgenic mouse models have provided information about several different molecules involved in the regulation. HFE, TfR2 and hemojuvelin (HJV) which are mutated in different forms of hemochromatosis, are thought to play a role in HEPC regulation (Viatte and Vaulont, 2009). Mutations in these genes result in decreased HEPC responsiveness to iron, and subsequent HEPC deficiency and iron overload (Kaplan et al., 2011). Conversely, mutations in the transmembrane protease serine 6 (TMPRSS6), which is associated with severe iron deficiency, inhibit downregulation of HEPC when body iron levels are low (Kaplan et al., 2011). Mouse models of hemachromatosis showed that components of the bone morphogenic protein (BMP) pathway are also necessary for HEPC regulation by iron. BMP6 knockout mice had low HEPC levels and developed severe iron overload (Meynard et al., 2009) . Thus, the regulation of HEPC expression by iron has been shown to involve several different molecules and pathways, and is still not completely understood. In addition, HEPC is downregulated by erythropoiesis, which could be mediated either by increased iron demands, bone marrow-derived factors (Pak et al., 2006; Vokurka et al., 2006) or higher oxygen requirements potentially regulating

HEPC via the hypoxia-inducible factors (Peyssonnaux et al., 2007). HEPC expression is upregulated by inflammation resulting in decreased plasma iron levels and subsequent "anemia of inflammation". This body defense mechanism limits iron supply to mircororganism and thus inhibits their proliferation. The major cytokine that induces the upregulation of HEPC in response to inflammation is IL-6 (Nemeth et al., 2003; Nemeth et al., 2004). IL-6 activates the Janus kinase (JAK)/signal transducer and activator of transcription (STAT) pathway, which activates the HEPC promoter via a STAT-binding motif (Fleming, 2007). Other cytokines and pathways are also involved in HEPC regulation (Lee and Beutler, 2009).

1.7 Iron homeostasis in Mitochondria

The main site of cellular iron utilization is the mitochondrion. This organelle requires iron for the synthesis of heme and iron-sulfur clusters (ISCs), two essential cofactors for many proteins including enzymes involved in mitochondrial oxidation (Levi and Rovida, 2009). Mitochondrial function is therefore highly dependent on adequate iron supply. The most prominent example of iron-dependent mitochondrial function is the electron transport chain, which relies on iron-containing redox systems to transport electrons from electron donors (NADH and succinate) to oxygen, ultimately resulting in ATP synthesis. These iron-dependent systems are enzyme complexes located in the inner mitochondrial membrane. Complex I-III contain ISCs in their active sites and in addition, complex III and complex IV contain cytochromes with heme as a prosthetic group (Gille and Reichmann, 2011). Despite the importance of iron in mitochondrial function, iron homeostatic mechanisms within mitochondria are still not fully understood. Different mechanisms have been suggested to mediate mitochondrial iron import. In case of TfR1-

mediated cellular iron uptake, the endosomal iron has been suggested to be directly transferred to the mitochondrion by transient fusion of the endosome with the mitochondrial membrane (Ponka, 1997). Iron could also be released from the endosome via DMT1 and then enter the mitochondrion via iron importers. Ferrous iron that is transported by DMT1 is thought to bind to low molecular-weight chaperones such as phosphate or citrate and then taken up by mitochondria as iron/chaperone complex (Shvartsman et al., 2007). In addition, two transport proteins, mitoferrin-1 and mitoferrin-2 have been identified in the inner mitochondrial membrane where they may play a role in mitochondrial iron uptake (Shaw et al., 2006). But it is still not understood how iron is transported across the outer mitochondrial membrane. Once inside the mitochondrion, iron can be used for heme and ISC synthesis or it can be stored in mitochondrial ferritin. Another protein suggested to bind or sequester mitochondrial iron is frataxin, a protein located in the mitochondrial matrix (Campuzano et al., 1997). Frataxin deficiency in mice and in Friedreich's Ataxia in humans results in reduced levels of ISC proteins suggesting a role for frataxin in ISC synthesis (Rotig et al., 1997; Puccio et al., 2001). Frataxin is thought to function as an iron chaperone by binding and delivering iron to the ISC and heme synthesis machinery (Yoon and Cowan, 2003, 2004). A great portion of the newly synthesized heme and ISCs is used by the mitochondrion itself for its own metabolism, while the remaining part is exported into the cytosol. Two Abc transporter, Abcb7 and Abc-me have been shown to be involved in the export of ISCs and heme, respectively (Shirihai et al., 2000; Pondarre et al., 2006). However, the exact export mechanisms are still unclear. Since mitochondria are major sources of cytotoxic ROS due to electron leak during oxidative phosphorylation, it is essential that mitochondrial iron metabolism is

tightly regulated in order to prevent further ROS generation through the Fenton reaction. Disturbances of mitochondrial iron homeostasis have been linked to human diseases such as Friedreich's Ataxia and sideroblastic anemia. Both diseases are caused by mutations in proteins involved in ISC and heme biosynthesis and are associated with mitochondrial iron overload (Levi and Rovida, 2009).

1.8 Iron homeostasis in the CNS

The CNS is highly metabolic active, consuming about 20% of the total body energy (Shulman et al., 2004) and thus, requires high iron levels to meet the metabolic needs. Iron deficiency during pregnancy and in infants has been associated with defects in brain development and cognition (Georgieff, 2008). In order to ensure proper development and functioning of the brain, a sufficient amount of iron has to be supplied to the CNS. In contrast to other organs, the CNS is separated from the circulation by an endothelial barrier, the blood brain barrier (BBB), consisting of brain capillary endothelial cells, a basement membrane and astrocytic endfeet. Due to lack of fenestrations that characterize capillaries of the systemic circulation, and the presence of tight junctions between the brain endothelial cells, nutrients cannot pass between these cells, but must be transported across the endothelial cells (Abbott et al., 2010). Studies using TF-bound radioactive iron or horse-radish peroxidase-labeled TF demonstrate that TF-bound iron from the circulation is taken up by brain capillary endothelial cells via TfR1-mediated endocytosis (Roberts et al., 1992; Moos and Morgan, 2000). TF itself does not cross the BBB suggesting that iron is released from TF within endosomes of the endothelial cells (Moos and Morgan, 2000). However, it is still unclear whether the iron transporter DMT1 that is required for the transfer of iron from the endosomes to the cytosol is expressed in

endothelial cells (Burdo et al., 2001; Moos and Morgan, 2004). The export of iron from endothelial cells into the CNS is thought to occur via Fpn (Wu et al., 2004). However, the expression of Fpn in endothelial cells is still under debate (Wu et al., 2004; Moos and Rosengren Nielsen, 2006). Since 95% of the endothelial surface in the CNS is covered by astrocytic endfeet, astrocytes are likely to take up the iron that is released from the endothelial cells and to distribute it to other CNS cells. The iron importer DMT1 is expressed in astrocytic endfeet (Burdo et al., 2001), where it could mediate the uptake of ferrous iron into astrocytes. Astrocytes also possess iron efflux mechanisms and are therefore capable of delivering iron to other cells in the CNS (Figure 4). Iron efflux from astrocytes is mediated by the iron exporter Fpn and the ferroxidase Cp (Jeong and David, 2003). Cp has been shown to physically interact with Fpn and to be essential for the iron efflux to occur (Jeong and David, 2003). It has been also suggested that astrocytic iron efflux is required for providing neurons with iron (Jeong and David, 2006). This study showed increased iron accumulation in astrocytes but not neurons with age in Cp null mice, which was associated with loss of both astrocytes and neurons in the cerebellum. Interestingly, the neurons showed upregulation of the iron importer, DMT1 suggesting that the neurons may be iron deprived because the iron remains trapped in the astrocytes. The neuronal cell death in these mice may however be due to either iron deprivation and /or loss of trophic support from astrocytes (Jeong and David, 2006). Ferrous iron effluxed from astrocytes is rapidly oxidized to its ferric form, which can bind to TF or other low molecular weight iron binding molecules. In the CNS, TF is primarily expressed by the choroid plexus and secreted into the cerebrospinal fluid (CSF). However, TF concentrations in the CSF are very low compared to TF in the plasma

(Bleijenberg et al., 1971; Moos, 2002). In addition, TF in the CSF is fully saturated with iron, whereas plasma TF is only up to 20-25% occupied by iron (Bradbury, 1997). Therefore, iron might not only be transported by TF but also by low molecular weight chaperones such as citrate or ATP (Moos et al., 2007). The presence of low molecular weight, non-transferrin bound iron has been also reported in the CSF (Moos and Morgan, 1998). Neurons are likely to take up TF-bound as well as non-TF bound iron as they express both TfR1 and DMT1 (Giometto et al., 1990; Moos, 1996; Burdo et al., 2001). A recent study provided evidence suggesting that neuronal iron export occurs via Fpn facilitated by APP, which has ferroxidase activity (Duce et al., 2010).

Iron import in developing oligodendrocytes may occur via TF-mediated endocytosis (Todorich et al., 2009). However, TfR1 expression has not been detected in mature oligodendrocytes (Moos, 1996) suggesting that mature oligodendrocytes take up non-TF bound iron. Oligodendrocytes could take up iron via DMT1 (Burdo et al., 2001) or via ferritin (Todorich et al., 2009). The ferritin receptor TIM-2 is expressed by oligodendrocytes and mediates the uptake of H-ferritin (Todorich et al., 2008a). However, physiological concentrations of ferritin in the CSF are very low (Moos and Morgan, 1998). The investigation of iron export mechanisms of oligodendrocytes is part of this thesis (chapter 2). It is still unclear how iron is released from the CNS. One possible route may be the release of iron into the CSF followed by the export to the blood via the arachnoid villi in the meninges (Moos et al., 2007).

1.9 CNS diseases with genetic defects in iron metabolism

Mutations in some iron homeostatic proteins have been directly linked to disturbances of iron homeostasis in the CNS, such as neuroferritinopathy, pantothenate kinase-associated neurodegeneration (PKAN), Friedreich's Ataxia, and aceruloplasminemia (Ponka, 2004). These diseases show iron accumulation in different brain regions accompanied by neurodegeneration.

1.9.1 Aceruloplasminemia

Mutations in human Cp result in an autosomal, recessive neurodegenerative disease called aceruloplasminemia (Harris et al., 1995). Patients with this disease exhibit mainly neurological symptoms such as involuntary movements, ataxia and dementia, but also develop diabetes and retinal degeneration (Miyajima et al., 1987). Besides increased iron depositions in the liver and the pancreas, iron accumulation can be especially seen in the basal ganglia and the deep cerebellar nuclei in brains of these patients. Mitochondrial dysfunction such as reduced enzymatic activity of complex I and IV of the respiratory chain is also associated with the disease (Kohno et al., 2000).

Cp null mice that have been generated by three different laboratories reflect well the pathology of the human disease. Cp null mice show iron accumulation in the liver, the spleen (Harris et al., 1999; Patel et al., 2002; Yamamoto et al., 2002), and the CNS (Patel et al., 2002; Jeong and David, 2006). It has been also shown that administration of Cp in these mice results in iron mobilization out of the liver (Bradley et al., 2000). In addition to iron deposits, Cp null mice show increased lipid peroxidation in the CNS, loss of dopaminergic neurons in the brainstem and decreased motor coordination (Patel et al., 2002). Cerebellar neurons purified from these mice are more susceptible to oxidative

damage *in vitro* (Patel et al., 2002). Further studies demonstrate iron accumulation in astrocytes in the cerebellum of Cp null mice with aging which was accompanied by a significant loss of these cells (Jeong and David, 2006). The loss of astrocytes has been suggested to be causative for the observed iron-deprivation of Purkinje neurons and their subsequent loss in the cerebellum of these mice (Jeong and David, 2006), indicating a role for astrocytes in delivering iron to neurons. Thus, the studies of Cp null mice and humans with aceruloplasminemia emphasize the important role for Cp in iron efflux from various tissues including the CNS.

1.9.2 Friedreich's Ataxia

Friedreich's Ataxia is an autosomal recessive neurodegenerative disease characterized by degeneration of large sensory neurons in the dorsal root ganglia (DRG) and spinocerebellar tracts, cardiomyopathy and an increased incidence of diabetes mellitus (Durr et al., 1996). It is caused by an abnormal expansion of a GAA triplet repeat in the first intron of the frataxin gene resulting in a severe reduction of frataxin protein levels (Campuzano et al., 1996). As discussed earlier, the physiological function of the mitochondrial protein frataxin is still not well understood. However, frataxin deficiency has been associated with mitochondrial iron accumulation, oxidative damage, reduction of ISC-containing proteins, and decreased respiratory chain activity (Rotig et al., 1997; Calabrese et al., 2005; Michael et al., 2006). The activities of the ISC-containing mitochondrial complexes I, II and III, as well as aconitase, were found to be highly reduced in endomyocardial biopsies of paients with Friedreich's Ataxia (Rotig et al., 1997; Bradley et al., 2000). Deficiency of ISC enzymes and mitochondrial iron accumulation were also observed in frataxin deficient mice (Puccio et al., 2001). These

mice also develop cardiomyopathy and sensory nerve defects. Thus, mitochondrial dysfunction appears to contribute to the pathophysiology of Friedreich's Ataxia.

1.9.3 Neuroferritinopathy

Mutations in the gene for L-ferritin result in a neurodegenerative disease called neuroferritinopathy. It has been characterized as an autosomal dominantly inherited basal ganglia disorder with late onset (Curtis et al., 2001). Patients with this disease exhibit motor symptoms such as choreoathetosis, spasticity, rigidity and dystonia. Interestingly, althouth ferritin is ubiquitiously expressed, only the CNS seems to be affected. Accumulation of iron and ferritin has been detected primarily in the globus pallidus, the forebrain and the cerebellum of patients (Curtis et al., 2001). Transgenic mice overexpressing a mutant form of L-ferritin exhibit a similar pathology with iron accumulation in the CNS and neurodegeneration (Vidal et al., 2008; Barbeito et al., 2009).

1.9.4 Pantothenate kinase-associated neurodegeneration

PKAN is a subtype of neurodegeneration with brain iron accumulation (NBIA) caused by a mutation in the pantothenate kinase 2 (PANK2) gene (Hayflick, 2003). It is a rare autosomal recessive disease characterized by extrapyramidal dysfunction such as generalized dystonia, rigidity and choreoathetosis, and a typical MRI pattern of iron accumulation in the globus pallidus ('eye of the tiger') (Swaiman, 2001). PANK2 is an enzyme involved in coenzyme A synthesis that phosphorylates panthothenate, which then condenses with cysteine. PANK2 deficiency thus results in the accumulation of cysteine (Perry et al., 1985), which in turn might cause iron accumulation due to the iron-chelating

properties of cysteine. However, another recently identified subtype of NBIA that is caused by a mutation in the calcium-independent group V phospholipase A2 shows an almost identical clinical phenotype but no disturbances in cysteine metabolism suggesting that also other mechanisms may underly the iron deposition (Schipper et al., 2011).

1.10 CNS diseases with secondary iron accumulation

Some diseases show iron accumulation in specific brain regions that are not due to genetic defects in iron homeostatic proteins. These iron-related disorders include neurodegenerative diseases such as amyotrophic lateral sclerosis (ALS), Alzheimer's disease, Parkinson's disease or multiple sclerosis (MS) (Carri et al., 2003; Levine and Chakrabarty, 2004; Zecca et al., 2004; Molina-Holgado et al., 2007). Iron also accumulates in the brain with normal aging, where it can promote oxidative damage, ultimately resulting in neurodegeneration (Zecca et al., 2004; Molina-Holgado et al., 2007). Our laboratory has been interested in ALS, a late-onset progressive neurodegenerative disease characterized by upper and lower motor neuron degeneration (Bento-Abreu et al., 2010). There are familial as well as sporadic forms of the disease. 20% of the familial ALS cases have been linked to a missense mutation in the superoxide dismutase 1 (SOD1) gene (Rosen, 1993). Iron accumulation and oxidative damage have been found in the CNS of patients with both, the sporadic and the familial forms of the disease (Kasarskis et al., 1995). Mouse models of the disease that have been generated by overexpressing mutant forms of SOD1, develop progressive weakness and muscle atrophy (Gurney, 1994). Our laboratory had shown recently that iron accumulates in neurons and glia in a mouse overexpressing mutant SOD1 (Jeong et al., 2009). Interestingly, this work showed that different molecular mechanisms might contribute to

the iron accumulation. Whereas in neurons the iron importer DMT1 was found to be upregulated, in glia cells, the increased expression of TfR1 might contribute to the observed iron deposition. The upregulation of TfR1 is likely to be mediated by an increase in IRP binding activity. Although IRP binding activity was increased, ferritin expression was not reduced, suggesting dysregulation of iron homeostasis in these mice. In addition, disruption of axonal transport which occurs in ALS mice was also shown to promote iron accumulation in the motor neurons in the ventral horn of the spinal cord (Jeong et al., 2009). This study also showed that administration of an iron chelator resulted in increased life span, increased survival of motor neurons and reduced iron accumulation (Jeong et al., 2009).

Iron has also been suggested to play a role in the pathogenesis of the demyelinating autoimmune disease MS and its animal model experimental autoimmune ancephalomyelitis (EAE) (Levine and Chakrabarty, 2004). Abnormal iron deposits have been found in CNS tissue of MS patients and EAE mice (LeVine, 1997; Bakshi et al., 2002; Levine and Chakrabarty, 2004). Moreover, oxidative stress seems to be an important factor in the pathogenesis of MS, which can be promoted by increased iron levels (Levine and Chakrabarty, 2004). Thus, dysregulation of cellular iron homeostasis has been associated with a variety of neurological diseases underlining the importance of understanding the mechanisms that control iron levels in CNS.

1.11 Iron deficiency and CNS pathology

As described above, iron accumulation is associated with neurodegenerative diseases. However, too low iron levels can also result in CNS pathology. Iron deficiency which is the most common nutrient deficiency in the world, has been linked to defects in brain

development including alterations in neurotransmitter synthesis, myelination and hippocampal structure (Georgieff, 2008). Iron-deficient children exhibit decreased cognitive abilities, poor school performance and behavior problems (Oski and Honig, 1978; Oski et al., 1983; Grantham-McGregor and Ani, 2001). Electrophysiological studies show increased latency of auditory brain stem potentials and visual evoked potentials in iron-deficient infants, which can be attributed to hypomyelination (Roncagliolo et al., 1998; Algarin et al., 2003; Lozoff et al., 2006). Other human studies report abnormal reflexes in premature iron-deficient infants suggesting either myelination or neurotransmitter deficits (Armony-Sivan et al., 2004). Most of what is known about the effects of iron deficiency in the CNS comes from animal studies. Studies in iron-deficient rodents show decreased levels of cytochrome c oxidase and reduced metabolites in different brain regions especially in the hippocampus emphasizing an important role of iron in brain energy metabolism (Dallman, 1986; de Deungria et al., 2000; Rao et al., 2003). It has been further demonstrated that iron is required for neurotransmitter synthesis as it is an essential cofactor for tyrosine hydroxylase (the enzyme required for dopamine and noradrenaline synthesis) and tryptophan hydroxylase (for serotonin synthesis) (Youdim and Green, 1978; Waldmeier et al., 1993; Beard and Connor, 2003). Iron is also required as a cofactor for HMG-CoA reductase and squalene epoxidase, two enzymes required for cholesterol synthesis, as well as for lipid saturase and desaturase enzymes involved in lipid synthesis (Lange and Que, 1998; Todorich et al., 2009). A decrease in stability and activity of these enzymes can therefore result in hypomyelination. Since oligodendrocytes are highly metabolically active during the phase of myelination, iron is also indirectly involved in myelination by maintaining a

high oxidative metabolism. Studies in rodents that were exposed to iron-deficiency during development show defects in oligodendrocyte precrusor cells (OPCs) proliferation and differentiation as well as reduced expression of myelin proteins (Morath and Mayer-Proschel, 2002; Beard et al., 2003; Ortiz et al., 2004). In addition, iron deficiency has been shown to affect the dendritic aborization in the rat hippocampus and the expression of proteins involved in synaptic plasticity, which has been suggested to underlie memory and learning deficits observed in iron-deficient infants (Jorgenson et al., 2003; Carlson et al., 2008). Expression of the microtubule-associated protein-2 (MAP-2) which is involved in dendritic scaffolding is reduced in the CA1 region of the hippocampus (Jorgenson et al., 2003) which could either result from lack of energy supply required for complex dendritic growth or from direct effects of iron-deficiency on MAP-2 expression, as has been found for various genes in different brain regions (Clardy et al., 2006; Carlson et al., 2008).

Besides the strong effects of iron deficiency on brain development, another pathological condition called restless leg syndrome (RLS) is associated with low brain iron levels. RLS is a sensorimotor disorder that is characterized by periodic leg movement, especially at rest and at night (Thorpy, 2005). Because symptoms can be alleviated by dopamine agonists, alterations in the dopaminergic systems have been suggested as a pathophysiological mechanism of the disease (Thorpy, 2005). The dopaminergic abnormalities have been confirmed in the substantia nigra and the putamen of RLS patients (Connor et al., 2009). In addition, low iron levels have been detected in the CSF and in different brain regions of RLS patients, in particular the substantia nigra (Allen et al., 2001; Mizuno et al., 2005). Insufficient brain iron is likely to contribute to

abnormalities in the dopaminergic system, because dopamine production requires iron as a cofactor for tyrosine hydroxylase, the rate-limiting enzyme of dopamine synthesis. A recent study further reported decreased CNS myelination in brains of RLS patients revealed by imaging analysis of the corpus callosum, anterior cingulum and precentral gyrus (Connor et al., 2011). In addition, similar to what has been demonstrated in iron-deficient animals (Yu et al., 1986; Ortiz et al., 2004), this study demonstrated reduced expression of myelin basic protein (MBP), proteolipid protein (PLP) and 3'5'-cyclic nucleotide phosphohydrolase (CNPase) in postmortem brain tissue of RLS patients (Connor et al., 2011). Thus, insufficient iron concentrations in brains of RLS patients appear to play an important role in the pathophysiology of the disease by affecting myelination as well as the dopaminergic system.

1.12 Remyelination in the CNS

Remyelination can occur spontaneously in response to myelin damage. New myelin sheaths are formed around demyelinated axons in order to prevent axonal damage and to restore saltatory conduction (Franklin and Ffrench-Constant, 2008). Remyelination in the CNS is carried out by OPCs that proliferate and differentiate into myelinating oligodendrocytes. Iron is required for the proliferation and differentiation of cells because it is an essential cofactor for the DNA ribonucleotide reductase and other enzymes involved in cell division (Hoffbrand et al., 1976; Cazzola et al., 1990). Iron also plays a role in proliferation and differentiation of OPCs *in vitro* and *in vivo* (Morath and Mayer-Proschel, 2001, 2002). Since iron is also directly involved in the synthesis of myelin (Connor and Menzies, 1996), it is likely to play an important role in the process of remyelination. Several other molecules have been implicated in proliferation and/or

differentiation of OPCs including growth factors such as platelet-derived growth factor-α (PDGF-α), fibroblast growth factor 2 (FGF-2), insulin-like growth factor-1 (IGF-1) and brain-derived neurotrophic factor (BDNF) (McKinnon et al., 1991; Mozell and McMorris, 1991). In addition, inflammation has been shown to influence remyelination. Animals lacking T cells or macrophages show impaired remyelination after chemically induced demyelination (Kotter et al., 2001; Bieber et al., 2003). The inflammatory cytokines, tumor necrosis factor α (TNF-α) and interleukin 1β (IL-1β) or the matrix metalloproteinase 9 also play a role in myelin repair (Arnett et al., 2001; Mason et al., 2001; Larsen et al., 2003). Several models of chemical-induced demyelination/ remyelination have been developed to study remyelination, including direct injection of lysophosphatdiylcholine (LPC) into the CNS, systemic delivery of cuprizone and ethidium bromide injections (Blakemore and Franklin, 2008). Our laboratory uses focal LPC injections into the dorsal white matter of the mouse spinal cord (Ousman and David, 2000, 2001; Ghasemlou et al., 2007) which induces demyelination within 2-3 days followed by clearance of myelin debris by macrophages (Hall, 1972; Ousman and David, 2000). Remyelination starts around day 7 after LPC-injection and is completed by day 28 (Jeffery and Blakemore, 1995). These models help identifying cellular and molecular events underlying successful remyelination, which is especially important for understanding demyelinating lesions in which remyelination fails, such as in MS.

1.13 Axonal mitochondria

Axonal mitochondria are important for providing ATP required for highly metabolic active processes along the axon. Mitochondria arise from the neuronal cell body and are

anterogradely and retrogradely transported along the axon at a rate of 0.7-1.5 μm/s (Forman et al., 1987). They are not evenly distributed along the length of the axon, but rather concentrate at sites of high energy demand such as synapses (Bogan and Cabot, 1991; Gotow et al., 1991), nodes of Ranvier (Fabricius et al., 1993), regions of demyelination (Mutsaers and Carroll, 1998) and active axonal growth cones (Morris and Hollenbeck, 1993; Ruthel and Hollenbeck, 2003). Neurological diseases in which either the axonal transport of mitochondria or mitochondrial function per se is impaired underline the importance of proper function of axonal mitochondria. Diseases in which axonal transport is disrupted affect mainly the peripheral nervous system due to the longer length of the axons. Several hereditary peripheral neuropathies such as Charcot-Marie-Tooth disease can result from mutations in genes involved in mitochondria dynamics (Baloh, 2008). However, hereditary paraparesis, which can involve the PNS and the CNS can also be caused by axonal transport defects (Baloh, 2008). Dysfunction of axonal mitochondria is also been associated with neurodegenerative diseases such as ALS or MS (Mahad et al., 2008). As discussed in section 1.7, iron is essential for proper mitochondrial function. However, not much is known about iron delivery to mitochondria within axons. Since axons, especially in the PNS are very long (up to 1 m), several sites of high metabolic demand are far away from the cell body. It is therefore conceivable that mitochondria not only receive iron in the region of the cell body but might also be able to acquire iron locally along the length of the axon. How this local supply might occur is part of the work done in chapter 4 of this thesis.

1.14 Axonal regeneration in the PNS

Following peripheral nerve injury, myelin breakdown and axonal fragmentation distal to the injury site (Wallerian degeneration) are initiated rapidly within hours. After the removal of axon and myelin debris by macrophages and Schwann cells which occurs over the period of the first 5 days, growth cone formation and axonal sprouting from the proximal stump begins. Schwann cells support and guide axonal regrowth in many ways. The Schwann cells in the denervated nerve align themselves longitudinal in cords called "bands of Büngner" and the axon growth promoting molecules found in the basal lamina they produce provide a tube through which newly regenerating axons regrow. In addition, Schwann cells also secrete a variety of neurotrophic factors which are recognized by axonal growth cones (Chen et al., 2007b; Vargas and Barres, 2007). Since axonal growth is a highly-energy demanding process, mitochondria are abundant in the axons and accumulate in growth cones, where their ATP-production is required for processes such as protein synthesis, axonal transport and cytoskeleton assembly (Bernstein and Bamburg, 2003). Mitochondrial function is highly dependent on iron, and thus, iron is likely to play a role in axonal regeneration. However, not much is known about the role of iron in axonal regeneration. One study reported upregulation of TF in Schwann cells after sciatic nerve crush injury (Salis et al., 2007). In addition,TfR1 levels have been shown to increase in Schwann cells and macrophages after sciatic nerve injury, accompanied by increased endoneural iron uptake as has been shown by intravenous injection of radiolabeled iron (Raivich et al., 1991). The increased iron uptake at the lesion site as well as distal to the lesion site paralleled the increased TfR1 expression. These findings suggest an increased iron demand of Schwann cells following peripheral nerve injury. The increased iron levels might either be required for Schwann cell

proliferation or Schwann cells may in turn deliver iron to regenerating axons. This is examined in the work presented in chapter 4.

1.15 Rationale

Iron plays an important role in establishing and maintaining proper functioning of the nervous system. However, iron in excess can lead to oxidative damage. Therefore, iron levels have to be tightly regulated. One way of controlling intracellular iron levels is iron export. Iron efflux might not only be important for maintaining intracellular iron homeostasis of that particular cell, but also for providing iron to neighboring cells. My thesis focuses on iron efflux mechanisms in the CNS and PNS and how iron efflux is involved in the transport of iron between cells of the nervous system.

1.16 Objectives and Hypotheses

1. Iron efflux from astrocytes has been shown to occur via Fpn facilitated by a GPI-anchored form of the ferroxidase Cp (Jeong and David, 2003). Since Cp is only expressed by astrocytes in the CNS, I sought to address in my thesis how other cells in the CNS export iron. Another ferroxidase that is thought to play a role in iron efflux from duodenal enterocytes is the Cp homologue Heph (Vulpe et al., 1999). ***I therefore hypothesized that Heph plays a role in iron efflux from CNS cells other than astrocytes.***

2. Iron efflux mechanisms in the CNS might be important for the delivery of iron from one cell type to another. Astrocytes which cover about 95% of the surface of blood vessels (capillaries) with their endfeet processes might play a key role in taking up iron

from the circulation and distributing it to other cells in the CNS. Data from our laboratory has suggested that astrocytes are involved in providing iron to neurons (Jeong and David, 2006). ***I therefore hypothesized that iron efflux from astrocytes also plays a role in delivering iron to oligodendrocytes, in particular in conditions that require high amounts of iron such as remyelination.***

3. Schwann cells which are in close association with axons in peripheral nerves may play a role in providing them with iron. Local iron supply by Schwann cells might be especially important for mitochondria within axons that are often far away from the cell body. Since axonal mitochondria are enriched in regions of high energy demand such as axonal growth cones, the acquisition of iron might be particularly important for axonal regeneration after peripheral nerve injury. ***I therefore hypothesized that iron efflux from Schwann cells is required for providing iron to mitochondria within peripheral axons for axonal regeneration.***

1.17 Specific Aims

1. To address the first hypothesis on the role of Heph in the CNS, I first examined the expression and role of Heph in CNS cells in culture. I also assessed the role of Heph in the CNS *in vivo* using the sex-lined anemia (sla) mouse, which carries a spontaneous, hypomorph mutation in the Heph gene. In addition, I investigated differences in iron efflux mechanisms utilized by grey and white matter oligodendrocytes. The results are presented in Chapter 2.

2. To address the second hypothesis, on the delivery of iron from astrocytes for remyelination in the CNS, I generated astrocyte-specific Fpn knockout mice using the inducible Cre-loxP system and assessed remyelination after LPC-induced demyelination. In addition, I carried out cell culture experiments on astrocytes and microglia to study possible effects of iron deficiency and iron overload on the expression of cytokines and growth factors in remyelination. These results are presented in chapter 3.

3. To address the third hypothesis on the delivery of iron from Schwann cells to peripheral axons for axon regeneration, I first assessed whether iron is required for axonal growth in an *in vitro* neurite outgrowth assay using dorsal root ganglia (DRG) neurons. To investigate whether iron efflux from Schwann cells is required for axonal regeneration, I performed sciatic nerve crush injuries in Cp knockout mice, in which iron efflux from Schwann cells would be impaired. The results of these experiments are presented in chapter 4.

1.18 References

Abbott NJ, Patabendige AA, Dolman DE, Yusof SR, Begley DJ (2010) Structure and function of the blood-brain barrier. Neurobiol Dis 37:13-25.

Abboud S, Haile DJ (2000) A novel mammalian iron-regulated protein involved in intracellular iron metabolism. J Biol Chem 275:19906-19912.

Algarin C, Peirano P, Garrido M, Pizarro F, Lozoff B (2003) Iron deficiency anemia in infancy: long-lasting effects on auditory and visual system functioning. Pediatr Res 53:217-223.

Allen RP, Barker PB, Wehrl F, Song HK, Earley CJ (2001) MRI measurement of brain iron in patients with restless legs syndrome. Neurology 56:263-265.

Anderson GJ, Darshan D, Wilkins SJ, Frazer DM (2007) Regulation of systemic iron homeostasis: how the body responds to changes in iron demand. Biometals 20:665-674.

Anderson GJ, Frazer DM, McKie AT, Wilkins SJ, Vulpe CD (2002) The expression and regulation of the iron transport molecules hephaestin and IREG1: implications for the control of iron export from the small intestine. Cell Biochem Biophys 36:137-146.

Andrews NC, Schmidt PJ (2007) Iron homeostasis. Annu Rev Physiol 69:69-85.

Armony-Sivan R, Eidelman AI, Lanir A, Sredni D, Yehuda S (2004) Iron status and neurobehavioral development of premature infants. J Perinatol 24:757-762.

Arnett HA, Mason J, Marino M, Suzuki K, Matsushima GK, Ting JP (2001) TNF alpha promotes proliferation of oligodendrocyte progenitors and remyelination. Nat Neurosci 4:1116-1122.

Arosio P, Levi S (2010) Cytosolic and mitochondrial ferritins in the regulation of cellular iron homeostasis and oxidative damage. Biochim Biophys Acta 1800:783-792.

Arosio P, Yokota M, Drysdale JW (1976) Structural and immunological relationships of isoferritins in normal and malignant cells. Cancer Res 36:1735-1739.

Bakshi R, Benedict RH, Bermel RA, Caruthers SD, Puli SR, Tjoa CW, Fabiano AJ, Jacobs L (2002) T2 hypointensity in the deep gray matter of patients with multiple sclerosis: a quantitative magnetic resonance imaging study. Arch Neurol 59:62-68.

Baloh RH (2008) Mitochondrial dynamics and peripheral neuropathy. Neuroscientist 14:12-18.

Bannerman RM, Cooper RG (1966) Sex-linked anemia: a hypochromic anemia of mice. Science 151:581-582.

Barbeito AG, Garringer HJ, Baraibar MA, Gao X, Arredondo M, Nunez MT, Smith MA, Ghetti B, Vidal R (2009) Abnormal iron metabolism and oxidative stress in mice expressing a mutant form of the ferritin light polypeptide gene. J Neurochem 109:1067-1078.

Beard JL, Connor JR (2003) Iron status and neural functioning. Annu Rev Nutr 23:41-58.

Beard JL, Connor JR, Jones BC (1993) Iron in the brain. Nutr Rev 51:157-170.

Beard JL, Wiesinger JA, Connor JR (2003) Pre- and postweaning iron deficiency alters myelination in Sprague-Dawley rats. Dev Neurosci 25:308-315.

Benkovic SA, Connor JR (1993) Ferritin, transferrin, and iron in selected regions of the adult and aged rat brain. J Comp Neurol 338:97-113.

Bento-Abreu A, Van Damme P, Van Den Bosch L, Robberecht W (2010) The neurobiology of amyotrophic lateral sclerosis. Eur J Neurosci 31:2247-2265.

Bento I, Peixoto C, Zaitsev VN, Lindley PF (2007) Ceruloplasmin revisited: structural and functional roles of various metal cation-binding sites. Acta Crystallogr D Biol Crystallogr 63:240-248.

Bernstein BW, Bamburg JR (2003) Actin-ATP hydrolysis is a major energy drain for neurons. J Neurosci 23:1-6.

Bieber AJ, Kerr S, Rodriguez M (2003) Efficient central nervous system remyelination requires T cells. Ann Neurol 53:680-684.

Bielli P, Calabrese L (2002) Structure to function relationships in ceruloplasmin: a 'moonlighting' protein. Cell Mol Life Sci 59:1413-1427.

Blakemore WF, Franklin RJ (2008) Remyelination in experimental models of toxin-induced demyelination. Curr Top Microbiol Immunol 318:193-212.

Bleijenberg BG, Van Eijk HG, Leijnse B (1971) The determination of non-heme iron and transferrin in cerebrospinal fluid. Clin Chim Acta 31:277-281.

Bloch B, Popovici T, Levin MJ, Tuil D, Kahn A (1985) Transferrin gene expression visualized in oligodendrocytes of the rat brain by using in situ hybridization and immunohistochemistry. Proc Natl Acad Sci U S A 82:6706-6710.

Bogan N, Cabot JB (1991) Light and electron microscopic analyses of intraspinal axon collaterals of sympathetic preganglionic neurons. Brain Res 541:241-251.

Bradbury MW (1997) Transport of iron in the blood-brain-cerebrospinal fluid system. J Neurochem 69:443-454.

Bradley JL, Blake JC, Chamberlain S, Thomas PK, Cooper JM, Schapira AH (2000) Clinical, biochemical and molecular genetic correlations in Friedreich's ataxia. Hum Mol Genet 9:275-282.

Burdo JR, Menzies SL, Simpson IA, Garrick LM, Garrick MD, Dolan KG, Haile DJ, Beard JL, Connor JR (2001) Distribution of divalent metal transporter 1 and metal transport protein 1 in the normal and Belgrade rat. J Neurosci Res 66:1198-1207.

Cai C, Ching A, Lagace C, Linsenmayer T (2008) Nuclear ferritin-mediated protection of corneal epithelial cells from oxidative damage to DNA. Dev Dyn 237:2676-2683.

Cai CX, Birk DE, Linsenmayer TF (1997) Ferritin is a developmentally regulated nuclear protein of avian corneal epithelial cells. J Biol Chem 272:12831-12839.

Cai CX, Birk DE, Linsenmayer TF (1998) Nuclear ferritin protects DNA from UV damage in corneal epithelial cells. Mol Biol Cell 9:1037-1051.

Calabrese V, Lodi R, Tonon C, D'Agata V, Sapienza M, Scapagnini G, Mangiameli A, Pennisi G, Stella AM, Butterfield DA (2005) Oxidative stress, mitochondrial dysfunction and cellular stress response in Friedreich's ataxia. J Neurol Sci 233:145-162.

Campuzano V, Montermini L, Lutz Y, Cova L, Hindelang C, Jiralerspong S, Trottier Y, Kish SJ, Faucheux B, Trouillas P, Authier FJ, Durr A, Mandel JL, Vescovi A, Pandolfo M, Koenig M (1997) Frataxin is reduced in Friedreich ataxia patients and is associated with mitochondrial membranes. Hum Mol Genet 6:1771-1780.

Campuzano V, Montermini L, Molto MD, Pianese L, Cossee M, Cavalcanti F, Monros E, Rodius F, Duclos F, Monticelli A, Zara F, Canizares J, Koutnikova H, Bidichandani SI, Gellera C, Brice A, Trouillas P, De Michele G, Filla A, De Frutos R, Palau F, Patel PI, Di Donato S, Mandel JL, Cocozza S, Koenig M,

Pandolfo M (1996) Friedreich's ataxia: autosomal recessive disease caused by an intronic GAA triplet repeat expansion. Science 271:1423-1427.

Carlson ES, Magid R, Petryk A, Georgieff MK (2008) Iron deficiency alters expression of genes implicated in Alzheimer disease pathogenesis. Brain Res 1237:75-83.

Carri MT, Ferri A, Cozzolino M, Calabrese L, Rotilio G (2003) Neurodegeneration in amyotrophic lateral sclerosis: the role of oxidative stress and altered homeostasis of metals. Brain Res Bull 61:365-374.

Cazzola M, Bergamaschi G, Dezza L, Arosio P (1990) Manipulations of cellular iron metabolism for modulating normal and malignant cell proliferation: achievements and prospects. Blood 75:1903-1919.

Cazzola M, Invernizzi R, Bergamaschi G, Levi S, Corsi B, Travaglino E, Rolandi V, Biasiotto G, Drysdale J, Arosio P (2003) Mitochondrial ferritin expression in erythroid cells from patients with sideroblastic anemia. Blood 101:1996-2000.

Cheah JH, Kim SF, Hester LD, Clancy KW, Patterson SE, 3rd, Papadopoulos V, Snyder SH (2006) NMDA receptor-nitric oxide transmission mediates neuronal iron homeostasis via the GTPase Dexras1. Neuron 51:431-440.

Chen H, Su T, Attieh ZK, Fox TC, McKie AT, Anderson GJ, Vulpe CD (2003) Systemic regulation of Hephaestin and Ireg1 revealed in studies of genetic and nutritional iron deficiency. Blood 102:1893-1899.

Chen H, Attieh ZK, Su T, Syed BA, Gao H, Alaeddine RM, Fox TC, Usta J, Naylor CE, Evans RW, McKie AT, Anderson GJ, Vulpe CD (2004) Hephaestin is a ferroxidase that maintains partial activity in sex-linked anemia mice. Blood 103:3933-3939.

Chen H, Attieh ZK, Syed BA, Kuo YM, Stevens V, Fuqua BK, Andersen HS, Naylor CE, Evans RW, Gambling L, Danzeisen R, Bacouri-Haidar M, Usta J, Vulpe CD, McArdle HJ (2010) Identification of zyklopen, a new member of the vertebrate multicopper ferroxidase family, and characterization in rodents and human cells. J Nutr 140:1728-1735.

Chen TT, Li L, Chung DH, Allen CD, Torti SV, Torti FM, Cyster JG, Chen CY, Brodsky FM, Niemi EC, Nakamura MC, Seaman WE, Daws MR (2005) TIM-2 is

expressed on B cells and in liver and kidney and is a receptor for H-ferritin endocytosis. J Exp Med 202:955-965.

Chen ZL, Yu WM, Strickland S (2007) Peripheral regeneration. Annu Rev Neurosci 30:209-233.

Clardy SL, Wang X, Zhao W, Liu W, Chase GA, Beard JL, True Felt B, Connor JR (2006) Acute and chronic effects of developmental iron deficiency on mRNA expression patterns in the brain. J Neural Transm Suppl:173-196.

Cohen LA, Gutierrez L, Weiss A, Leichtmann-Bardoogo Y, Zhang DL, Crooks DR, Sougrat R, Morgenstern A, Galy B, Hentze MW, Lazaro FJ, Rouault TA, Meyron-Holtz EG (2010) Serum ferritin is derived primarily from macrophages through a nonclassical secretory pathway. Blood 116:1574-1584.

Connor JR, Fine RE (1986) The distribution of transferrin immunoreactivity in the rat central nervous system. Brain Res 368:319-328.

Connor JR, Menzies SL (1996) Relationship of iron to oligodendrocytes and myelination. Glia 17:83-93.

Connor JR, Boeshore KL, Benkovic SA, Menzies SL (1994) Isoforms of ferritin have a specific cellular distribution in the brain. J Neurosci Res 37:461-465.

Connor JR, Wang XS, Allen RP, Beard JL, Wiesinger JA, Felt BT, Earley CJ (2009) Altered dopaminergic profile in the putamen and substantia nigra in restless leg syndrome. Brain 132:2403-2412.

Connor JR, Ponnuru P, Lee BY, Podskalny GD, Alam S, Allen RP, Earley CJ, Yang QX (2011) Postmortem and imaging based analyses reveal CNS decreased myelination in restless legs syndrome. Sleep Med.

Curtis AR, Fey C, Morris CM, Bindoff LA, Ince PG, Chinnery PF, Coulthard A, Jackson MJ, Jackson AP, McHale DP, Hay D, Barker WA, Markham AF, Bates D, Curtis A, Burn J (2001) Mutation in the gene encoding ferritin light polypeptide causes dominant adult-onset basal ganglia disease. Nat Genet 28:350-354.

Dallman PR (1986) Biochemical basis for the manifestations of iron deficiency. Annu Rev Nutr 6:13-40.

Danzeisen R, Ponnambalam S, Lea RG, Page K, Gambling L, McArdle HJ (2000) The effect of ceruloplasmin on iron release from placental (BeWo) cells; evidence for an endogenous Cu oxidase. Placenta 21:805-812.

Danzeisen R, Fosset C, Chariana Z, Page K, David S, McArdle HJ (2002) Placental ceruloplasmin homolog is regulated by iron and copper and is implicated in iron metabolism. Am J Physiol Cell Physiol 282:C472-478.

Dautry-Varsat A (1986) Receptor-mediated endocytosis: the intracellular journey of transferrin and its receptor. Biochimie 68:375-381.

Dautry-Varsat A, Ciechanover A, Lodish HF (1983) pH and the recycling of transferrin during receptor-mediated endocytosis. Proc Natl Acad Sci U S A 80:2258-2262.

Davies P, Moualla D, Brown DR (2011) Alpha-synuclein is a cellular ferrireductase. PLoS One 6:e15814.

de Arriba Zerpa GA, Saleh MC, Fernandez PM, Guillou F, Espinosa de los Monteros A, de Vellis J, Zakin MM, Baron B (2000) Alternative splicing prevents transferrin secretion during differentiation of a human oligodendrocyte cell line. J Neurosci Res 61:388-395.

de Deungria M, Rao R, Wobken JD, Luciana M, Nelson CA, Georgieff MK (2000) Perinatal iron deficiency decreases cytochrome c oxidase (CytOx) activity in selected regions of neonatal rat brain. Pediatr Res 48:169-176.

De Domenico I, Ward DM, Musci G, Kaplan J (2006a) Iron overload due to mutations in ferroportin. Haematologica 91:92-95.

De Domenico I, Vaughn MB, Paradkar PN, Lo E, Ward DM, Kaplan J (2011) Decoupling ferritin synthesis from free cytosolic iron results in ferritin secretion. Cell Metab 13:57-67.

De Domenico I, Vaughn MB, Li L, Bagley D, Musci G, Ward DM, Kaplan J (2006b) Ferroportin-mediated mobilization of ferritin iron precedes ferritin degradation by the proteasome. Embo J 25:5396-5404.

De Domenico I, Ward DM, di Patti MC, Jeong SY, David S, Musci G, Kaplan J (2007a) Ferroxidase activity is required for the stability of cell surface ferroportin in cells expressing GPI-ceruloplasmin. Embo J 26:2823-2831.

De Domenico I, Ward DM, Langelier C, Vaughn MB, Nemeth E, Sundquist WI, Ganz T, Musci G, Kaplan J (2007b) The molecular mechanism of hepcidin-mediated ferroportin down-regulation. Mol Biol Cell 18:2569-2578.

Donovan A, Lima CA, Pinkus JL, Pinkus GS, Zon LI, Robine S, Andrews NC (2005) The iron exporter ferroportin/Slc40a1 is essential for iron homeostasis. Cell Metab 1:191-200.

Donovan A, Brownlie A, Zhou Y, Shepard J, Pratt SJ, Moynihan J, Paw BH, Drejer A, Barut B, Zapata A, Law TC, Brugnara C, Lux SE, Pinkus GS, Pinkus JL, Kingsley PD, Palis J, Fleming MD, Andrews NC, Zon LI (2000) Positional cloning of zebrafish ferroportin1 identifies a conserved vertebrate iron exporter. Nature 403:776-781.

Du Y, Fischer TZ, Clinton-Luke P, Lercher LD, Dreyfus CF (2006) Distinct effects of p75 in mediating actions of neurotrophins on basal forebrain oligodendrocytes. Mol Cell Neurosci 31:366-375.

Du Y, Fischer TZ, Lee LN, Lercher LD, Dreyfus CF (2003) Regionally specific effects of BDNF on oligodendrocytes. Dev Neurosci 25:116-126.

Duce JA, Tsatsanis A, Cater MA, James SA, Robb E, Wikhe K, Leong SL, Perez K, Johanssen T, Greenough MA, Cho HH, Galatis D, Moir RD, Masters CL, McLean C, Tanzi RE, Cappai R, Barnham KJ, Ciccotosto GD, Rogers JT, Bush AI (2010) Iron-export ferroxidase activity of beta-amyloid precursor protein is inhibited by zinc in Alzheimer's disease. Cell 142:857-867.

Durr A, Cossee M, Agid Y, Campuzano V, Mignard C, Penet C, Mandel JL, Brice A, Koenig M (1996) Clinical and genetic abnormalities in patients with Friedreich's ataxia. N Engl J Med 335:1169-1175.

Eisenstein RS (2000) Iron regulatory proteins and the molecular control of mammalian iron metabolism. Annu Rev Nutr 20:627-662.

Fabricius C, Berthold CH, Rydmark M (1993) Axoplasmic organelles at nodes of Ranvier. II. Occurrence and distribution in large myelinated spinal cord axons of the adult cat. J Neurocytol 22:941-954.

Fisher J, Devraj K, Ingram J, Slagle-Webb B, Madhankumar AB, Liu X, Klinger M, Simpson IA, Connor JR (2007) Ferritin: a novel mechanism for delivery of iron to the brain and other organs. Am J Physiol Cell Physiol 293:C641-649.

Flanagan JM, Truksa J, Peng H, Lee P, Beutler E (2007) In vivo imaging of hepcidin promoter stimulation by iron and inflammation. Blood Cells Mol Dis 38:253-257.

Fleming MD, Romano MA, Su MA, Garrick LM, Garrick MD, Andrews NC (1998) Nramp2 is mutated in the anemic Belgrade (b) rat: evidence of a role for Nramp2 in endosomal iron transport. Proc Natl Acad Sci U S A 95:1148-1153.

Fleming MD, Trenor CC, 3rd, Su MA, Foernzler D, Beier DR, Dietrich WF, Andrews NC (1997) Microcytic anaemia mice have a mutation in Nramp2, a candidate iron transporter gene. Nat Genet 16:383-386.

Fleming RE (2007) Hepcidin activation during inflammation: make it STAT. Gastroenterology 132:447-449.

Forman DS, Lynch KJ, Smith RS (1987) Organelle dynamics in lobster axons: anterograde, retrograde and stationary mitochondria. Brain Res 412:96-106.

Fraenkel PG, Traver D, Donovan A, Zahrieh D, Zon LI (2005) Ferroportin1 is required for normal iron cycling in zebrafish. J Clin Invest 115:1532-1541.

Franklin RJ, Ffrench-Constant C (2008) Remyelination in the CNS: from biology to therapy. Nat Rev Neurosci 9:839-855.

Frazer DM, Vulpe CD, McKie AT, Wilkins SJ, Trinder D, Cleghorn GJ, Anderson GJ (2001) Cloning and gastrointestinal expression of rat hephaestin: relationship to other iron transport proteins. Am J Physiol Gastrointest Liver Physiol 281:G931-939.

Fruttiger M, Karlsson L, Hall AC, Abramsson A, Calver AR, Bostrom H, Willetts K, Bertold CH, Heath JK, Betsholtz C, Richardson WD (1999) Defective oligodendrocyte development and severe hypomyelination in PDGF-A knockout mice. Development 126:457-467.

Galy B, Ferring D, Hentze MW (2005) Generation of conditional alleles of the murine Iron Regulatory Protein (IRP)-1 and -2 genes. Genesis 43:181-188.

Galy B, Ferring-Appel D, Kaden S, Grone HJ, Hentze MW (2008) Iron regulatory proteins are essential for intestinal function and control key iron absorption molecules in the duodenum. Cell Metab 7:79-85.

Gambling L, Lang C, McArdle HJ (2011) Fetal regulation of iron transport during pregnancy. Am J Clin Nutr.

Ganz T (2003) Hepcidin, a key regulator of iron metabolism and mediator of anemia of inflammation. Blood 102:783-788.

Georgieff MK (2008) The role of iron in neurodevelopment: fetal iron deficiency and the developing hippocampus. Biochem Soc Trans 36:1267-1271.

Ghasemlou N, Jeong SY, Lacroix S, David S (2007) T cells contribute to lysophosphatidylcholine-induced macrophage activation and demyelination in the CNS. Glia 55:294-302.

Gille G, Reichmann H (2011) Iron-dependent functions of mitochondria--relation to neurodegeneration. J Neural Transm 118:349-359.

Giometto B, Bozza F, Argentiero V, Gallo P, Pagni S, Piccinno MG, Tavolato B (1990) Transferrin receptors in rat central nervous system. An immunocytochemical study. J Neurol Sci 98:81-90.

Gotow T, Miyaguchi K, Hashimoto PH (1991) Cytoplasmic architecture of the axon terminal: filamentous strands specifically associated with synaptic vesicles. Neuroscience 40:587-598.

Grantham-McGregor S, Ani C (2001) A review of studies on the effect of iron deficiency on cognitive development in children. J Nutr 131:649S-666S; discussion 666S-668S.

Gunshin H, Mackenzie B, Berger UV, Gunshin Y, Romero MF, Boron WF, Nussberger S, Gollan JL, Hediger MA (1997) Cloning and characterization of a mammalian proton-coupled metal-ion transporter. Nature 388:482-488.

Gunshin H, Starr CN, Direnzo C, Fleming MD, Jin J, Greer EL, Sellers VM, Galica SM, Andrews NC (2005) Cybrd1 (duodenal cytochrome b) is not necessary for dietary iron absorption in mice. Blood 106:2879-2883.

Gunshin H, Allerson CR, Polycarpou-Schwarz M, Rofts A, Rogers JT, Kishi F, Hentze MW, Rouault TA, Andrews NC, Hediger MA (2001) Iron-dependent regulation of the divalent metal ion transporter. FEBS Lett 509:309-316.

Guo B, Phillips JD, Yu Y, Leibold EA (1995) Iron regulates the intracellular degradation of iron regulatory protein 2 by the proteasome. J Biol Chem 270:21645-21651.

Gurney ME (1994) Transgenic-mouse model of amyotrophic lateral sclerosis. N Engl J Med 331:1721-1722.

Gutteridge JM (1994) Hydroxyl radicals, iron, oxidative stress, and neurodegeneration. Ann N Y Acad Sci 738:201-213.

Hadziahmetovic M, Dentchev T, Song Y, Haddad N, He X, Hahn P, Pratico D, Wen R, Harris ZL, Lambris JD, Beard J, Dunaief JL (2008) Ceruloplasmin/hephaestin knockout mice model morphologic and molecular features of AMD. Invest Ophthalmol Vis Sci 49:2728-2736.

Hahn P, Dentchev T, Qian Y, Rouault T, Harris ZL, Dunaief JL (2004a) Immunolocalization and regulation of iron handling proteins ferritin and ferroportin in the retina. Mol Vis 10:598-607.

Hahn P, Qian Y, Dentchev T, Chen L, Beard J, Harris ZL, Dunaief JL (2004b) Disruption of ceruloplasmin and hephaestin in mice causes retinal iron overload and retinal degeneration with features of age-related macular degeneration. Proc Natl Acad Sci U S A 101:13850-13855.

Hall SM (1972) The effect of injections of lysophosphatidyl choline into white matter of the adult mouse spinal cord. J Cell Sci 10:535-546.

Halliwell B (2006) Oxidative stress and neurodegeneration: where are we now? J Neurochem 97:1634-1658.

Halliwell B, Gutteridge JM (1990) Role of free radicals and catalytic metal ions in human disease: an overview. Methods Enzymol 186:1-85.

Han O, Wessling-Resnick M (2002) Copper repletion enhances apical iron uptake and transepithelial iron transport by Caco-2 cells. Am J Physiol Gastrointest Liver Physiol 282:G527-533.

Han O, Kim EY (2007) Colocalization of ferroportin-1 with hephaestin on the basolateral membrane of human intestinal absorptive cells. J Cell Biochem 101:1000-1010.

Harris ZL, Durley AP, Man TK, Gitlin JD (1999) Targeted gene disruption reveals an essential role for ceruloplasmin in cellular iron efflux. Proc Natl Acad Sci U S A 96:10812-10817.

Harris ZL, Takahashi Y, Miyajima H, Serizawa M, MacGillivray RT, Gitlin JD (1995) Aceruloplasminemia: molecular characterization of this disorder of iron metabolism. Proc Natl Acad Sci U S A 92:2539-2543.

Harrison PM, Arosio P (1996) The ferritins: molecular properties, iron storage function and cellular regulation. Biochim Biophys Acta 1275:161-203.

Harrison PM, Fischbach FA, Hoy TG, Haggis GH (1967) Ferric oxyhydroxide core of ferritin. Nature 216:1188-1190.

Hayflick SJ (2003) Unraveling the Hallervorden-Spatz syndrome: pantothenate kinase-associated neurodegeneration is the name. Curr Opin Pediatr 15:572-577.

Hetet G, Devaux I, Soufir N, Grandchamp B, Beaumont C (2003) Molecular analyses of patients with hyperferritinemia and normal serum iron values reveal both L ferritin IRE and 3 new ferroportin (slc11A3) mutations. Blood 102:1904-1910.

Hoffbrand AV, Ganeshaguru K, Hooton JW, Tattersall MH (1976) Effect of iron deficiency and desferrioxamine on DNA synthesis in human cells. Br J Haematol 33:517-526.

Holmberg CG, Laurell CB (1948) Histaminolytic activity of a copper protein in serum. Nature 161:236.

Hubert N, Hentze MW (2002) Previously uncharacterized isoforms of divalent metal transporter (DMT)-1: implications for regulation and cellular function. Proc Natl Acad Sci U S A 99:12345-12350.

Jeffery ND, Blakemore WF (1995) Remyelination of mouse spinal cord axons demyelinated by local injection of lysolecithin. J Neurocytol 24:775-781.

Jeong SY, David S (2003) Glycosylphosphatidylinositol-anchored ceruloplasmin is required for iron efflux from cells in the central nervous system. J Biol Chem 278:27144-27148.

Jeong SY, David S (2006) Age-related changes in iron homeostasis and cell death in the cerebellum of ceruloplasmin-deficient mice. J Neurosci 26:9810-9819.

Jeong SY, Rathore KI, Schulz K, Ponka P, Arosio P, David S (2009) Dysregulation of iron homeostasis in the CNS contributes to disease progression in a mouse model of amyotrophic lateral sclerosis. J Neurosci 29:610-619.

Jorgenson LA, Wobken JD, Georgieff MK (2003) Perinatal iron deficiency alters apical dendritic growth in hippocampal CA1 pyramidal neurons. Dev Neurosci 25:412-420.

Kaplan J, Ward DM, De Domenico I (2011) The molecular basis of iron overload disorders and iron-linked anemias. Int J Hematol 93:14-20.

Kasarskis EJ, Tandon L, Lovell MA, Ehmann WD (1995) Aluminum, calcium, and iron in the spinal cord of patients with sporadic amyotrophic lateral sclerosis using laser microprobe mass spectroscopy: a preliminary study. J Neurol Sci 130:203-208.

Kawabata H, Yang R, Hirama T, Vuong PT, Kawano S, Gombart AF, Koeffler HP (1999) Molecular cloning of transferrin receptor 2. A new member of the transferrin receptor-like family. J Biol Chem 274:20826-20832.

Keel SB, Doty RT, Yang Z, Quigley JG, Chen J, Knoblaugh S, Kingsley PD, De Domenico I, Vaughn MB, Kaplan J, Palis J, Abkowitz JL (2008) A heme export protein is required for red blood cell differentiation and iron homeostasis. Science 319:825-828.

Kidane TZ, Sauble E, Linder MC (2006) Release of iron from ferritin requires lysosomal activity. Am J Physiol Cell Physiol 291:C445-455.

Klomp LW, Gitlin JD (1996) Expression of the ceruloplasmin gene in the human retina and brain: implications for a pathogenic model in aceruloplasminemia. Hum Mol Genet 5:1989-1996.

Klomp LW, Farhangrazi ZS, Dugan LL, Gitlin JD (1996) Ceruloplasmin gene expression in the murine central nervous system. J Clin Invest 98:207-215.

Koeller DM, Horowitz JA, Casey JL, Klausner RD, Harford JB (1991) Translation and the stability of mRNAs encoding the transferrin receptor and c-fos. Proc Natl Acad Sci U S A 88:7778-7782.

Koeppen AH, Dentinger MP (1988) Brain hemosiderin and superficial siderosis of the central nervous system. J Neuropathol Exp Neurol 47:249-270.

Kohno S, Miyajima H, Takahashi Y, Suzuki H, Hishida A (2000) Defective electron transfer in complexes I and IV in patients with aceruloplasminemia. J Neurol Sci 182:57-60.

Kotter MR, Setzu A, Sim FJ, Van Rooijen N, Franklin RJ (2001) Macrophage depletion impairs oligodendrocyte remyelination following lysolecithin-induced demyelination. Glia 35:204-212.

Krause A, Neitz S, Magert HJ, Schulz A, Forssmann WG, Schulz-Knappe P, Adermann K (2000) LEAP-1, a novel highly disulfide-bonded human peptide, exhibits antimicrobial activity. FEBS Lett 480:147-150.

Krishnamurthy P, Schuetz JD (2006) Role of ABCG2/BCRP in biology and medicine. Annu Rev Pharmacol Toxicol 46:381-410.

Krishnamurthy P, Xie T, Schuetz JD (2007) The role of transporters in cellular heme and porphyrin homeostasis. Pharmacol Ther 114:345-358.

Lange SJ, Que L, Jr. (1998) Oxygen activating nonheme iron enzymes. Curr Opin Chem Biol 2:159-172.

Larsen PH, Wells JE, Stallcup WB, Opdenakker G, Yong VW (2003) Matrix metalloproteinase-9 facilitates remyelination in part by processing the inhibitory NG2 proteoglycan. J Neurosci 23:11127-11135.

Laufberger V (1937) Sur la cristallization de la ferritine. Bull Soc Chim biol, Paris, 19:1575-1582.

LaVaute T, Smith S, Cooperman S, Iwai K, Land W, Meyron-Holtz E, Drake SK, Miller G, Abu-Asab M, Tsokos M, Switzer R, 3rd, Grinberg A, Love P, Tresser N, Rouault TA (2001) Targeted deletion of the gene encoding iron regulatory protein-2 causes misregulation of iron metabolism and neurodegenerative disease in mice. Nat Genet 27:209-214.

Lee PL, Beutler E (2009) Regulation of hepcidin and iron-overload disease. Annu Rev Pathol 4:489-515.

Levi S, Arosio P (2004) Mitochondrial ferritin. Int J Biochem Cell Biol 36:1887-1889.

Levi S, Rovida E (2009) The role of iron in mitochondrial function. Biochim Biophys Acta 1790:629-636.

Levi S, Luzzago A, Cesareni G, Cozzi A, Franceschinelli F, Albertini A, Arosio P (1988) Mechanism of ferritin iron uptake: activity of the H-chain and deletion mapping of the ferro-oxidase site. A study of iron uptake and ferro-oxidase activity of human liver, recombinant H-chain ferritins, and of two H-chain deletion mutants. J Biol Chem 263:18086-18092.

Levi S, Corsi B, Bosisio M, Invernizzi R, Volz A, Sanford D, Arosio P, Drysdale J (2001) A human mitochondrial ferritin encoded by an intronless gene. J Biol Chem 276:24437-24440.

Levi S, Santambrogio P, Cozzi A, Rovida E, Corsi B, Tamborini E, Spada S, Albertini A, Arosio P (1994) The role of the L-chain in ferritin iron incorporation. Studies of homo and heteropolymers. J Mol Biol 238:649-654.

LeVine SM (1997) Iron deposits in multiple sclerosis and Alzheimer's disease brains. Brain Res 760:298-303.

LeVine SM, Macklin WB (1990) Iron-enriched oligodendrocytes: a reexamination of their spatial distribution. J Neurosci Res 26:508-512.

Levine SM, Chakrabarty A (2004) The role of iron in the pathogenesis of experimental allergic encephalomyelitis and multiple sclerosis. Ann N Y Acad Sci 1012:252-266.

Li JY, Paragas N, Ned RM, Qiu A, Viltard M, Leete T, Drexler IR, Chen X, Sanna-Cherchi S, Mohammed F, Williams D, Lin CS, Schmidt-Ott KM, Andrews NC, Barasch J (2009) Scara5 is a ferritin receptor mediating non-transferrin iron delivery. Dev Cell 16:35-46.

Linder MC, Schaffer KJ, Hazegh-Azam M, Zhou CY, Tran TN, Nagel GM (1996) Serum ferritin: does it differ from tissue ferritin? J Gastroenterol Hepatol 11:1033-1036.

Liuzzi JP, Aydemir F, Nam H, Knutson MD, Cousins RJ (2006) Zip14 (Slc39a14) mediates non-transferrin-bound iron uptake into cells. Proc Natl Acad Sci U S A 103:13612-13617.

Lou DQ, Nicolas G, Lesbordes JC, Viatte L, Grimber G, Szajnert MF, Kahn A, Vaulont S (2004) Functional differences between hepcidin 1 and 2 in transgenic mice. Blood 103:2816-2821.

Lozoff B, Jimenez E, Smith JB (2006) Double burden of iron deficiency in infancy and low socioeconomic status: a longitudinal analysis of cognitive test scores to age 19 years. Arch Pediatr Adolesc Med 160:1108-1113.

Lymboussaki A, Pignatti E, Montosi G, Garuti C, Haile DJ, Pietrangelo A (2003) The role of the iron responsive element in the control of ferroportin1/IREG1/MTP1 gene expression. J Hepatol 39:710-715.

Magrane J, Manfredi G (2009) Mitochondrial function, morphology, and axonal transport in amyotrophic lateral sclerosis. Antioxid Redox Signal 11:1615-1626.

Mahad D, Lassmann H, Turnbull D (2008) Review: Mitochondria and disease progression in multiple sclerosis. Neuropathol Appl Neurobiol 34:577-589.

Marro S, Chiabrando D, Messana E, Stolte J, Turco E, Tolosano E, Muckenthaler MU (2010) Heme controls ferroportin1 (FPN1) transcription involving Bach1, Nrf2 and a MARE/ARE sequence motif at position -7007 of the FPN1 promoter. Haematologica 95:1261-1268.

Mason JL, Suzuki K, Chaplin DD, Matsushima GK (2001) Interleukin-1beta promotes repair of the CNS. J Neurosci 21:7046-7052.

McKie AT (2005) A ferrireductase fills the gap in the transferrin cycle. Nat Genet 37:1159-1160.

McKie AT (2008) The role of Dcytb in iron metabolism: an update. Biochem Soc Trans 36:1239-1241.

McKie AT, Marciani P, Rolfs A, Brennan K, Wehr K, Barrow D, Miret S, Bomford A, Peters TJ, Farzaneh F, Hediger MA, Hentze MW, Simpson RJ (2000) A novel duodenal iron-regulated transporter, IREG1, implicated in the basolateral transfer of iron to the circulation. Mol Cell 5:299-309.

McKie AT, Barrow D, Latunde-Dada GO, Rolfs A, Sager G, Mudaly E, Mudaly M, Richardson C, Barlow D, Bomford A, Peters TJ, Raja KB, Shirali S, Hediger MA, Farzaneh F, Simpson RJ (2001) An iron-regulated ferric reductase associated with the absorption of dietary iron. Science 291:1755-1759.

McKinnon RD, Matsui T, Aranda M, Dubois-Dalcq M (1991) A role for fibroblast growth factor in oligodendrocyte development. Ann N Y Acad Sci 638:378-386.

Meyer LA, Durley AP, Prohaska JR, Harris ZL (2001) Copper transport and metabolism are normal in aceruloplasminemic mice. J Biol Chem 276:36857-36861.

Meynard D, Kautz L, Darnaud V, Canonne-Hergaux F, Coppin H, Roth MP (2009) Lack of the bone morphogenetic protein BMP6 induces massive iron overload. Nat Genet 41:478-481.

Meyron-Holtz EG, Ghosh MC, Rouault TA (2004a) Mammalian tissue oxygen levels modulate iron-regulatory protein activities in vivo. Science 306:2087-2090.

Meyron-Holtz EG, Ghosh MC, Iwai K, LaVaute T, Brazzolotto X, Berger UV, Land W, Ollivierre-Wilson H, Grinberg A, Love P, Rouault TA (2004b) Genetic ablations of iron regulatory proteins 1 and 2 reveal why iron regulatory protein 2 dominates iron homeostasis. Embo J 23:386-395.

Michael S, Petrocine SV, Qian J, Lamarche JB, Knutson MD, Garrick MD, Koeppen AH (2006) Iron and iron-responsive proteins in the cardiomyopathy of Friedreich's ataxia. Cerebellum 5:257-267.

Mikhael M, Sheftel AD, Ponka P (2010) Ferritin does not donate its iron for haem synthesis in macrophages. Biochem J 429:463-471.

Mittal B, Doroudchi MM, Jeong SY, Patel BN, David S (2003) Expression of a membrane-bound form of the ferroxidase ceruloplasmin by leptomeningeal cells. Glia 41:337-346.

Miyajima H, Nishimura Y, Mizoguchi K, Sakamoto M, Shimizu T, Honda N (1987) Familial apoceruloplasmin deficiency associated with blepharospasm and retinal degeneration. Neurology 37:761-767.

Mizuno S, Mihara T, Miyaoka T, Inagaki T, Horiguchi J (2005) CSF iron, ferritin and transferrin levels in restless legs syndrome. J Sleep Res 14:43-47.

Molina-Holgado F, Hider RC, Gaeta A, Williams R, Francis P (2007) Metals ions and neurodegeneration. Biometals 20:639-654.

Montosi G, Donovan A, Totaro A, Garuti C, Pignatti E, Cassanelli S, Trenor CC, Gasparini P, Andrews NC, Pietrangelo A (2001) Autosomal-dominant hemochromatosis is associated with a mutation in the ferroportin (SLC11A3) gene. J Clin Invest 108:619-623.

Moos T (1996) Immunohistochemical localization of intraneuronal transferrin receptor immunoreactivity in the adult mouse central nervous system. J Comp Neurol 375:675-692.

Moos T (2002) Brain iron homeostasis. Dan Med Bull 49:279-301.

Moos T, Morgan EH (1998) Evidence for low molecular weight, non-transferrin-bound iron in rat brain and cerebrospinal fluid. J Neurosci Res 54:486-494.

Moos T, Morgan EH (2000) Transferrin and transferrin receptor function in brain barrier systems. Cell Mol Neurobiol 20:77-95.

Moos T, Morgan EH (2004) The significance of the mutated divalent metal transporter (DMT1) on iron transport into the Belgrade rat brain. J Neurochem 88:233-245.

Moos T, Rosengren Nielsen T (2006) Ferroportin in the postnatal rat brain: implications for axonal transport and neuronal export of iron. Semin Pediatr Neurol 13:149-157.

Moos T, Rosengren Nielsen T, Skjorringe T, Morgan EH (2007) Iron trafficking inside the brain. J Neurochem 103:1730-1740.

Morath DJ, Mayer-Proschel M (2001) Iron modulates the differentiation of a distinct population of glial precursor cells into oligodendrocytes. Dev Biol 237:232-243.

Morath DJ, Mayer-Proschel M (2002) Iron deficiency during embryogenesis and consequences for oligodendrocyte generation in vivo. Dev Neurosci 24:197-207.

Morris RL, Hollenbeck PJ (1993) The regulation of bidirectional mitochondrial transport is coordinated with axonal outgrowth. J Cell Sci 104 (Pt 3):917-927.

Mozell RL, McMorris FA (1991) Insulin-like growth factor I stimulates oligodendrocyte development and myelination in rat brain aggregate cultures. J Neurosci Res 30:382-390.

Muckenthaler MU, Galy B, Hentze MW (2008) Systemic iron homeostasis and the iron-responsive element/iron-regulatory protein (IRE/IRP) regulatory network. Annu Rev Nutr 28:197-213.

Mutsaers SE, Carroll WM (1998) Focal accumulation of intra-axonal mitochondria in demyelination of the cat optic nerve. Acta Neuropathol 96:139-143.

Nemeth E, Valore EV, Territo M, Schiller G, Lichtenstein A, Ganz T (2003) Hepcidin, a putative mediator of anemia of inflammation, is a type II acute-phase protein. Blood 101:2461-2463.

Nemeth E, Tuttle MS, Powelson J, Vaughn MB, Donovan A, Ward DM, Ganz T, Kaplan J (2004) Hepcidin regulates cellular iron efflux by binding to ferroportin and inducing its internalization. Science 306:2090-2093.

Nicolas G, Bennoun M, Devaux I, Beaumont C, Grandchamp B, Kahn A, Vaulont S (2001) Lack of hepcidin gene expression and severe tissue iron overload in upstream stimulatory factor 2 (USF2) knockout mice. Proc Natl Acad Sci U S A 98:8780-8785.

Nicolas G, Bennoun M, Porteu A, Mativet S, Beaumont C, Grandchamp B, Sirito M, Sawadogo M, Kahn A, Vaulont S (2002) Severe iron deficiency anemia in transgenic mice expressing liver hepcidin. Proc Natl Acad Sci U S A 99:4596-4601.

Nittis T, Gitlin JD (2004) Role of copper in the proteosome-mediated degradation of the multicopper oxidase hephaestin. J Biol Chem 279:25696-25702.

Njajou OT, Vaessen N, Joosse M, Berghuis B, van Dongen JW, Breuning MH, Snijders PJ, Rutten WP, Sandkuijl LA, Oostra BA, van Duijn CM, Heutink P (2001) A mutation in SLC11A3 is associated with autosomal dominant hemochromatosis. Nat Genet 28:213-214.

Ohgami RS, Campagna DR, McDonald A, Fleming MD (2006) The Steap proteins are metalloreductases. Blood 108:1388-1394.

Ohgami RS, Campagna DR, Greer EL, Antiochos B, McDonald A, Chen J, Sharp JJ, Fujiwara Y, Barker JE, Fleming MD (2005) Identification of a ferrireductase required for efficient transferrin-dependent iron uptake in erythroid cells. Nat Genet 37:1264-1269.

Ortiz E, Pasquini JM, Thompson K, Felt B, Butkus G, Beard J, Connor JR (2004) Effect of manipulation of iron storage, transport, or availability on myelin composition and brain iron content in three different animal models. J Neurosci Res 77:681-689.

Osaki S, Johnson DA (1969) Mobilization of liver iron by ferroxidase (ceruloplasmin). J Biol Chem 244:5757-5758.

Oski FA, Honig AS (1978) The effects of therapy on the developmental scores of iron-deficient infants. J Pediatr 92:21-25.

Oski FA, Honig AS, Helu B, Howanitz P (1983) Effect of iron therapy on behavior performance in nonanemic, iron-deficient infants. Pediatrics 71:877-880.

Ousman SS, David S (2000) Lysophosphatidylcholine induces rapid recruitment and activation of macrophages in the adult mouse spinal cord. Glia 30:92-104.

Ousman SS, David S (2001) MIP-1alpha, MCP-1, GM-CSF, and TNF-alpha control the immune cell response that mediates rapid phagocytosis of myelin from the adult mouse spinal cord. J Neurosci 21:4649-4656.

Pak M, Lopez MA, Gabayan V, Ganz T, Rivera S (2006) Suppression of hepcidin during anemia requires erythropoietic activity. Blood 108:3730-3735.

Pantopoulos K, Hentze MW (1998) Activation of iron regulatory protein-1 by oxidative stress in vitro. Proc Natl Acad Sci U S A 95:10559-10563.

Park CH, Valore EV, Waring AJ, Ganz T (2001) Hepcidin, a urinary antimicrobial peptide synthesized in the liver. J Biol Chem 276:7806-7810.

Patel BN, David S (1997) A novel glycosylphosphatidylinositol-anchored form of ceruloplasmin is expressed by mammalian astrocytes. J Biol Chem 272:20185-20190.

Patel BN, Dunn RJ, David S (2000) Alternative RNA splicing generates a glycosylphosphatidylinositol-anchored form of ceruloplasmin in mammalian brain. J Biol Chem 275:4305-4310.

Patel BN, Dunn RJ, Jeong SY, Zhu Q, Julien JP, David S (2002) Ceruloplasmin regulates iron levels in the CNS and prevents free radical injury. J Neurosci 22:6578-6586.

Perry TL, Norman MG, Yong VW, Whiting S, Crichton JU, Hansen S, Kish SJ (1985) Hallervorden-Spatz disease: cysteine accumulation and cysteine dioxygenase deficiency in the globus pallidus. Ann Neurol 18:482-489.

Petrak J, Vyoral D (2005) Hephaestin--a ferroxidase of cellular iron export. Int J Biochem Cell Biol 37:1173-1178.

Peyssonnaux C, Zinkernagel AS, Schuepbach RA, Rankin E, Vaulont S, Haase VH, Nizet V, Johnson RS (2007) Regulation of iron homeostasis by the hypoxia-inducible transcription factors (HIFs). J Clin Invest 117:1926-1932.

Picard V, Govoni G, Jabado N, Gros P (2000) Nramp 2 (DCT1/DMT1) expressed at the plasma membrane transports iron and other divalent cations into a calcein-accessible cytoplasmic pool. J Biol Chem 275:35738-35745.

Pietrangelo A (2004) The ferroportin disease. Blood Cells Mol Dis 32:131-138.

Pigeon C, Ilyin G, Courselaud B, Leroyer P, Turlin B, Brissot P, Loreal O (2001) A new mouse liver-specific gene, encoding a protein homologous to human antimicrobial peptide hepcidin, is overexpressed during iron overload. J Biol Chem 276:7811-7819.

Pinnix ZK, Miller LD, Wang W, D'Agostino R, Jr., Kute T, Willingham MC, Hatcher H, Tesfay L, Sui G, Di X, Torti SV, Torti FM (2010) Ferroportin and iron regulation in breast cancer progression and prognosis. Sci Transl Med 2:43ra56.

Pondarre C, Antiochos BB, Campagna DR, Clarke SL, Greer EL, Deck KM, McDonald A, Han AP, Medlock A, Kutok JL, Anderson SA, Eisenstein RS, Fleming MD (2006) The mitochondrial ATP-binding cassette transporter Abcb7 is essential in mice and participates in cytosolic iron-sulfur cluster biogenesis. Hum Mol Genet 15:953-964.

Ponka P (1997) Tissue-specific regulation of iron metabolism and heme synthesis: distinct control mechanisms in erythroid cells. Blood 89:1-25.

Ponka P (1999) Cellular iron metabolism. Kidney Int Suppl 69:S2-11.

Ponka P (2004) Hereditary causes of disturbed iron homeostasis in the central nervous system. Ann N Y Acad Sci 1012:267-281.

Puccio H, Simon D, Cossee M, Criqui-Filipe P, Tiziano F, Melki J, Hindelang C, Matyas R, Rustin P, Koenig M (2001) Mouse models for Friedreich ataxia exhibit cardiomyopathy, sensory nerve defect and Fe-S enzyme deficiency followed by intramitochondrial iron deposits. Nat Genet 27:181-186.

Qiu A, Jansen M, Sakaris A, Min SH, Chattopadhyay S, Tsai E, Sandoval C, Zhao R, Akabas MH, Goldman ID (2006) Identification of an intestinal folate transporter and the molecular basis for hereditary folate malabsorption. Cell 127:917-928.

Quigley JG, Yang Z, Worthington MT, Phillips JD, Sabo KM, Sabath DE, Berg CL, Sassa S, Wood BL, Abkowitz JL (2004) Identification of a human heme exporter that is essential for erythropoiesis. Cell 118:757-766.

Raivich G, Graeber MB, Gehrmann J, Kreutzberg GW (1991) Transferrin Receptor Expression and Iron Uptake in the Injured and Regenerating Rat Sciatic Nerve. Eur J Neurosci 3:919-927.

Rambod M, Kovesdy CP, Kalantar-Zadeh K (2008) Combined high serum ferritin and low iron saturation in hemodialysis patients: the role of inflammation. Clin J Am Soc Nephrol 3:1691-1701.

Rao R, Tkac I, Townsend EL, Gruetter R, Georgieff MK (2003) Perinatal iron deficiency alters the neurochemical profile of the developing rat hippocampus. J Nutr 133:3215-3221.

Rice AE, Mendez MJ, Hokanson CA, Rees DC, Bjorkman PJ (2009) Investigation of the Biophysical and Cell Biological Properties of Ferroportin, a Multipass Integral Membrane Protein Iron Exporter. J Mol Biol.

Roberts R, Sandra A, Siek GC, Lucas JJ, Fine RE (1992) Studies of the mechanism of iron transport across the blood-brain barrier. Ann Neurol 32 Suppl:S43-50.

Roetto A, Papanikolaou G, Politou M, Alberti F, Girelli D, Christakis J, Loukopoulos D, Camaschella C (2003) Mutant antimicrobial peptide hepcidin is associated with severe juvenile hemochromatosis. Nat Genet 33:21-22.

Roncagliolo M, Garrido M, Walter T, Peirano P, Lozoff B (1998) Evidence of altered central nervous system development in infants with iron deficiency anemia at 6 mo: delayed maturation of auditory brainstem responses. Am J Clin Nutr 68:683-690.

Rosen DR (1993) Mutations in Cu/Zn superoxide dismutase gene are associated with familial amyotrophic lateral sclerosis. Nature 364:362.

Roth JA, Singleton S, Feng J, Garrick M, Paradkar PN (2010) Parkin regulates metal transport via proteasomal degradation of the 1B isoforms of divalent metal transporter 1 J Neurochem 113:454-464.

Rotig A, de Lonlay P, Chretien D, Foury F, Koenig M, Sidi D, Munnich A, Rustin P (1997) Aconitase and mitochondrial iron-sulphur protein deficiency in Friedreich ataxia. Nat Genet 17:215-217.

Rouault TA (2006) The role of iron regulatory proteins in mammalian iron homeostasis and disease. Nat Chem Biol 2:406-414.

Rouault TA, Klausner RD (1996) Iron-sulfur clusters as biosensors of oxidants and iron. Trends Biochem Sci 21:174-177.

Ruthel G, Hollenbeck PJ (2003) Response of mitochondrial traffic to axon determination and differential branch growth. J Neurosci 23:8618-8624.

Sakakibara S, Aoyama Y (2002) Dietary iron-deficiency up-regulates hephaestin mRNA level in small intestine of rats. Life Sci 70:3123-3129.

Salahudeen AA, Thompson JW, Ruiz JC, Ma HW, Kinch LN, Li Q, Grishin NV, Bruick RK (2009) An E3 ligase possessing an iron-responsive hemerythrin domain is a regulator of iron homeostasis. Science 326:722-726.

Salazar J, Mena N, Hunot S, Prigent A, Alvarez-Fischer D, Arredondo M, Duyckaerts C, Sazdovitch V, Zhao L, Garrick LM, Nunez MT, Garrick MD, Raisman-Vozari R, Hirsch EC (2008) Divalent metal transporter 1 (DMT1) contributes to neurodegeneration in animal models of Parkinson's disease. Proc Natl Acad Sci U S A 105:18578-18583.

Salis C, Setton CP, Soto EF, Pasquini JM (2007) The mRNA of transferrin is expressed in Schwann cells during their maturation and after nerve injury. Exp Neurol 207:85-94.

Salzer JL, Lovejoy L, Linder MC, Rosen C (1998) Ran-2, a glial lineage marker, is a GPI-anchored form of ceruloplasmin. J Neurosci Res 54:147-157.

Santambrogio P, Biasiotto G, Sanvito F, Olivieri S, Arosio P, Levi S (2007) Mitochondrial ferritin expression in adult mouse tissues. J Histochem Cytochem 55:1129-1137.

Schade AL, Caroline L (1946) An Iron-binding Component in Human Blood Plasma. Science 104:340-341.

Schipper HM (1999) Neurodegeneration with brain iron accumulation - Clinical syndromes and neuroimaging. Biochim Biophys Acta. [Epub ahead of print]

Shaw GC, Cope JJ, Li L, Corson K, Hersey C, Ackermann GE, Gwynn B, Lambert AJ, Wingert RA, Traver D, Trede NS, Barut BA, Zhou Y, Minet E, Donovan A, Brownlie A, Balzan R, Weiss MJ, Peters LL, Kaplan J, Zon LI, Paw BH (2006) Mitoferrin is essential for erythroid iron assimilation. Nature 440:96-100.

Shayeghi M, Latunde-Dada GO, Oakhill JS, Laftah AH, Takeuchi K, Halliday N, Khan Y, Warley A, McCann FE, Hider RC, Frazer DM, Anderson GJ, Vulpe CD, Simpson RJ, McKie AT (2005) Identification of an intestinal heme transporter. Cell 122:789-801.

Shirihai OS, Gregory T, Yu C, Orkin SH, Weiss MJ (2000) ABC-me: a novel mitochondrial transporter induced by GATA-1 during erythroid differentiation. Embo J 19:2492-2502.

Shulman RG, Rothman DL, Behar KL, Hyder F (2004) Energetic basis of brain activity: implications for neuroimaging. Trends Neurosci 27:489-495.

Shvartsman M, Kikkeri R, Shanzer A, Cabantchik ZI (2007) Non-transferrin-bound iron reaches mitochondria by a chelator-inaccessible mechanism: biological and clinical implications. Am J Physiol Cell Physiol 293:C1383-1394.

Sibille JC, Kondo H, Aisen P (1988) Interactions between isolated hepatocytes and Kupffer cells in iron metabolism: a possible role for ferritin as an iron carrier protein. Hepatology 8:296-301.

Smith SR, Ghosh MC, Ollivierre-Wilson H, Hang Tong W, Rouault TA (2006) Complete loss of iron regulatory proteins 1 and 2 prevents viability of murine zygotes beyond the blastocyst stage of embryonic development. Blood Cells Mol Dis 36:283-287.

Stuart KA, Anderson GJ, Frazer DM, Powell LW, McCullen M, Fletcher LM, Crawford DH (2003) Duodenal expression of iron transport molecules in untreated haemochromatosis subjects. Gut 52:953-959.

Swaiman KF (2001) Hallervorden-Spatz syndrome. Pediatr Neurol 25:102-108.

Syed BA, Beaumont NJ, Patel A, Naylor CE, Bayele HK, Joannou CL, Rowe PS, Evans RW, Srai SK (2002) Analysis of the human hephaestin gene and protein: comparative modelling of the N-terminus ecto-domain based upon ceruloplasmin. Protein Eng 15:205-214.

Thompson KJ, Fried MG, Ye Z, Boyer P, Connor JR (2002) Regulation, mechanisms and proposed function of ferritin translocation to cell nuclei. J Cell Sci 115:2165-2177.

Thorpy MJ (2005) New paradigms in the treatment of restless legs syndrome. Neurology 64:S28-33.

Todorich B, Zhang X, Slagle-Webb B, Seaman WE, Connor JR (2008b) Tim-2 is the receptor for H-ferritin on oligodendrocytes. J Neurochem.

Todorich B, Pasquini JM, Garcia CI, Paez PM, Connor JR (2009) Oligodendrocytes and myelination: the role of iron. Glia 57:467-478.

Vargas ME, Barres BA (2007) Why is Wallerian degeneration in the CNS so slow? Annu Rev Neurosci 30:153-179.

Vashisht AA, Zumbrennen KB, Huang X, Powers DN, Durazo A, Sun D, Bhaskaran N, Persson A, Uhlen M, Sangfelt O, Spruck C, Leibold EA, Wohlschlegel JA (2009) Control of iron homeostasis by an iron-regulated ubiquitin ligase. Science 326:718-721.

Viatte L, Vaulont S (2009) Hepcidin, the iron watcher. Biochimie 91:1223-1228.

Vidal R, Miravalle L, Gao X, Barbeito AG, Baraibar MA, Hekmatyar SK, Widel M, Bansal N, Delisle MB, Ghetti B (2008) Expression of a mutant form of the ferritin light chain gene induces neurodegeneration and iron overload in transgenic mice. J Neurosci 28:60-67.

Vokurka M, Krijt J, Sulc K, Necas E (2006) Hepcidin mRNA levels in mouse liver respond to inhibition of erythropoiesis. Physiol Res 55:667-674.

Vulpe CD, Kuo YM, Murphy TL, Cowley L, Askwith C, Libina N, Gitschier J, Anderson GJ (1999) Hephaestin, a ceruloplasmin homologue implicated in intestinal iron transport, is defective in the sla mouse. Nat Genet 21:195-199.

Waldmeier PC, Buchle AM, Steulet AF (1993) Inhibition of catechol-O-methyltransferase (COMT) as well as tyrosine and tryptophan hydroxylase by the orally active iron chelator, 1,2-dimethyl-3-hydroxypyridin-4-one (L1, CP20), in rat brain in vivo. Biochem Pharmacol 45:2417-2424.

Watkins JA, Altazan JD, Elder P, Li CY, Nunez MT, Cui XX, Glass J (1992) Kinetic characterization of reductant dependent processes of iron mobilization from endocytic vesicles. Biochemistry 31:5820-5830.

Wessling-Resnick M (2006) Iron imports. III. Transfer of iron from the mucosa into circulation. Am J Physiol Gastrointest Liver Physiol 290:G1-6.

Wrighting DM, Andrews NC (2008) Iron homeostasis and erythropoiesis. Curr Top Dev Biol 82:141-167.

Wu LJ, Leenders AG, Cooperman S, Meyron-Holtz E, Smith S, Land W, Tsai RY, Berger UV, Sheng ZH, Rouault TA (2004) Expression of the iron transporter ferroportin in synaptic vesicles and the blood-brain barrier. Brain Res 1001:108-117.

Xu X, Pin S, Gathinji M, Fuchs R, Harris ZL (2004) Aceruloplasminemia: an inherited neurodegenerative disease with impairment of iron homeostasis. Ann N Y Acad Sci 1012:299-305.

Yamamoto K, Yoshida K, Miyagoe Y, Ishikawa A, Hanaoka K, Nomoto S, Kaneko K, Ikeda S, Takeda S (2002) Quantitative evaluation of expression of iron-metabolism genes in ceruloplasmin-deficient mice. Biochim Biophys Acta 1588:195-202.

Yeh KY, Yeh M, Mims L, Glass J (2009) Iron feeding induces ferroportin 1 and hephaestin migration and interaction in rat duodenal epithelium. Am J Physiol Gastrointest Liver Physiol 296:G55-65.

Yoon T, Cowan JA (2003) Iron-sulfur cluster biosynthesis. Characterization of frataxin as an iron donor for assembly of [2Fe-2S] clusters in ISU-type proteins. J Am Chem Soc 125:6078-6084.

Yoon T, Cowan JA (2004) Frataxin-mediated iron delivery to ferrochelatase in the final step of heme biosynthesis. J Biol Chem 279:25943-25946.

Youdim MB, Green AR (1978) Iron deficiency and neurotransmitter synthesis and function. Proc Nutr Soc 37:173-179.

Yu GS, Steinkirchner TM, Rao GA, Larkin EC (1986) Effect of prenatal iron deficiency on myelination in rat pups. Am J Pathol 125:620-624.

Zaitsev VN, Zaitseva I, Papiz M, Lindley PF (1999) An X-ray crystallographic study of the binding sites of the azide inhibitor and organic substrates to ceruloplasmin, a multi-copper oxidase in the plasma. J Biol Inorg Chem 4:579-587.

Zecca L, Youdim MB, Riederer P, Connor JR, Crichton RR (2004) Iron, brain ageing and neurodegenerative disorders. Nat Rev Neurosci 5:863-873.

Zechel S, Huber-Wittmer K, von Bohlen und Halbach O (2006) Distribution of the iron-regulating protein hepcidin in the murine central nervous system. J Neurosci Res 84:790-800.

Zhang DL, Hughes RM, Ollivierre-Wilson H, Ghosh MC, Rouault TA (2009) A ferroportin transcript that lacks an iron-responsive element enables duodenal and erythroid precursor cells to evade translational repression. Cell Metab 9:461-473.

Zoller H, Theurl I, Koch RO, McKie AT, Vogel W, Weiss G (2003) Duodenal cytochrome b and hephaestin expression in patients with iron deficiency and hemochromatosis. Gastroenterology 125:746-754.

1.19 Figures

Figure 1

The transferrin cycle. Holo-TF binds to the TfR1 at the suface of many cells. The TF/TfR1-complex is then endocytosed via clathrin-coated vesicles. Following endocytosis, Fe^{3+} is released from the TF/TfR1-complex in the acidified endosome, converted into Fe^{2+} by the ferric reductase STEAP3 and transported into the cytosol via DMT1. The apo-TF/TfR1-complex is recycled to the cell surface where the extracellular neutral pH causes the release of the apo-TF.

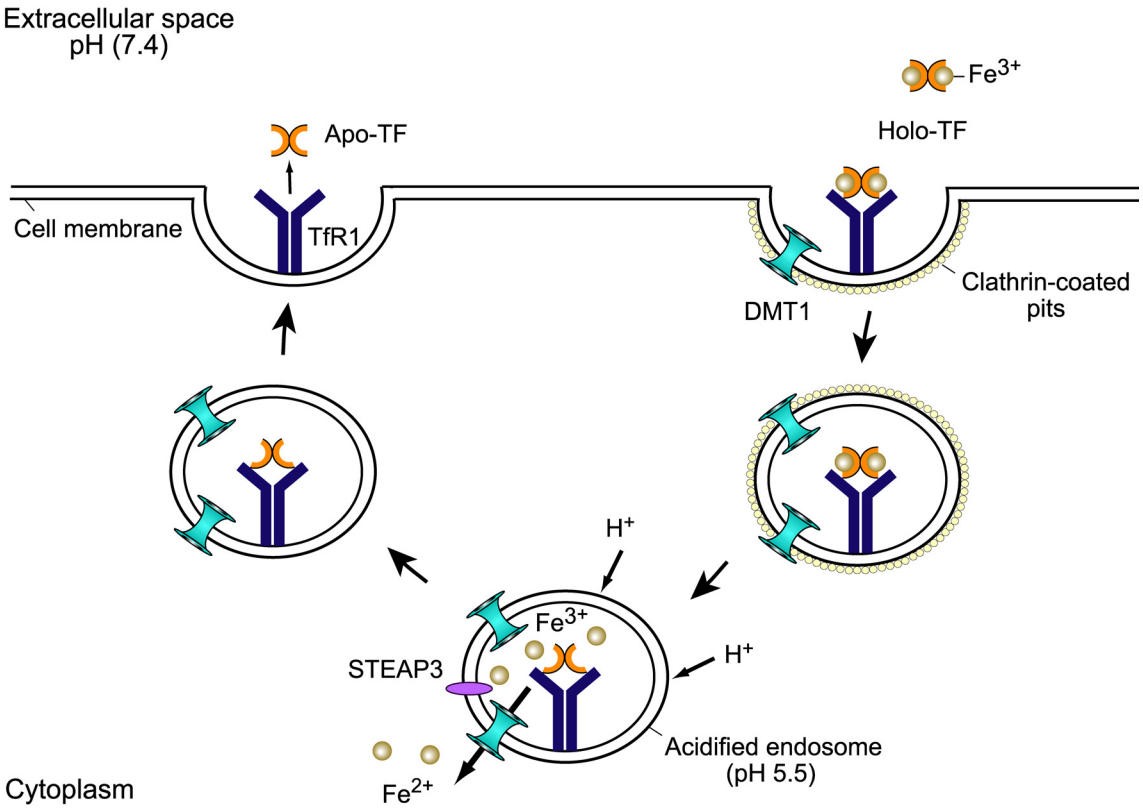
Extracellular space
pH (7.4)
Fe3+
Holo-TF
Apo-TF
Cell membrane
TfR1
DMT1
Clathrin-coated
pits
H+
Fe3+
H+
STEAP3
Acidified endosome
(pH 5.5)
Cytoplasm
Fe2+

Figure 2

Intestinal iron absorption. Dietary non-haem iron is reduced by the actions of the ferric reductase Dcytb at the brush border of duodenal enterocytes to yield Fe^{2+} which subsequently enters the enterocytes through DMT1. Dietary heme can be absorbed via HCP1. Once inside the enterocytes, iron is either stored bound to ferritin or exported into the circulation through Fpn on the basolateral membrane of the enterocytes. The transport of Fe^{2+} is facilitated by Heph which oxidizes it to Fe^{3+}, thereby enabling iron loading onto plasma TF.

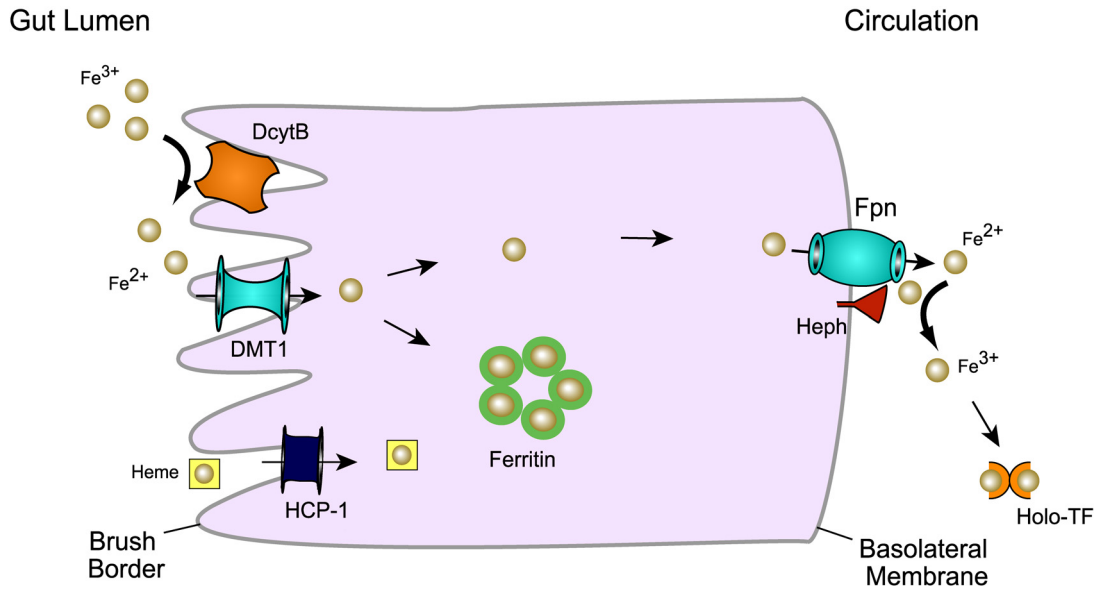
Gut Lumen
Circulation
Fe3+
DcytB
Fe2+
DMT1
Fpn
Fe2+
Heph
Fe3+
Ferritin
Heme
HCP-1
Holo-TF
Brush
Border
Basolateral
Membrane

Figure 3

The IRE/IRP system. (**A**) In iron-deficient cells, IRPs bind to stem loop structures (IRE motives) in UTRs of certain mRNAs encoding iron homeostatic proteins. In the case of ferritin, IRP binding to a single IRE in the 5' UTR of the mRNA inhibits its translation resulting in a reduction of ferritin synthesis. In the case of TfR1, IRP binding to multiple IREs in the 3' UTR of the mRNA increases its stability leading to increased TfR1 protein expression. (**B**) In iron-replete cells, the level of functional IRE-binding IRPs is reduced resulting in increased ferritin translation and decreased TfR1 mRNA stability.

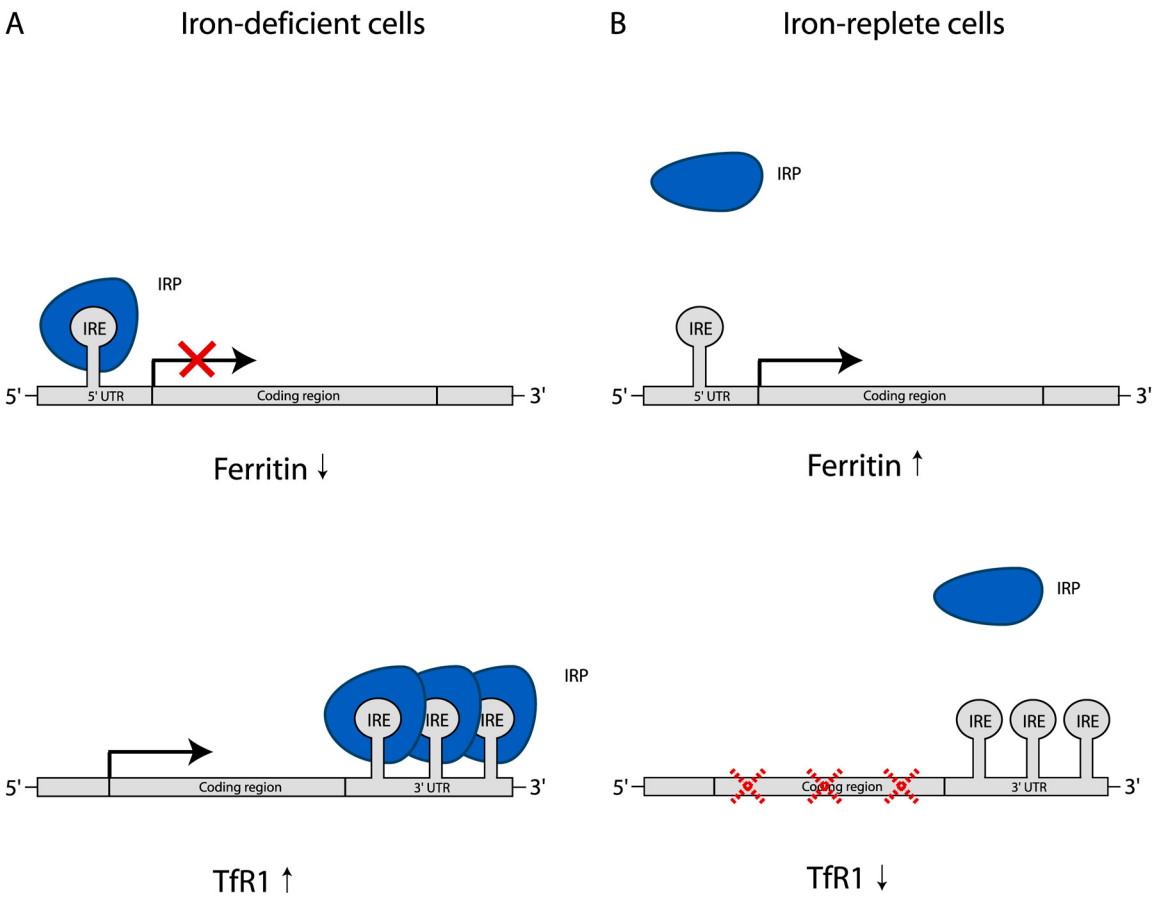
A
Iron-deficient cells
B
Iron-replete cells
IRP
IRE
5'
5' UTR
Coding region
3'
Ferritin ↓
Ferritin ↑
IRP
IRE
IRE
IRE
5'
Coding region
3' UTR
3'
TfR1 ↑
IRP
IRE
IRE
IRE
5'
Coding region
3' UTR
3'
TfR1 ↓

Figure 4

Iron homeostatic mechanisms in astrocytes. Extracellular Fe^{3+} is reduced to Fe^{2+} by the ferric reductase DcytB on the cell surface of astrocytes and transported into the cell via DMT1. The iron that is not immediately used by the cell is either stored bound to ferritin and in the labile iron pool (LIP), or released through the iron exporter Fpn. The iron efflux mechanism involves the action of a GPI-anchored form of Cp on the cell surface of astrocytes which oxidizes the Fe^{2+} that is transported through Fpn into Fe^{3+} which can then bind to extracellular iron-binding proteins.

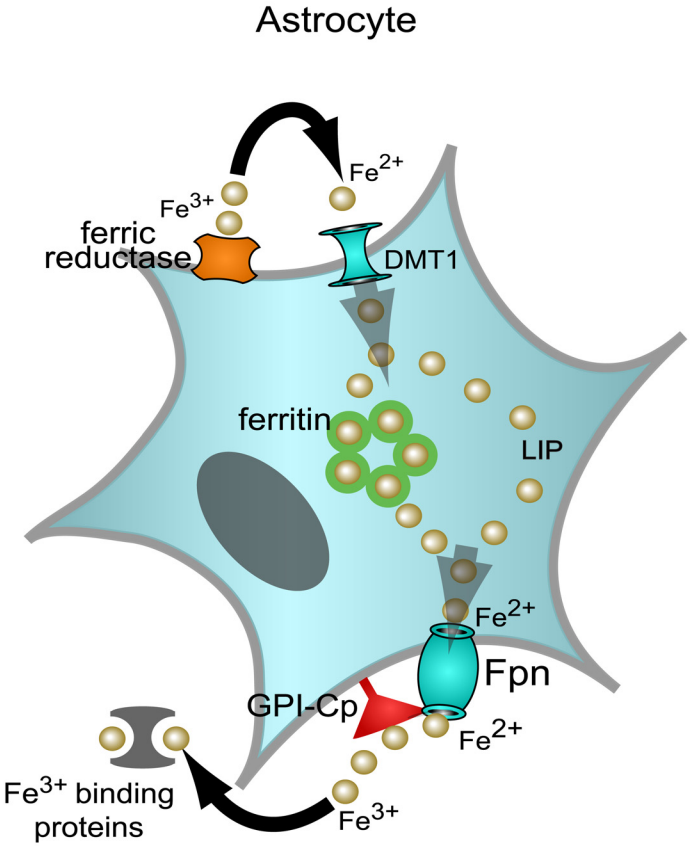
Astrocyte
Fe2+
Fe3+
ferric
reductase
DMT1
ferritin
LIP
Fe2+
Fpn
GPI-Cp
Fe2+
Fe3+ binding
proteins
Fe3+

Chapter 2

Iron Efflux from Oligodendrocytes is Differentially Regulated in Grey and White Matter

Katrin Schulz, Chris D. Vulpe, Leah Z. Harris and Samuel David

*The work presented in this chapter has been published

2.1 Preface

The regulation of iron homeostasis in the CNS is crucial, as disturbances of CNS iron metabolism are associated with several pathological conditions. However, the iron homeostatic mechanisms in the CNS underlying this regulation are still not well characterized. One fundamental iron homeostatic mechanism is cellular iron efflux. In astrocytes, iron efflux occurs via the iron exporter Fpn mediated by a GPI-anchored form of the ferroxidase Cp (Jeong and David, 2003). However, Cp is only expressed by astrocytes in the CNS. In the present chapter, I studied the role of another ferroxidase, Heph, in iron efflux from oligodendrocytes.

2.2 Abstract

Accumulation of iron occurs in the central nervous system in several neurodegenerative diseases. Iron is essential for life but also has the ability to generate toxic free radicals if not properly handled. Iron homeostasis at the cellular level is therefore important to maintain proper cellular function, and its dysregulation can contribute to neurodegenerative diseases. Iron export, a key mechanism to maintain proper iron levels in cells occurs via ferroportin, a ubiquitously expressed transmembrane protein that partners with a ferroxidase. A membrane-bound form of the ferroxidase ceruloplasmin is expressed by astrocytes in the central nervous system and regulates iron efflux. We now show that oligodendrocytes utilize another ferroxidase, called hephaestin, which was first identified in enterocytes in the gut. Mice with mutations in the hephaestin gene (sex-linked anemia mice) show iron accumulation in oligodendrocytes in the grey matter but not white matter, and exhibit motor deficits. This was accompanied by a marked

reduction in the levels of the paranodal proteins contactin-associated protein 1 (Caspr) and reticulon-4 (Nogo A). We show that the sparing of iron accumulation in white matter oligodendrocytes in sex-linked anemia mice is due to compensatory upregulation of ceruloplasmin in these cells. This was further confirmed in ceruloplasmin/hephaestin double mutant mice, which show iron accumulation in both grey and white matter oligodendrocytes. These data indicate that grey and white matter oligodendrocytes can utilize different iron efflux mechanisms to maintain iron homeostasis. Dysregulation of such efflux mechanisms leads to iron accumulation in the CNS.

2.3 Introduction

Iron is an essential trace metal required for many biological functions including oxygen transport, DNA synthesis, and mitochondrial oxidation. Iron can cycle between the ferrous (Fe^{2+}) and ferric (Fe^{3+}) states. This ability to accept and donate electrons allows it to serve as an important cofactor for enzymes. However, ferrous iron can generate highly reactive free radicals, which can cause oxidative damage (Berg et al., 2004). Excessive iron in the CNS has been implicated in several neurodegenerative conditions (LeVine, 1997; Bakshi et al., 2001; Carri et al., 2003; Zecca et al., 2004; Molina-Holgado et al., 2007).

In the CNS, iron levels are highest in myelin and oligodendrocytes (Connor and Menzies, 1996; Erb et al., 1996). In these cells, iron is needed for biosynthetic enzymes involved in lipid and cholesterol synthesis, as well as enzymes required for the increased metabolic demands of myelination (Hill and Switzer, 1984; LeVine and Macklin, 1990). Oligodendrocytes synthesize high levels of ferritin (Connor et al., 1994) and therefore

possess a high buffering capacity for iron. Although this buffering capacity offers some protection, excessive iron load can be expected to disrupt some aspects of oligodendrocyte function. To prevent overload, iron levels in all cells, including oligodendrocytes, are tightly regulated.

One mechanism by which cells regulate intracellular iron levels is via iron efflux through the ubiquitously expressed iron exporter ferroportin (Fpn) (Donovan et al., 2000). Ferroportin partners with ferroxidases to efflux iron (Jeong and David, 2003). The multi-copper ferroxidase ceruloplasmin (Cp), a serum protein secreted by the liver, has been shown to mediate iron efflux from hepatocytes and macrophages (Osaki and Johnson, 1969; Harris et al., 1999). We have shown previously that an alternatively spliced, glycosylphosphatidylinositol (GPI)-anchored form of Cp is expressed by astrocytes (Patel and David, 1997; Patel et al., 2000) and is required for iron efflux from these cells (Jeong and David, 2003). This suggests that ferrous iron effluxed via Fpn requires oxidation by a ferroxidase such as Cp for proper iron release. Another copper-dependent ferroxidase, hephaestin (Heph), was identified in duodenal enterocytes (Vulpe et al., 1999), and also shown to play a role in iron efflux. In the sex-linked anemia (sla) mouse, a partial deletion of the *heph* gene results in the expression of a truncated Heph protein that exhibits only partial ferroxidase activity (Vulpe et al., 1999; Chen et al., 2004).

Heph and Cp are expressed in retinal Muller glia and in retinal pigment epithelial cells and are thought to mediate iron efflux from these cells (Hahn et al., 2004b). To date, the mechanisms of iron efflux from non-astrocytic cells in the CNS and the possible role of Heph in this process are not known. We therefore examined the expression and

function of Heph in the mammalian CNS. We provide *in vitro* and *in vivo* evidence that Heph is expressed by mature oligodendrocytes and plays a role in regulating iron efflux from these cells. In addition, our data suggest that grey and white matter oligodendrocytes can use different ferroxidases to regulate iron homeostasis.

2.4 Materials and Methods

Animals. Sla mice were purchased from Jackson Laboratories and C57BL/6 mice and Sprague Dawley rats from Charles River. Animals of either sex were used for all experiments. All procedures were approved by the McGill University Animal Care committee and followed the guidelines of the Canadian Council on Animal Care.

Purification of oligodendrocyte precursor cells (OPCs), astrocytes, and microglia from neonatal rat cerebral cortex. Astrocytes were purified from neonatal rat cerebral cortex as described previously (Jeong and David, 2003). Microglia and OPCs were purified from neonatal rat cortex as described elsewhere (Chen et al., 2007a). Briefly, to obtain microglia, mixed glial cultures were prepared and plated in Dulbecco's modified Eagle's medium (DMEM, Invitrogen) containing 10% fetal bovine serum (FBS, Invitrogen). After 10-14 days, microglia were shaken off for 3 hrs and cultured in DMEM/F12 (Invitrogen) containing 10% FBS. Mixed glia cultures were shaken again overnight to detach oligodendrocytes. The detached cells were plated on uncoated Petri dishes for 3 hrs to remove residual microglia. The non-adherent OPCs were then plated on poly-L-lysine coated tissue culture flasks in oligodendrocyte-specific medium (DMEM/F12 containing 5 µg/mL insulin, 50 µg/mL human transferrin, 16 µg/mL

putrescine, 30 nM triiodothyronine 10 mM HEPES, 0.1% BSA, 20 nM hydrocortisone, 20 nM progesterone, 10 nM biotin, 30 nM selenium) supplemented with 2.5 ng/mL platelet derived growth factor (PDGF)-AA and 2.5 ng/mL basic fibroblast growth factor (bFGF) (all from Sigma-Aldrich). For differentiation of OPCs, PDGF-AA and bFGF were removed.

Purification of OPCs from neonatal mouse cerebral cortex. For work on sla and wildtype mice, neural progenitor cells were isolated from neonatal mouse cerebral cortex and differentiated into OPCs using neurosphere cultures as previously described (Chen et al., 2007a) with the following modifications: neonatal mouse cerebral cortex was triturated with a fire-polished pipette, passed through a 40 μm cell strainer, and plated onto 6-well plates (1 brain/6-well plate) in neurosphere growth medium (NPM) consisting of DMEM/F12 with B27 supplement (Invitrogen) containing 20 ng/mL epidermal growth factor (EGF) and 20 ng/mL bFGF. To generate oligospheres, the neurosphere medium was gradually changed to oligosphere medium (NPM/conditioned media of B104 cells, 7:3) by replacing one-fourth of the former medium with the latter every other day. After 7 days in culture, oligospheres were mechanically dissociated and resuspended in oligosphere medium. After 2-4 days, oligospheres were again dissociated and replated. For proliferation of OPCs, the cell suspension was plated onto poly-L-lysine coated 6-well plates in oligodendrocyte-specific medium supplemented with 5.0 ng/mL PDGF-AA and 5.0 ng/mL bFGF. For differentiation of OPCs into oligodendrocytes, PDGF-AA and bFGF were removed.

Iron efflux study. Oligodendrocytes that were differentiated from OPCs purified from sla and wildtype mice were plated 2 days prior to use in a 6-well plate at a density of 1 x 10^6 cells/well. Cells were incubated in serum- and transferrin-free oligodendrocyte medium (SFM) for 1 h to remove any transferrin-bound iron. Radiolabeled iron ($^{55}FeCl_3$; PerkinElmer Life Science) was mixed with non-labeled $FeCl_3$ (total of 40 μM) and L-ascorbate (Sigma-Aldrich) was added (molar ratio of $FeCl_3$ to L-ascorbate was 1:44). Cells were then incubated with SFM containing radiolabeled iron-ascorbate (1 μCi/well) for 6 h. After iron loading, cells were washed and incubated with fresh SFM without radiolabeled iron. At each time point (0, 12, and 24 h) cells were washed three times with PBS, detached, pelleted, and treated with PRONASE (Calbiochem) for 1 h at 4 °C to remove membrane-bound iron. Cells were lysed in 0.1 N NaOH, and radioactivity was measured using a liquid scintillation counter. Sister cultures were treated in the same way without radioactive iron, and viable cell numbers were estimated by trypan blue (Sigma) exclusion. The radioactivity taken up by the cells was normalized to value per 10^6 cells. The radioactivity within cells at time point 0 h was set to 100%. Measurements at each time point were done in triplicate and repeated in three separate experiments (n=3). Results are shown as mean ± SEM. Two-way ANOVA was used to determine statistical significance.

Immunofluorescence labeling. Immunostaining was performed on cultures of neonatal rat oligodendrocytes grown on poly-L-lysine coated 12 mm round glass coverslips. Cells were stained for 30 min at room temperature with mouse anti-A2B5 (R&D Systems; 1:100), mouse anti-O4 (1:100; Chemicon) or mouse anti-Gal-C (1:100; Chemicon) and

rabbit anti-Heph (1:400; C. Vulpe) or rabbit anti-Fpn (1:200; Alpha Diagnostics). Primary antibodies were visualized with rhodamine-conjugated goat anti-mouse IgG (1:400, Jackson ImmunoResearch) and Alexa 488-conjugated goat anti-rabbit IgG (1:400; Invitrogen) for 30 min at room temperature. Cells were fixed in acetic acid/ethanol (5:95 (v/v)) at -20 °C for 10 min and coverslipped with mounting medium containing 100 ng/mL 4'-6-diamidino-2-phenylindole (DAPI) (Vector Laboratories) to visualize cell nuclei.

For immunofluorescence labeling of tissue sections, sla and wildtype mice were perfused with 4% paraformaldehyde (PFA) in 0.1 M phosphate buffer, pH 7.4. Cryostat sections (14 μm) were incubated with different combinations of the following primary antibodies (mouse anti-CC1 (1:200; Chemicon), rabbit anti-Fpn (1:200; Alpha Diagnostics); rabbit anti-Heph (1:400; C. Vulpe), rabbit anti-ferritin (1:200; DakoCytomation), rabbit anti-Caspr (1:800; Abcam), rabbit anti-Nogo A (1:100; Santa Cruz; Biotech), and secondary antibodies (rhodamine-conjugated goat anti-mouse IgG (1:400, Jackson ImmunoResearch) and Alexa488-conjugated goat anti-rabbit IgG (1:400; Invitrogen) as described previously (Jeong and David, 2006; Rathore et al., 2008). Sections were coverslipped with DAPI containing medium.

Quantification of immunofluorescence labeling. Images were captured with a Retiga 1300 C digital camera (QImaging Corp., Burnaby, British Columbia) using a Zeiss AxioSkop II light microscope (Carl Zeiss Canada Ltd., Toronto), and analyzed with the BioQuant Nova Prime image analysis system (BioQuant Image Analysis Corp., Nashville). Heph and Fpn expression *in vitro* were quantified by counting the numbers of

cells double-labeled for Heph or Fpn and either A2B5, O4 or GAL-C in 4 different fields of 2 coverslips for 3 experimental groups. Statistical significance was determined using the Student's *t*-test.

Caspr and NogoA immunostainings were quantified by pixel density. Thresholds for detection of Caspr and NogoA immunoreactivity were first established and then applied throughout. The pixel density of Caspr immunoreactivity was measured within a fixed area in the ventral horn and the ventral white matter in cross-sections of cervical, thoracic and lumbar spinal cord and divided by the size of the area (3 sections per animal, 3 mice; n=3). The pixel density of Nogo A immunoreactivity was determined per CC1-positive cell in the grey matter of the lumbar spinal cord (30 cells per section, 3 sections per animal, 3 mice; n=3). The respective background was determined and subtracted for each section. The area of each cell was measured and the pixel density per μm^2 was calculated. The data obtained for Caspr and Nogo A immunoreactivity were analyzed for statistical significance by two-way RM-ANOVA, and Student's *t*-test, respectively. The data are plotted as means ± SEM.

Heph expression *in vivo* was analyzed in the grey and white matter of the spinal cord by counting Heph positive, CC1 positive and Heph/CC1 double-labeled cells in a fixed area and the percentage of Heph expression in CC1 positive cells and the percentage of CC1 expression in Heph positive cells was determined (3 sections per animal, 3 mice; n=3). The pixel density of Heph immunoreactivity was determined per CC1-positive cell in the spinal cord grey and white matter (30 cells per section, 3 sections per animal, 3 mice; n=3). The respective background was determined and subtracted for each section. The

area of each cell was measured and the pixel density per μm² was calculated. Statistical significance for all Heph expression analyses was determined using the Student's *t*-test. The numbers of Cp-positive cells and CC1-positive cells in the combined ISH/immunostaining were quantified by counting the respective cells in a fixed area of the white and grey matter spinal cord and divided by the area (3 sections per animal, 3 mice; n=3). Student's *t*-test was performed to determine statistical significance.

Perl's Histochemistry. Wildtype and sla mice were perfused with 4% PFA in 0.1 M phosphate buffer, pH 7.4. Modified enhanced Perl's histochemistry was performed on 14 μm-thick cryostat sections of the spinal cord to detect iron accumulation as described previously (Smith et al., 1997). Briefly, sections were incubated for 10 minutes with 4% potassium ferrocyanide only, followed by a 50-minute incubation with 4% HCl and 4% potassium ferrocyanide (1:1). The reaction product was enhanced with diaminobenzidine (DAB). Sections were counterstained with methyl green and mounted with Entellan (all from Sigma-Aldrich).

Perfusion-Perl's method for electron microscopy. Wildtype and sla mice were perfused with the perfusion-Perl's method, and spinal cords were prepared for electron microscopy according to a previously described protocol (Meguro et al., 2005). In brief, mice were first perfused with 0.1 M phosphate buffer (pH 7.4) containing heparin (10 units/mL), then with 4% PFA and 1.5% glutaraldehyde in 0.1 M phosphate buffer (pH 7.4) followed by 4% paraformaldehyde, 1% glutaraldehyde and 1% potassium ferrocyanide in distilled H_2O (pH 1.0). Spinal cords were dissected out and post-fixed

overnight in 4% paraformaldehyde and 1.5% glutaraldehyde in 0.1 M phosphate buffer (pH 7.4). Vibratome sections (100 μm) were obtained and washed twice with PBS and once with PBS containing 0.3% H_2O_2 and 0.1 M NaN_3. Sections were incubated for 10 min in 0.025% DAB and 0.005% H_2O_2 in PBS. Tissue sections were then post-fixed in 2% osmium tetroxide for 1 hr and processed for embedding in Epon. Thin sections (1 nm) picked-up on copper grids were stained with lead citrate and viewed with a Philips CM 10 electron microscope.

Western Blotting. Total protein was extracted from spinal cord tissue, separated by SDS-PAGE and transferred to a polyvinylidene difluoride membrane (Bio-Rad). The membrane was incubated overnight with rabbit anti-Heph (1:600; Vulpe), rabbit anti-Fpn (1:1000, Alpha Diagnostics), rabbit anti-Cp (1:800, DakoCytomation) or rabbit anti-β-actin (1:400, Sigma-Aldrich). Blots were then incubated with peroxidase-conjugated anti-rabbit IgG, (1:500,000; Jackson ImmunoResearch) and developed with enhanced chemiluminescence (PerkinElmer Life Sciences).

RT-PCR. RNA was purified from whole spinal cord or cultured oligodendrocytes and Caco2 cells using the RNeasy Lipid Tissue Mini Kit (Qiagen). RT-PCR was performed using the Omniscript RT Kit (Qiagen) and the following primers: Cp_forward :5′-TGG GAC TAT GCT TCT GGC AGT GAA-3’; Cp_reverse: 5′-TTG GCA CGC AGA ACG TAC AAA TAC-3’ ; DMT1_forward: 5′-ACA AAT ATG GCT TGC GGA AGC TGG -3′ ; DMT1_reverse: 5′-ACA TGT TGT GCG GCA TGA TCA CAG -3′; Fpn_forward: 5′-TCA GGA CTG GCT CAG CTT TCT TGT-3′ ; Fpn_reverse: 5′-CAG CAA TGA CTC

CTG CAA ACA GCA-3′; Heph_forward: 5′-ATG GAC CGG GAA TTT GCC TTG TTG-3’; Heph_reverse: 5′-TCA TGC CCA GCA TCT TCA CAT TGC-3’; TIM-2_forward: 5′-ATC CCT CCA CAG AAG CCA CAG AAA-3′; TIM-2_reverse: 5′-ACT GAG GCG GTG CTG ATA CAA GAA-3′; TfR1_forward: 5′-AGC AGC ATC TGC TAA TGA GAC CCA-3′; TfR1_reverse: 5′-TGC AAG CTT TGT CTT CCC AAC AAC -3′.

In Situ Hybridization. Sla and wildtype mice were perfused with 4% paraformaldehyde in 0.1 M phosphate buffer (pH 7.4). Cryostat sections (14 µm) were obtained and *in situ* hybridization was performed with Digoxygenin (DIG)-labeled locked nucleic acids (LNAs) (Exiqon) using a modified version of a protocol that has been described previously (Obernosterer et al., 2007). Briefly, tissue sections were fixed in 4% PFA for 10 min at room temperature, then washed three times for 3 min in PBS and incubated 10 min in acetylation solution (1.3% Triethanolamine, 0.25% acetic anhydride, 0.17% concentrated HCl in DEPC-treated dH_2O) to reduce background binding. Sections were then washed in PBS for 5 min and incubated 5 min with proteinase K (5 µg/mL in PBS) to increase permeability and hybridization efficiency. After three more washes for 3 min in PBS, prehybridization was carried out in hybridization buffer (50% formamide, 5x saline-sodium citrate (SSC), 5x Denhardt’s, 200 µg/m l yeast RNA, 0.4 g Roche blocking reagents in DEPC-treated dH_2O) for 5 hrs at room temperature. Sections were then incubated with 1 pM of the Cp LNA DIG-labeled probe in denaturizing hybridization buffer (hybridization buffer containing 0.25% CHAPS) overnight at 52 °C. Slides were soaked in pre-warmed 60 °C 5 x SSC, incubated in 0.2 x SSC at 60 °C for 1 h and

washed in B1 solution (0.1 M Tris pH 7.5, 0.15 M NaCl) at room temperature for 10 min. After an incubation in blocking solution (1% FBS and 0.05% Tween20 in B1 solution) for 1 h at room temperature, slides were incubated with a sheep anti-DIG fluoresein-coupled antibody (1:200 in blocking solution, Roche) overnight at 4 °C. Slides were washed three times for 5 min in PBST, mounted with DAPI. Up to the hybridization step, everything was carried out with DEPC-treated dH_2O under RNAse free conditions.

Rotorod assay. Motor performance was assessed using a rotorod test (Steele et al., 1998). Mice were made to walk on the rotating rod for a maximum duration of 3 min at a constant speed of 16 rpm. Each mouse was given 3 trials with an inter-trial interval of 5 minutes. 6 animals per group were tested (n=6). Results are shown as a mean ± SEM. Two-way ANOVA was used to determine statistical significance.

2.5 Results

Hephaestin and ferroportin are expressed in mature oligodendrocytes. We first assessed the expression of Heph in primary cultures of the neonatal rat CNS. Mixed cerebellar cultures exhibit Heph expression in oligodendrocytes and microglia but not in astrocytes or neurons (Fig. 1). Furthermore, quantification of Heph staining in glial cell cultures from the neonatal cerebral cortex indicates that 100% of the oligodendrocytes express Heph, whereas none of the astrocytes express this ferroxidase.

Oligodendrocytes *in vitro* go through a series of well-defined maturational stages that are delineated by the expression of various cell surface antigens. One series of maturational changes involves the temporal shift in expression of A2B5 to O4 and

eventually to galactocerebroside (Gal-C) antigens (Gard and Pfeiffer, 1993). We therefore assessed the stage of oligodendrocyte maturation in which Heph expression first occurs. Our immunofluorescence analysis indicate that Heph is expressed only by the more mature Gal-C expressing oligodendrocytes (100 ± 0.0%) but not by A2B5-expressing early OPCs (1 ± 0.004%) or by O4-expressing late OPCs (2 ± 0.048%) (Fig. 2A-I). As Heph would likely partner with an iron transporter to efflux iron, we assessed the expression of Fpn at different stages of oligodendrocyte maturation. Double immunofluorescence labeling shows that Fpn, like Heph, is expressed by the more mature Gal-C expressing oligodendrocytes (99 ± 0.009%) but not by $A2B5^+$ (0%) or $O4^+$ OPCs (0%) (Fig. 2J-R).

Hephaestin and ferroportin are expressed in the adult mouse spinal cord. To confirm the expression of Heph and Fpn *in vivo*, we carried out double immunofluorescence labeling on spinal cord tissue sections of adult mice using antibodies against Heph or Fpn combined with an antibody against the oligodendrocyte specific maker CC1. Heph is expressed in the majority of $CC1^+$ oligodendrocytes in the spinal cord (Fig. 3A-C). About 80% of oligodendrocytes in the grey and white matter express Heph (white matter = 83.42 ± 4.44%; grey matter = 78.98 ± 3.1%). Furthermore, almost 90% of the $Heph^+$ cells are $CC1^+$ oligodendrocytes (white matter = 88.6 ± 1.6%; grey matter = 89.77 ± 3.25%). Quantification of the intensity of Heph immunostaining in $CC1^+$ oligodendrocytes as an index of expression per cell showed higher Heph expression in white matter oligodendrocytes (71.47 ± 3.89 pixel density/μm^2) as compared to grey matter oligodendrocytes (36.95 ± 7.23 pixel density/μm^2), suggesting that white matter

oligodendrocytes have a greater requirement for ferroxidase activity than those in the grey matter. The efflux iron transporter, ferroportin (Fpn), a ubiquitously expressed molecule, is expressed by both $CC1^+$ oligodendrocytes as well as by $CC1^-$ cells (Fig. 3D-F). We have evidence that Fpn is also expressed in astrocytes and neurons (data not shown). As mentioned previously, sla mutant mice express a truncated, partially active form of Heph in non-CNS tissues (Vulpe et al., 1999; Chen et al., 2004). We therefore compared the expression of Heph and Fpn in the CNS of sla and wildtype mice by Western blot analysis. Spinal cord tissue from sla mice contains low levels of the truncated form of Heph relative to the full-length form in wildtype mice (Fig. 3G), a decrease likely due to the rapid degradation of the truncated protein *in vivo*. In contrast, expression of the iron exporter Fpn is similar in the spinal cords of wildtype and sla mice (Fig. 3G).

Hephaestin mediates iron efflux from oligodendrocytes. Using an *in vitro* iron efflux assay, we next assessed the involvement of Heph in iron efflux from oligodendrocytes. Oligodendrocyte precursor cells were first purified from the brains of neonatal sla and wildtype mice and allowed to mature *in vitro.* After loading with radiolabeled iron, mature oligodendrocyte cultures were incubated with fresh medium and assayed for iron retention at several time-points. In oligodendrocytes from wildtype mice, ~60% of the radiolabeled iron is effluxed after 24 h, whereas iron efflux from oligodendrocytes from sla mice is severely impaired (Fig. 3H). The iron uptake was not significantly different in wildtype and sla oligodendrocytes, similar to the finding reported for astrocytes lacking Cp (Jeong and David, 2003). These data provide direct evidence that Heph is required for

iron efflux from oligodendrocytes and demonstrate that the low amount of functionally impaired Heph present in the sla mice is insufficient to mediate iron efflux.

Iron accumulates in oligodendrocytes in sla mice. Since Heph was found to be involved in iron export from oligodendrocytes in culture, we reasoned that iron would accumulate in oligodendrocytes of sla mice *in vivo*. Iron accumulation in the CNS of sla mice was assessed by enhanced Perl's histochemistry on tissue sections of mice aged 3-, 6- and 10-months (Fig. 4A-H). Iron accumulation in the spinal cord of sla mice is seen as early as 3 months of age (Fig. 4C and F). Interestingly, cells labeled for iron are located primarily in the grey matter (Fig. 4B) and display the process-bearing morphology characteristic of oligodendrocytes (Fig. 4H). Iron accumulation in these cells increases at 6 and 10 months of age in sla mice but not in wildtype controls (Fig. 4D-H). To confirm that these iron-loaded cells are indeed oligodendrocytes, we performed double immunofluorescence labeling for the iron binding protein, ferritin (a sensitive surrogate marker for increased cellular iron load), and the oligodendrocyte marker CC1. These studies clearly demonstrate that $CC1^+$ oligodendrocytes in the spinal cord grey matter of sla mice but not wildtype mice express high levels of ferritin (Fig. 4I-N). Sla mice also show enhanced iron accumulation relative to wildtype mice in other CNS grey matter regions including the brainstem and the deep cerebellar nuclei (data not shown). We analyzed the iron deposits within these cells further, using the perfusion-Perl's enhancement technique and electron microscopy. This ultrastructural analysis revealed iron deposits in the cytosol of oligodendrocytes in the grey matter of the spinal cord in 10-month old sla mice (Fig. 5C, D). Such deposits are not seen in oligodendrocytes of wildtype mice (Fig. 5A, B). The

iron accumulation in sla mice is unlikely to be due to increased iron influx, as the mRNA expression of the iron importers, transferrin receptor 1 (TfR1) and divalent metal transporter 1 (DMT1) is not increased (Fig. 5E). Furthermore, the expression of the ferritin receptor TIM-2, which is thought to mediate influx of ferritin-bound iron into oligodendrocytes (Todorich et al., 2008a), is decreased in sla mice, possibly in an effort to minimize iron overload in oligodendrocytes (Fig. 5E).

Sla mice show deficits in motor performance with age. Motor control of sla and wildtype mice was tested at 3, 6, and 9 months of age using the rotorod test. Whereas wildtype mice remain on the rotorod for about 180 seconds (maximum test duration), sla mice fall off after ~100 seconds at 9 months of age, suggesting that motor coordination in sla mice is impaired with age (Fig. 5F).

Expression of the paranodal proteins Caspr and Nogo A is reduced in the spinal cord of sla mice. Iron efflux from glia may be an important route for iron availability to neurons. If this were the case, impaired iron efflux in grey matter oligodendrocytes in sla mice might lead to neuronal, axonal, or synaptic abnormalities due to a lack of iron. We therefore assessed neuronal numbers in spinal cord tissue sections of 10-months old sla and wildtype mice stained with cresyl violet. In addition, we assessed the expression of the synaptic membrane protein, synapsin, by Western blotting using protein extracted from spinal cords of 10-months old animals. No differences between wildtype and sla mice were observed in either of these neuronal indicators. Furthermore, despite the marked iron accumulation in oligodendrocytes, there is no loss of $CC1^+$ oligodendrocytes

in the grey matter of sla mice at 10 months of age, indicating that oligodendrocytes have a high iron-buffering capacity. In addition, the overall extent of myelination as determined by Luxol fast blue staining appeared unchanged in sla mice (data not shown). To further confirm this, we also examined whether myelin thickness is affected in the sla mice by quantifying the g-ratio from electron micrographs of the spinal cord grey and white matter. The g-ratio is obtained by dividing the axon diameter by the fiber diameter (axon diameter plus myelin). This analysis revealed no differences between sla and wildtype mice (mean g-ratio in the grey matter in wildtype mice = 0.77 ± 0.01, in sla mice = 0.75 ± 0.02; the mean g-ratio in the white matter in wildtype mice = 0.74 ± 0.01, sla mice = 0.73 ± 0.02; n=3). We therefore assessed sla mice for subtle disruptions of myelination, such as altered expression of paranodal proteins. It has been reported that impaired expression of the axonal protein Caspr at the paranodal junction results in subtle morphological changes that lead to behavioral deficits (Berglund et al., 1999; Boyle et al., 2001). Interestingly, we found that immunofluorescence labeling for Caspr in spinal cord sections is reduced in 10-months old sla mice relative to wildtype mice (Fig. 6A-D*)*. Quantification of the immunofluorescence staining in the cervical, thoracic, and lumbar spinal cord shows a significant reduction in Caspr expression in the grey and white matter in sla mice relative to wildtype controls (Fig. 6E and F). To rule out the possibility that the reduced Caspr expression in sla mice might be due to axonal loss, we performed immunofluorescence labeling for neurofilaments. Quantification of the neurofilament immunostaining shows no difference between sla (ventral grey matter: 1.30 ± 0.18 pixel density/μm^2; ventral white matter: 1.73 ± 0.18 pixel density/μm^2; n=3) and wildtype mice (ventral grey matter: 1.39 ± 0.31 pixel density/μm^2; ventral white matter: 1.74 ± 0.30

pixel density/μm²; n=3). We next assessed the expression of Nogo A, a known partner of Caspr that is expressed by oligodendrocytes in the CNS (Nie et al., 2003). Double immunofluorescence labeling shows reduction of Nogo A expression in oligodendrocytes in the grey matter in the sla spinal cord as compared to wildtype mice (Fig. 7A-F). Quantification of Nogo A immunolabeling in $CC1^+$ oligodendrocytes in the lumbar spinal cord shows a marked decrease of Nogo A expression levels in the grey and white matter in sla mice relative to wildtype mice (Fig. 7G).

Abnormal paranodal structure in the spinal cord of sla mice. Paranodal proteins at the axonal membrane and the terminal myelin loops form paranodal junctions that are important in establishing and maintaining the structure of the paranodes. We therefore assessed by electron microscopy whether the reduced expression of the paranodal proteins Caspr and Nogo A affects paranodal structure in the spinal cord grey matter of sla as compared to wildtype mice. The paranodal region in sla mice showed abnormal separation of the myelin sheath into multiple distinct myelin lamellae (Fig. 7J, K), as well as floating terminal myelin loops that are not attached to the axonal membrane (Fig. 7J, K). In contrast, the paranodal loops in wildtype animals are properly aligned and in close association with the axonal membrane and did not show splitting of the myelin at the paranodal region (Fig. 7H, I). The paranodal abnormalities seen in sla mice are similar to those reported in Caspr mutant and contactin mutant mice, which were also associated with functional defects (Berglund et al., 1999; Bhat et al., 2001; Boyle et al., 2001). These results indicate that although the overall myelination (g-ratio) is not impaired in sla

mice, the structure of the paranodes is severely disrupted, which could account for the motor deficits seen in these mice.

Ceruloplasmin compensates for the loss of Heph function in white matter oligodendrocytes. It was surprising to see that iron accumulation in sla mice was limited to grey matter oligodendrocytes. We hypothesized that the absence of iron accumulation in white matter oligodendrocytes of sla mice might be due to upregulation of the other known ferroxidase, Cp. Although oligodendrocytes do not express Cp at the protein level (data not shown), RT-PCR analysis indicate that oligodendrocytes *in vitro* do express Cp mRNA (Fig. 8A). Interestingly, in support of our hypothesis, Western blot analysis shows that Cp is upregulated at the protein level in the spinal cord of sla mice (Fig. 8B and C). To assess whether Cp expression is upregulated in oligodendrocytes in spinal cord white matter of sla mice, we performed *in situ* hybridization. We see high Cp mRNA expression in the white matter of sla but not wildtype mice (Fig. 8D and E). In addition, quantification of the numbers of cells expressing Cp in the sla spinal cord showed 4-fold greater induction in white matter (29.28 cells/100 μm^2) as compared to grey matter (7.25 cells/100 μm^2) (Fig. 8F). This is not due to differences in the number of oligodendrocytes ($CC1^+$ cells) in grey and white matter (white matter = 36.33 ± 3.04 cells/100 μm^2; grey matter = 39.68 ± 0.18 cells/100 μm^2). This compensatory upregulation of Cp expression further points to the greater need for ferroxidase activity in white matter oligodendrocytes. Furthermore, *in situ* hybridization for Cp combined with immunofluorescence labeling for oligodendrocytes using an anti-CC1 antibody shows

that Cp is upregulated in $CC1^+$ oligodendrocytes in the white matter of the spinal cord in sla mice (Fig. 8G-I) but not in wildtype mice (Fig. 8J-L).

To determine if the compensatory upregulation of Cp in white matter oligodendrocytes in sla mice rescues them from iron accumulation, we generated $Heph^{sla}/Cp^{-/-}$ double mutant mice and performed iron histochemistry. Enhanced Perl's histochemistry of 9-12 month old animals shows iron accumulation in both the grey and white matter of the spinal cord in the $Heph^{sla}/Cp^{-/-}$ double mutants (Fig. 9A-D). The iron-loaded cells in the white matter of the double mutant mice display the morphology of oligodendrocytes with processes surrounding axons (Fig. 9D). Immunofluorescence labeling with anti-ferritin as a surrogate marker for iron shows high ferritin levels in both the grey and white matter of the spinal cord in $Heph^{sla}/Cp^{-/-}$ double mutants, but only in the grey matter in sla mice (Fig. 9E-G). To determine whether the ferritin positive cells in the white matter of the $Heph^{sla}/Cp^{-/-}$ mice were oligodendrocytes, we carried out double immunofluorescence labeling for ferritin and the oligodendrocyte marker CC1 and found high levels of ferritin predominantly in $CC1^+$ oligodendrocytes (Fig. 9H-M). These results suggest that oligodendrocytes in the white matter are able to compensate for the loss of Heph function by upregulating Cp expression. We also examined whether the $Heph^{sla}/Cp^{-/-}$ double mutant mice show increased motor deficits on rotorod analysis. $Heph^{sla}/Cp^{-/-}$ mice at 6 months of age fell off the rotating rod earlier than wildtype and sla mice (wildtype mice, mean = 174 s (n=6); sla mice, mean = 143.5 s (n=6); $Heph^{sla}/Cp^{-/-}$ mice, mean = 80 s (n=2)). These data indicate that increased iron accumulation in white and grey matter in $Heph^{sla}/Cp^{-/-}$ mice are associated with even earlier impairment of

motor control as compared to sla mice, further supporting the importance of compensatory upregulation of Cp in white matter oligodendrocytes in sla mice.

2.6 Discussion

Astrocytes efflux iron via Fpn and its interactions with the GPI-anchored form of the ferroxidase Cp (Jeong and David, 2003). Ceruloplasmin, however, is not expressed by oligodendrocytes in the normal CNS. We show here that another ferroxidase, Heph, is expressed by oligodendrocytes and plays an important role in iron efflux from these cells.

Heph mediates iron efflux from duodenal enterocytes into the circulation via interactions with Fpn (Wessling-Resnick, 2006; Yeh et al., 2008). We also found expression of Fpn in oligodendrocytes and show that expression of Fpn and Heph is restricted to mature oligodendrocytes. The lack of Fpn and Heph expression in earlier stages of the oligodendrocyte lineage suggests that iron efflux is a feature of mature oligodendrocytes. OPCs might have a greater need to acquire and retain iron, as iron is required for the proliferation and differentiation of OPCs,as well as for myelination (Morath and Mayer-Proschel, 2001; Schonberg and McTigue, 2009; Todorich et al., 2009). After myelination is complete, oligodendrocytes likely require less iron, and maintain stable iron levels through iron efflux. In support of this idea, oligodendrocytes also down-regulate expression of the iron importer TfR1 after differentiation is completed (Hill et al., 1985; Han et al., 2003). Nevertheless, OPCs and mature oligodendrocytes express ferritin receptors that permit uptake of extracellular ferritin-bound iron (Todorich et al., 2008a), suggesting that mature oligodendrocytes also require basal levels of iron influx.

Cells handle increased intracellular iron load in a variety of ways. One mechanism is the upregulation of the iron-binding protein ferritin in the cytosol. The age-associated increase in ferritin immunostaining seen in oligodendrocytes in sla mice suggests an increased iron load. Another way in which cells control high intracellular iron levels is by decreasing iron influx. However, despite the high iron levels in oligodendrocytes in sla mice, TfR1 mRNA level in the spinal cord remains unchanged from normal levels. As expression of TfR1 in mature oligodendrocytes is generally low (Hill et al., 1985; Han et al., 2003), a further decrease in TFR1 expression via the iron regulatory protein-iron response element (IRP-IRE) system (Pantopoulos, 2004) may be undetectable in sla mice. However, expression of the ferritin receptor TIM-2, which is likely to function as an iron importer in mature oligodendrocytes, is reduced in sla mice. This data suggests that oligodendrocytes in sla mice may be attempting to minimize iron uptake in response to high intracellular iron levels; however, this compensatory mechanism appears to be insufficient as iron overload continues to occur with age in sla oligodendrocytes.

Cells also handle increased intracellular iron through efflux of excess iron. Our *in vitro* studies show that the reduction of Heph in sla mice leads to impaired iron efflux from oligodendrocytes. Heph likely regulates iron efflux from oligodendrocytes by converting ferrous iron transported via Fpn into its ferric form. The immediate oxidation of ferrous iron appears to be necessary for its efflux, as has been shown for Cp and Fpn in astrocytes (Jeong and David, 2003). *In vitro* studies with astrocytes and C6 glioma cells indicate that, in the absence of GPI-Cp, cell surface Fpn gets internalized and rapidly degraded (De Domenico et al., 2007a). In contrast to this, we have evidence that Fpn remains on the cell surface of oligodendrocytes from sla mice (data not shown). Whether

this is due to the presence of low levels of mutant Heph in the membrane is currently not known. Consistent with the role of Heph in iron efflux from oligodendrocytes in cell culture, we found iron accumulation in oligodendrocytes *in vivo* in the CNS of sla mice with age. Our data indicate that the residual activity of Heph in sla mice is insufficient to mediate effective iron efflux from oligodendrocytes *in vitro* and *in vivo*.

Interestingly, iron accumulation in sla mice occurs only in grey matter oligodendrocytes, suggesting differential requirements for the management of iron homeostasis in grey and white matter oligodendrocytes. Grey and white matter oligodendrocytes differ in their metabolic function and in their capacity to handle metabolic stress (D'Amelio et al., 1990; Bauer et al., 2002). Because white matter oligodendrocytes are involved in myelination of long fiber tracts in the CNS, they may require higher iron levels than their counterparts in the grey matter. Since high intracellular iron levels are likely to cause oxidative damage if not properly controlled, white matter oligodendrocytes may need to be equipped with additional iron efflux mechanisms to prevent intracellular iron overload and potential damage to white matter tracts. Interestingly, we observed upregulation of Cp expression in white matter oligodendrocytes in sla mice, indicating that Cp compensates for the loss of Heph function. Additionally, the extensive iron accumulation in white matter oligodendrocytes in the $Heph^{sla}/Cp^{-/-}$ double mutant mice further supports the proposed view that expression of Cp in white matter oligodendrocytes in sla mice protects these cells from iron accumulation. The severe motor defects in $Heph^{sla}/Cp^{-/-}$ double mutant mice further emphasize the importance of Cp upregulation in white matter oligodendrocytes in sla mice. The ability of Cp to function as a fail-safe mechanism has also been demonstrated

in the gut in sla mice where it is thought to rescue these mice from early onset microcytic anemia (Bannerman and Cooper, 1966; Cherukuri et al., 2005).

We show here that motor coordination of sla mice is impaired, suggesting that some aspect of neuronal function is affected. Unlike myelin-producing white matter oligodendrocytes, the function of grey matter oligodendrocytes remains incompletely understood. However, perineuronal oligodendrocytes have been shown to provide trophic factor support for neurons (Du and Dreyfus, 2002). We did not observe any loss in the number of neurons in the sla spinal cord, nor was there an increase in the number of apoptotic cells, as assessed by annexin V staining (data not shown). Similarly, no differences were seen in the expression of the synaptic protein, synapsin, in the spinal cord of sla and wildtype mice (data not shown). Despite increased iron accumulation in grey matter oligodendrocytes in sla mice, their numbers were not diminished. This is in contrast to the marked loss of astrocytes in Cp null mice which exhibit iron accumulation in astrocytes (Jeong and David, 2006). Collectively, these findings suggest that oligodendrocytes, which have a higher requirement for iron, appear to have a better capacity to buffer increased iron load and to remain viable relative to astrocytes. Also myelination overall is not affected as assessed by Luxol Fast blue staining and g-ratio analysis. However, there is decreased expression of the paranodal proteins Nogo A and Caspr in the spinal cord of sla mice. Nogo A is expressed by oligodendrocytes and is localized to the paranodal loops of myelin where it partners with the axonal protein Caspr (Nie et al., 2003). Caspr is a main component of the paranodal region, and plays an important role in establishing and maintaining the paranodal junctions (Einheber et al., 1997). These axoglial junctions form a critical barrier between the voltage-gated Na^+

channels at the node and the delayed rectifier K^+ channels in the juxtaparanodal region, and are therefore crucial for the propagation of action potentials via saltatory conduction (Waxman and Ritchie, 1993; Denisenko-Nehrbass et al., 2002). The reduction of Caspr and Nogo A in sla mice was observed in the grey as well as white matter. Since Caspr is a neuronal/axonal protein, its reduction in the white matter might be due to the involvement of the neuronal cell bodies of projecting neurons that are located in the grey matter in other regions of the CNS. We observed iron accumulation in grey matter regions throughout the CNS of sla mice (data not shown). The reduced expression of Caspr in sla mice may also be due to the loss of its binding partner Nogo A in oligodendrocytes, which may result from indirect effects of increased iron load. The reduction of the two paranodal proteins Caspr and NogoA is likely to result in the structural abnormalities of the paranodes that were observed in sla mice. Alterations of the paranodal loops seen by electron microscopy may contribute to the motor deficits in these animals. This is supported by previous work demonstrating functional deficits caused by reduction of Caspr and ultrastructural abnormalities of the paranodal loops (Bhat et al., 2001; Boyle et al., 2001).

In summary, our data show that Heph is expressed by mature oligodendrocytes and plays a role in iron efflux from these cells. The findings presented here also indicate that white and grey matter oligodendrocytes can regulate iron efflux differently. We show that in the absence of Heph, white matter oligodendrocytes upregulate the expression of Cp, likely as a fail-safe mechanism. The lack of such compensatory upregulation of Cp in grey matter oligodendrocytes results in severe iron accumulation. We show that although oligodendrocytes have a high capacity to buffer excess iron, the increased iron load in

grey matter oligodendrocytes leads to paranodal abnormalities that likely contribute to the motor deficits seen in the sla mutants. The present study reveals the first clear demonstration of a ferroxidase that is required for iron efflux from oligodendrocytes. This knowledge will help in future studies on iron homeostasis in various neurodegenerative diseases in which iron accumulation occurs.

2.7 References

Bakshi R, Dmochowski J, Shaikh ZA, Jacobs L (2001) Gray matter T2 hypointensity is related to plaques and atrophy in the brains of multiple sclerosis patients. J Neurol Sci 185:19-26.

Bannerman RM, Cooper RG (1966) Sex-linked anemia: a hypochromic anemia of mice. Science 151:581-582.

Bauer J, Bradl M, Klein M, Leisser M, Deckwerth TL, Wekerle H, Lassmann H (2002) Endoplasmic reticulum stress in PLP-overexpressing transgenic rats: gray matter oligodendrocytes are more vulnerable than white matter oligodendrocytes. J Neuropathol Exp Neurol 61:12-22.

Berg D, Youdim MB, Riederer P (2004) Redox imbalance. Cell Tissue Res 318:201-213.

Berglund EO, Murai KK, Fredette B, Sekerkova G, Marturano B, Weber L, Mugnaini E, Ranscht B (1999) Ataxia and abnormal cerebellar microorganization in mice with ablated contactin gene expression. Neuron 24:739-750.

Bhat MA, Rios JC, Lu Y, Garcia-Fresco GP, Ching W, St Martin M, Li J, Einheber S, Chesler M, Rosenbluth J, Salzer JL, Bellen HJ (2001) Axon-glia interactions and the domain organization of myelinated axons requires neurexin IV/Caspr/Paranodin. Neuron 30:369-383.

Boyle ME, Berglund EO, Murai KK, Weber L, Peles E, Ranscht B (2001) Contactin orchestrates assembly of the septate-like junctions at the paranode in myelinated peripheral nerve. Neuron 30:385-397.

Carri MT, Ferri A, Cozzolino M, Calabrese L, Rotilio G (2003) Neurodegeneration in amyotrophic lateral sclerosis: the role of oxidative stress and altered homeostasis of metals. Brain Res Bull 61:365-374.

Chen H, Attieh ZK, Su T, Syed BA, Gao H, Alaeddine RM, Fox TC, Usta J, Naylor CE, Evans RW, McKie AT, Anderson GJ, Vulpe CD (2004) Hephaestin is a ferroxidase that maintains partial activity in sex-linked anemia mice. Blood 103:3933-3939.

Chen Y, Balasubramaniyan V, Peng J, Hurlock EC, Tallquist M, Li J, Lu QR (2007) Isolation and culture of rat and mouse oligodendrocyte precursor cells. Nat Protoc 2:1044-1051.

Cherukuri S, Potla R, Sarkar J, Nurko S, Harris ZL, Fox PL (2005) Unexpected role of ceruloplasmin in intestinal iron absorption. Cell Metab 2:309-319.

Connor JR, Menzies SL (1996) Relationship of iron to oligodendrocytes and myelination. Glia 17:83-93.

Connor JR, Boeshore KL, Benkovic SA, Menzies SL (1994) Isoforms of ferritin have a specific cellular distribution in the brain. J Neurosci Res 37:461-465.

D'Amelio F, Eng LF, Gibbs MA (1990) Glutamine synthetase immunoreactivity is present in oligodendroglia of various regions of the central nervous system. Glia 3:335-341.

De Domenico I, Ward DM, di Patti MC, Jeong SY, David S, Musci G, Kaplan J (2007) Ferroxidase activity is required for the stability of cell surface ferroportin in cells expressing GPI-ceruloplasmin. Embo J 26:2823-2831.

Denisenko-Nehrbass N, Faivre-Sarrailh C, Goutebroze L, Girault JA (2002) A molecular view on paranodal junctions of myelinated fibers. J Physiol Paris 96:99-103.

Donovan A, Brownlie A, Zhou Y, Shepard J, Pratt SJ, Moynihan J, Paw BH, Drejer A, Barut B, Zapata A, Law TC, Brugnara C, Lux SE, Pinkus GS, Pinkus JL, Kingsley PD, Palis J, Fleming MD, Andrews NC, Zon LI (2000) Positional cloning of zebrafish ferroportin1 identifies a conserved vertebrate iron exporter. Nature 403:776-781.

Du Y, Dreyfus CF (2002) Oligodendrocytes as providers of growth factors. J Neurosci Res 68:647-654.

Einheber S, Zanazzi G, Ching W, Scherer S, Milner TA, Peles E, Salzer JL (1997) The axonal membrane protein Caspr, a homologue of neurexin IV, is a component of the septate-like paranodal junctions that assemble during myelination. J Cell Biol 139:1495-1506.

Erb GL, Osterbur DL, LeVine SM (1996) The distribution of iron in the brain: a phylogenetic analysis using iron histochemistry. Brain Res Dev Brain Res 93:120-128.

Gard AL, Pfeiffer SE (1993) Glial cell mitogens bFGF and PDGF differentially regulate development of O4+GalC- oligodendrocyte progenitors. Dev Biol 159:618-630.

Hahn P, Qian Y, Dentchev T, Chen L, Beard J, Harris ZL, Dunaief JL (2004) Disruption of ceruloplasmin and hephaestin in mice causes retinal iron overload and retinal degeneration with features of age-related macular degeneration. Proc Natl Acad Sci U S A 101:13850-13855.

Han J, Day JR, Connor JR, Beard JL (2003) Gene expression of transferrin and transferrin receptor in brains of control vs. iron-deficient rats. Nutr Neurosci 6:1-10.

Harris ZL, Durley AP, Man TK, Gitlin JD (1999) Targeted gene disruption reveals an essential role for ceruloplasmin in cellular iron efflux. Proc Natl Acad Sci U S A 96:10812-10817.

Hill JM, Switzer RC, 3rd (1984) The regional distribution and cellular localization of iron in the rat brain. Neuroscience 11:595-603.

Hill JM, Ruff MR, Weber RJ, Pert CB (1985) Transferrin receptors in rat brain: neuropeptide-like pattern and relationship to iron distribution. Proc Natl Acad Sci U S A 82:4553-4557.

Jeong SY, David S (2003) Glycosylphosphatidylinositol-anchored ceruloplasmin is required for iron efflux from cells in the central nervous system. J Biol Chem 278:27144-27148.

Jeong SY, David S (2006) Age-related changes in iron homeostasis and cell death in the cerebellum of ceruloplasmin-deficient mice. J Neurosci 26:9810-9819.

LeVine SM (1997) Iron deposits in multiple sclerosis and Alzheimer's disease brains. Brain Res 760:298-303.

LeVine SM, Macklin WB (1990) Iron-enriched oligodendrocytes: a reexamination of their spatial distribution. J Neurosci Res 26:508-512.

Meguro R, Asano Y, Odagiri S, Li C, Iwatsuki H, Shoumura K (2005) The presence of ferric and ferrous iron in the nonheme iron store of resident macrophages in different tissues and organs: histochemical demonstrations by the perfusion-Perls and -Turnbull methods in the rat. Arch Histol Cytol 68:171-183.

Molina-Holgado F, Hider RC, Gaeta A, Williams R, Francis P (2007) Metals ions and neurodegeneration. Biometals 20:639-654.

Morath DJ, Mayer-Proschel M (2001) Iron modulates the differentiation of a distinct population of glial precursor cells into oligodendrocytes. Dev Biol 237:232-243.

Nie DY, Zhou ZH, Ang BT, Teng FY, Xu G, Xiang T, Wang CY, Zeng L, Takeda Y, Xu TL, Ng YK, Faivre-Sarrailh C, Popko B, Ling EA, Schachner M, Watanabe K, Pallen CJ, Tang BL, Xiao ZC (2003) Nogo-A at CNS paranodes is a ligand of Caspr: possible regulation of K(+) channel localization. Embo J 22:5666-5678.

Obernosterer G, Martinez J, Alenius M (2007) Locked nucleic acid-based in situ detection of microRNAs in mouse tissue sections. Nat Protoc 2:1508-1514.

Osaki S, Johnson DA (1969) Mobilization of liver iron by ferroxidase (ceruloplasmin). J Biol Chem 244:5757-5758.

Pantopoulos K (2004) Iron metabolism and the IRE/IRP regulatory system: an update. Ann N Y Acad Sci 1012:1-13.

Patel BN, David S (1997) A novel glycosylphosphatidylinositol-anchored form of ceruloplasmin is expressed by mammalian astrocytes. J Biol Chem 272:20185-20190.

Patel BN, Dunn RJ, David S (2000) Alternative RNA splicing generates a glycosylphosphatidylinositol-anchored form of ceruloplasmin in mammalian brain. J Biol Chem 275:4305-4310.

Rathore KI, Kerr BJ, Redensek A, Lopez-Vales R, Jeong SY, Ponka P, David S (2008) Ceruloplasmin protects injured spinal cord from iron-mediated oxidative damage. J Neurosci 28:12736-12747.

Schonberg DL, McTigue DM (2009) Iron is essential for oligodendrocyte genesis following intraspinal macrophage activation. Exp Neurol 218:64-74.

Smith MA, Harris PL, Sayre LM, Perry G (1997) Iron accumulation in Alzheimer disease is a source of redox-generated free radicals. Proc Natl Acad Sci U S A 94:9866-9868.

Steele PM, Medina JF, Nores WL, Mauk MD (1998) Using genetic mutations to study the neural basis of behavior. Cell 95:879-882.

Todorich B, Zhang X, Slagle-Webb B, Seaman WE, Connor JR (2008) Tim-2 is the receptor for H-ferritin on oligodendrocytes. J Neurochem.

Todorich B, Pasquini JM, Garcia CI, Paez PM, Connor JR (2009) Oligodendrocytes and myelination: the role of iron. Glia 57:467-478.

Vulpe CD, Kuo YM, Murphy TL, Cowley L, Askwith C, Libina N, Gitschier J, Anderson GJ (1999) Hephaestin, a ceruloplasmin homologue implicated in intestinal iron transport, is defective in the sla mouse. Nat Genet 21:195-199.

Waxman SG, Ritchie JM (1993) Molecular dissection of the myelinated axon. Ann Neurol 33:121-136.

Wessling-Resnick M (2006) Iron imports. III. Transfer of iron from the mucosa into circulation. Am J Physiol Gastrointest Liver Physiol 290:G1-6.

Yeh KY, Yeh M, Mims L, Glass J (2008) Iron Feeding Induces Ferroportin 1 and Hephaestin Migration and Interaction in Rat Duodenal Epithelium. Am J Physiol Gastrointest Liver Physiol.

Zecca L, Youdim MB, Riederer P, Connor JR, Crichton RR (2004) Iron, brain ageing and neurodegenerative disorders. Nat Rev Neurosci 5:863-873.

2.8 Figures

Figure 1

Expression of Heph in mixed cerebellar cultures. Double immunofluorescence labeling with anti-Heph (**A, D, G, J**) and antibodies against the oligodendrocyte marker Gal-C (**B**), astrocyte maker GFAP (**E**), microglial marker OX42 (**H**) or the neuronal marker NeuN (**K**). Note that Heph is expressed in oligodendrocytes and microglia but not in astrocytes or neurons. Merged images showing the nuclear DAPI staining are shown in panels **C, F, I and L**. Scale bar in L=50 μm.

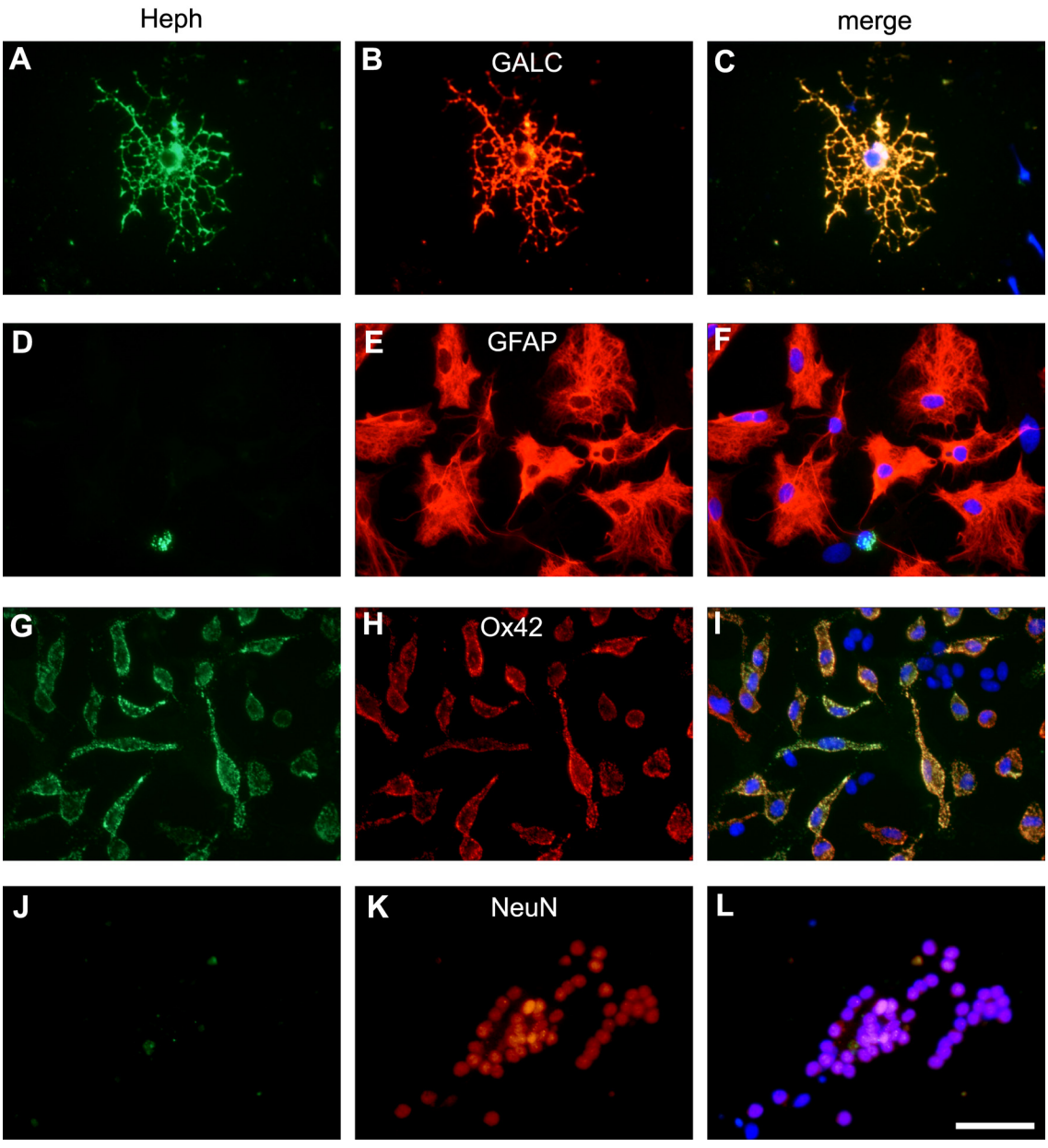
Heph
merge
A
B
GALC
C
D
E
GFAP
F
G
H
Ox42
I
J
K
NeuN
L

Figure 2

Heph and Fpn are only expressed in mature oligodendrocytes. Oligodendrocyte precursor cells were purified from neonatal rat cerebral cortex, allowed to mature *in vitro*, and double immunofluorescence labeling carried out. Staining with anti-Heph (**A, D, G**) or with Fpn (**J, M, P**) and the early OPC marker anti-A2B5 (**B, K**), the late OPC marker anti-O4 (**E, N**) or the marker for more mature oligodendrocytes anti-Gal-C (**H, Q**) shows that Heph and Fpn are only expressed in mature Gal-C^+ oligodendrocytes. Merged figures including DAPI staining of the nuclei are shown in **C, F, I, L, O** and **R**. Scale bar in R=50 μm.

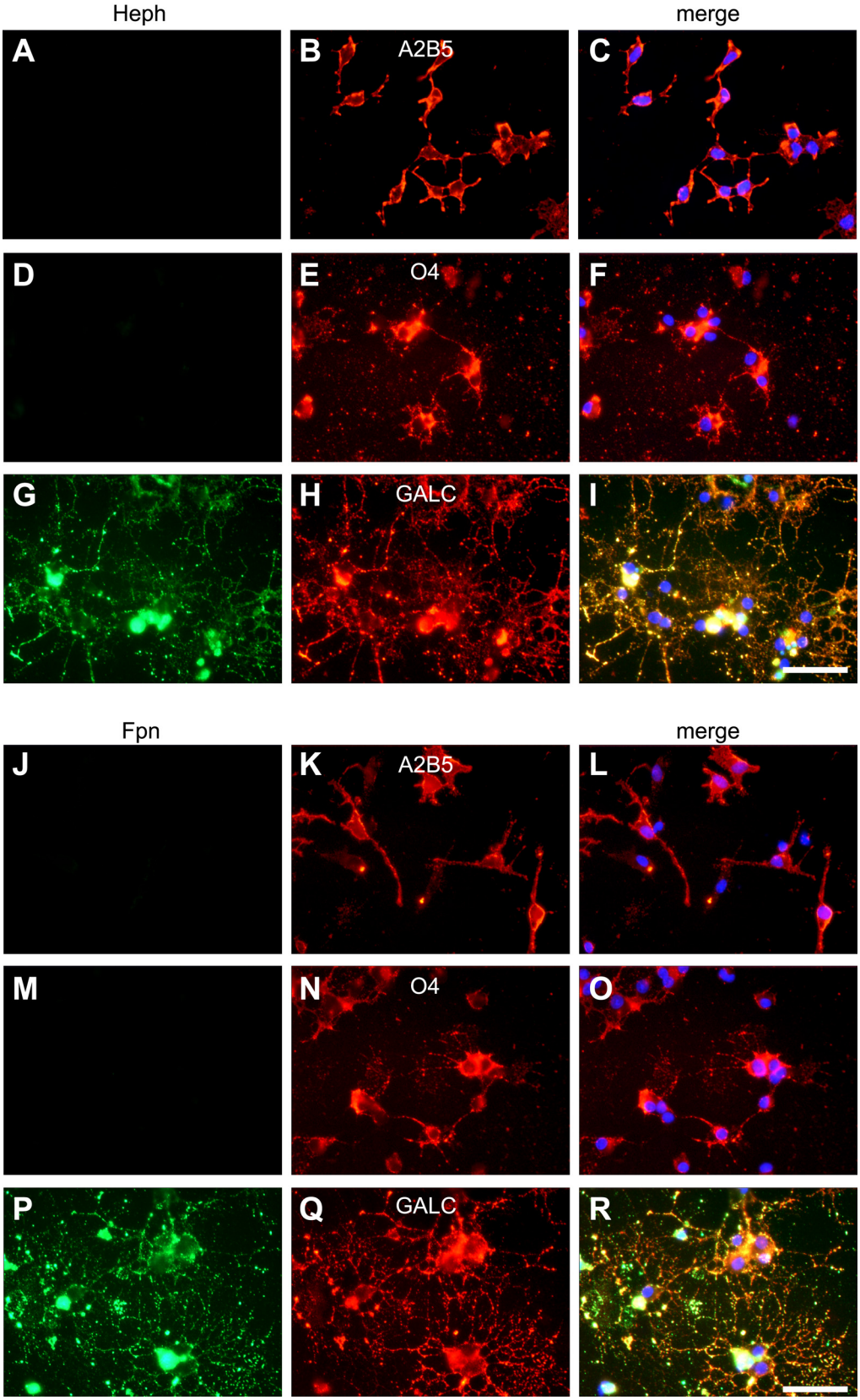
Heph
merge
A
B
A2B5
C
D
E
O4
F
G
H
GALC
I
Fpn
merge
J
K
A2B5
L
M
N
O4
O
P
Q
GALC
R

Figure 3

In vivo **expression of Heph and Fpn in the spinal cord and the role of Heph in iron efflux.** Double immunofluorescence labeling shows expression of Heph (**A**) and Fpn (**D**) in CC1-labeled oligodendrocytes (**B, E**) in a cross section of the adult mouse spinal cord. Arrows indicate cells that are double labeled for Heph/CC1 or Fpn/CC1. Arrowheads indicate CC1-negative cells that are Fpn^{+}. Panels **C** and **F** show merged images that include the nuclear DAPI labeling. Note also that Fpn is ubiquitously expressed. Scale bar in F=100 μm; inset=20 μm. **(G)** Western blot shows reduced expression of Heph in the spinal cord of sla mice which carries a mutation in the *heph* gene as compared to wildtype (WT) mice. Reprobing the blot for Fpn demonstrates equal Fpn levels in sla and WT mice. β-actin was used as a protein loading control. **(H)** An *in vitro* iron efflux assay using radiolabeled iron (^{55}Fe) was performed with oligodendrocytes obtained from neonatal sla and wildtype mice. Cells were loaded with iron-ascorbate containing ^{55}Fe for 6 h, washed, and cultured in non-radioactive medium. The amount of radiolabeled iron in the cell pellets was measured at 0, 12 and 24 h. Marked impairment of iron efflux is seen in cultures of sla oligodendrocytes as compared to wildtype cells. Measurements at each time point were done in triplicates and repeated in three separate experiments. Results are shown as mean ± SEM (n=3; *$p \leq 0.05$; Two-way ANOVA).

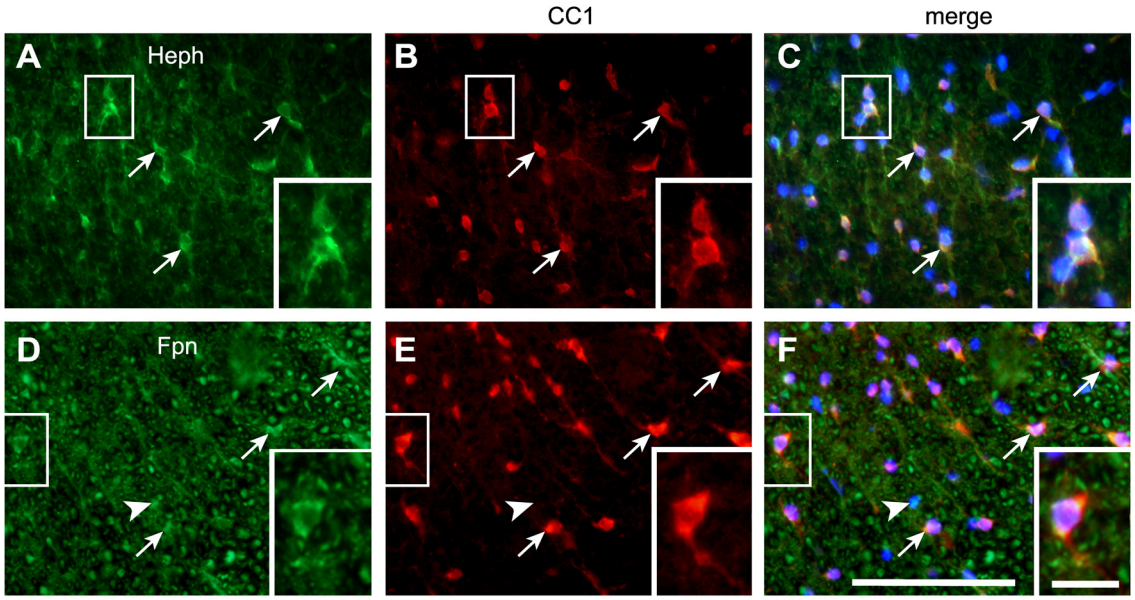
CC1
merge
A
Heph
B
C
D
Fpn
E
F

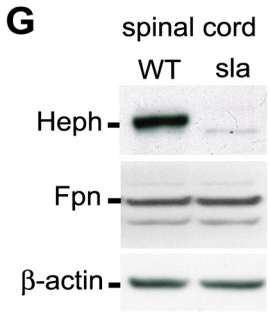
G
spinal cord
WT
sla
Heph
Fpn
β-actin

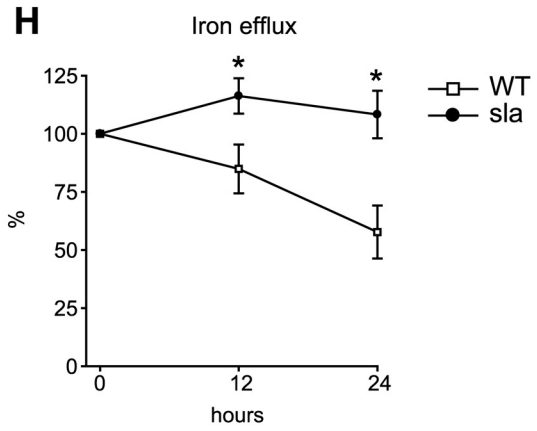
H
Iron efflux
125
100
75
50
25
0
%
0
12
24
hours
*
*
WT
sla

Figure 4

Iron accumulates in grey matter oligodendrocytes in the spinal cord of sla mice. (**A**) Perl's histochemistry shows no labeling for iron in 6 month-old wildtype mouse spinal cord. (**B**) In contrast, iron accumulation is abundant in the spinal cord grey matter in 6 month-old sla mouse. (**C-E**) Higher magnification images showing Perl's histochemistry of the ventral grey matter of the spinal cord shows that there is no iron accumulation in the grey matter of wildtype mice between 3 and 10 months of age. In contrast, increasing iron accumulation is seen in sla mice with age, at 3 months (**F**), 6 months (**G**) and 10 months (**H**) of age. Arrows in panel **F** indicate iron-loaded cells. Note in the inset in panel **H**, of an iron-containing cell that has a long processes resembling oligodendrocytes. Further confirmation that iron accumulation in the spinal cord grey matter of sla mice occurs in oligodendrocytes was obtained by double immunofluorescence labeling with anti-ferritin (**I, L**) as a surrogate marker for iron, and anti-CC1 (**J, M**) for oligodendrocytes. Merged images including DAPI stained nuclei are shown in panels **K and N**. Note the ferritin/CC1 double labeled cells in the sla spinal cord, indicated by arrows (**L-N**). Scale bars in B=500 μm; H=100 μm (inset=30 μm); N=50 μm.

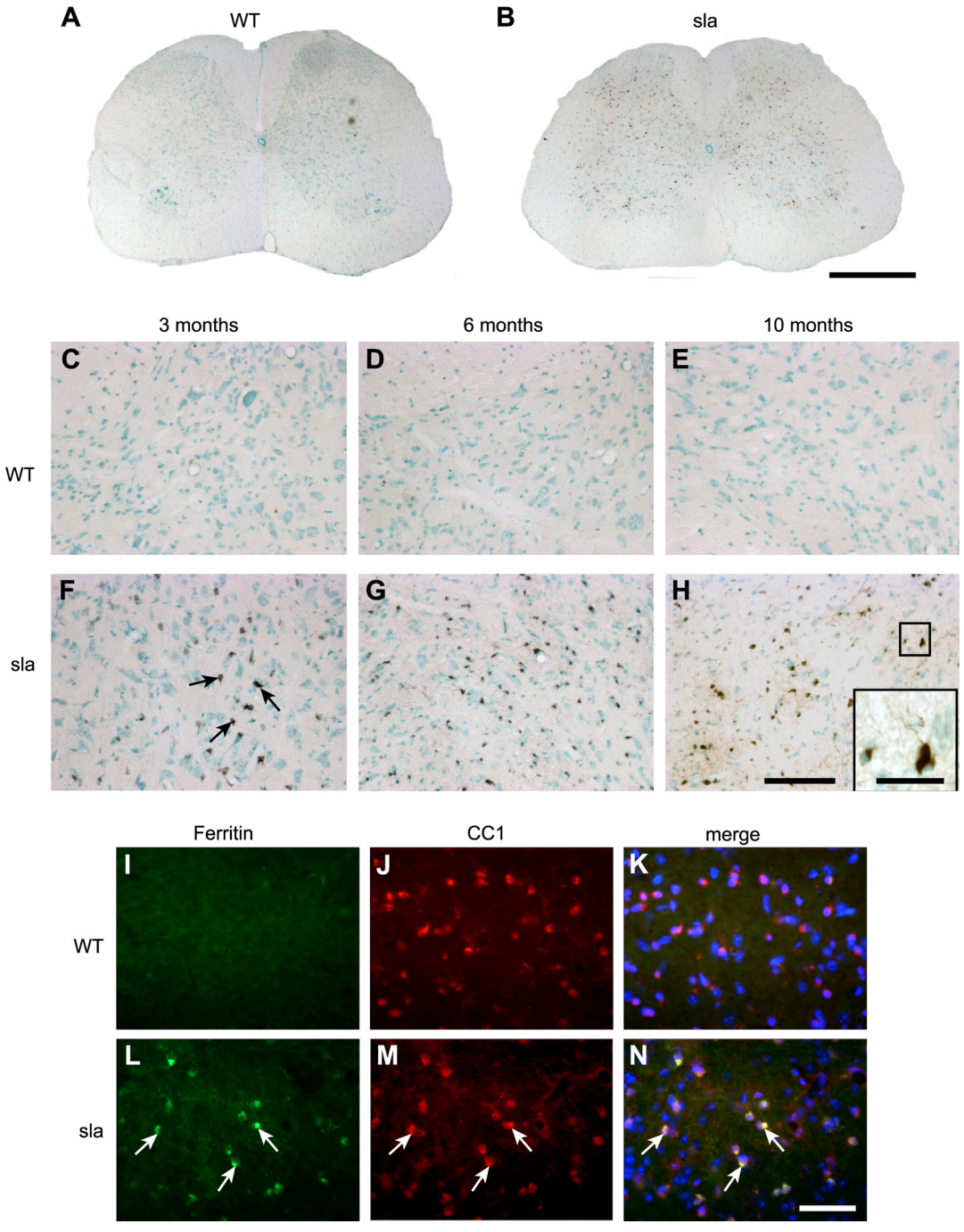
A
WT
B
sla
3 months
6 months
10 months
C
D
E
WT
F
G
H
sla
Ferritin
CC1
merge
I
J
K
WT
L
M
N
sla

Figure 5

Ultrastructural evidence of iron accumulation in oligodendrocytes in sla mice, the expression of iron influx proteins and effects on motor coordination. (**A**) Electron micrograph of oligodendrocyte from wildtype mouse shows no evidence of iron deposits in tissue prepared by perfusion Perl's histochemistry. (**B**) Higher magnification of the area outlined in panel A. (**C**) In contrast, electron micrograph of oligodendrocyte in a sla mouse shows clear evidence of iron deposits detected by perfusion Perl's histochemistry. Note the dark diaminobenzidine (DAB) reaction product indicating iron deposits. (**D**) Higher magnification of the area outlined in panel C showing the dark deposits of iron in the cytosol. Scale bars in A, B=2 μm; C, D=1 μm. (**E**) RT-PCR data showing mRNA expression of TfR1 and DMT1 are not significantly different in the sla spinal cord as compared to wildtype mice, whereas TIM-2 mRNA levels are decreased in the sla spinal cord. Results are shown as mean ± SEM (n=3; *$p \leq 0.05$; Student's *t* test). (**F**) Rotorod analysis shows that motor function in sla mice is significantly impaired at 9 months of age as compared to age-matched wildtype mice. The results are shown as the mean ± SEM (n=6; *$p \leq 0.05$; Two-way ANOVA).

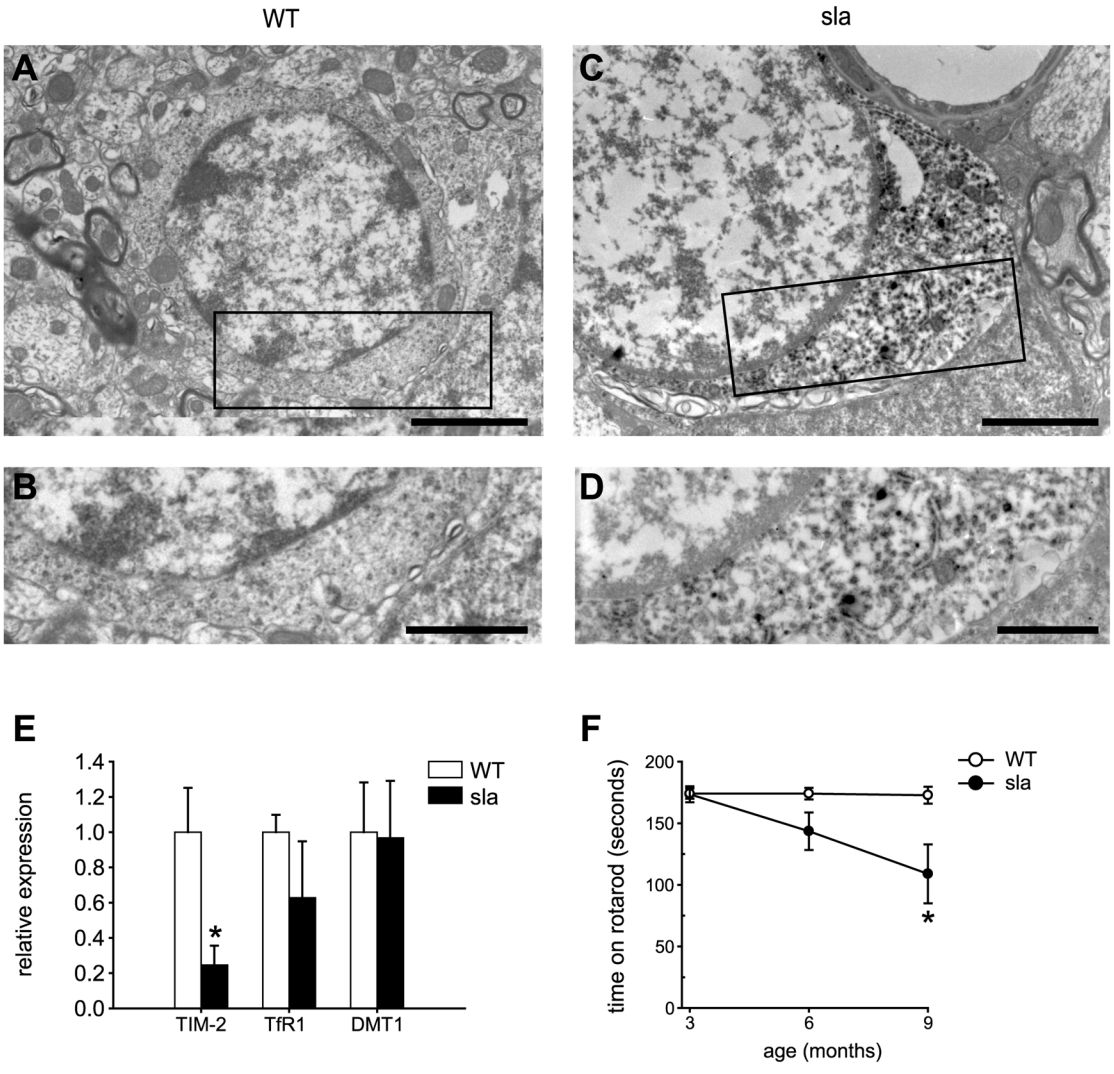
WT
sla
A
B
C
D
E
relative expression
1.4
1.2
1.0
0.8
0.6
0.4
0.2
0.0
WT
sla
*
TIM-2
TfR1
DMT1
F
time on rotarod (seconds)
200
150
100
50
0
WT
sla
*
3
6
9
age (months)

Figure 6

Expression of the paranodal protein Caspr is reduced in the sla spinal cord. (**A**) Cross section of wildtype mouse spinal cord shows strong immunofluorescence labeling for Caspr in grey and white matter. (**B**) In contrast, Caspr labeling is very weak in the sla spinal cord. The areas outlined in panels A an B are shown at higher magnification in panels **C** and **D,** respectively. (**E** and **F**) Quantification of the pixel density per μm^2 in the grey matter of the ventral horn and the ventral white matter of the cervical, thoracic and lumbar spinal cord shows a significant reduction of Caspr expression in sla mice as compared to wildtype mice. Results are shown as mean ± SEM (n=3; *$p \leq 0.05$; Two-way RM-ANOVA). Scale bars in B=500 μm; D=200 μm.

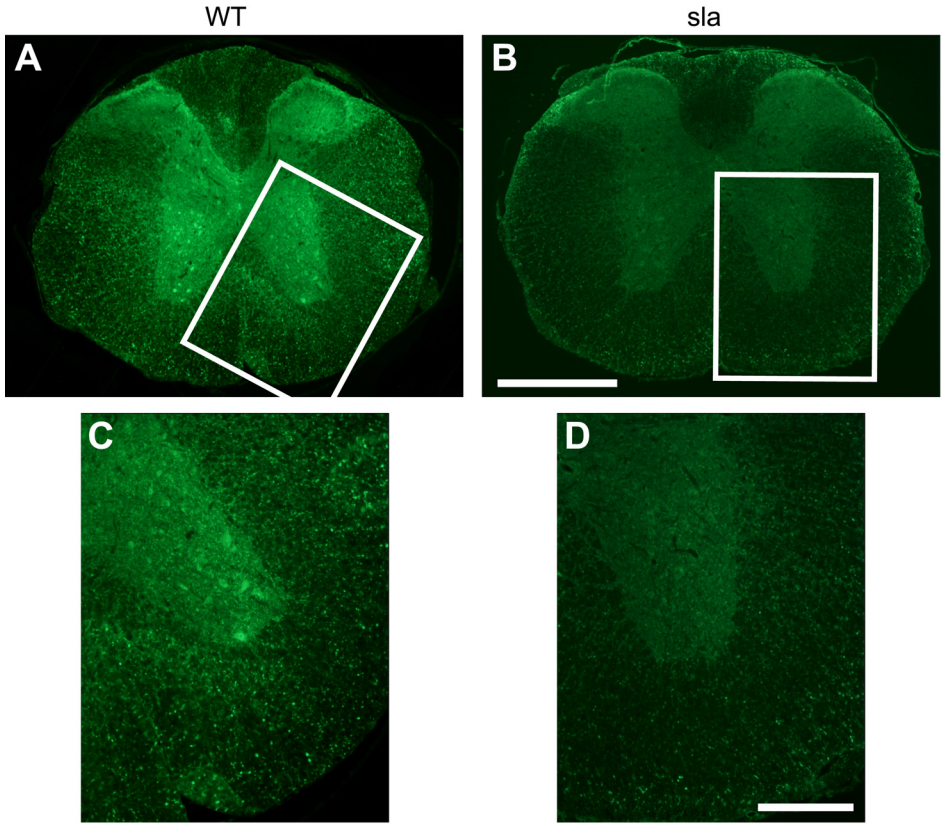
WT
sla
A
B
C
D

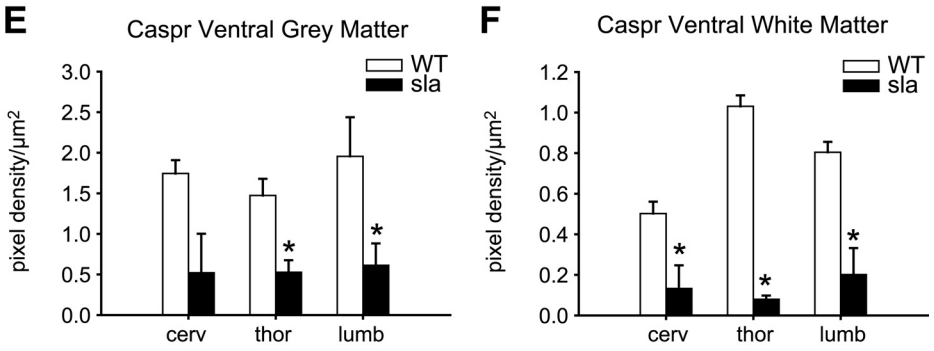
E
Caspr Ventral Grey Matter
WT
sla
pixel density/µm²
3.0
2.5
2.0
1.5
1.0
0.5
0.0
cerv
thor
lumb
F
Caspr Ventral White Matter
WT
sla
pixel density/µm²
1.2
1.0
0.8
0.6
0.4
0.2
0.0
cerv
thor
lumb

Figure 7

Reduced expression of Nogo A in oligodendrocytes in the sla spinal cord and ultrastructural abnormalities at the paranodal region in sla mice. (**A-C**) Wildtype spinal cord shows strong immunofluorescence labeling for Nogo A (arrows in A) in CC1 labeled oligodendrocytes (arrows in B). (**D-F**) In contrast, sla spinal cord shows markedly reduced labeling for Nogo A (arrows in D) in CC1 labeled oligodendrocytes (E). Panels C and F show merged images. (**G**) Quantification of the Nogo A pixel density per μm² of individual CC1-positive cells (30 per animal, n=3 mice) in the grey and white matter of the lumbar spinal cord shows a significant reduction of Nogo A expression in sla mice as compared to wildtype mice. Results are shown as mean ± SEM (n=3; *p≤0.05; Student's *t*-test). Scale bar in F=30 μm. (**H**) Electron micrograph of a paranodal region in the grey matter of a wildtype mouse. (**I**) The area of the paranode outlined in the rectangle in panel H is shown at higher magnification. Note the regularly arranged terminal myelin loops that are closely associated with the axonal membrane of the paranodal region. (**J**) In contrast, the paranodal region in the sla spinal cord grey matter shows abnormal structure. (**K**) shows a higher magnification of the area outlined in the rectangle in panel J. Note the multiple loops of myelin (labeled 1, 2, and 3), and the floating paranodal loops that fail to make contact with the axonal membrane (asterisks). Scale bars in H, J=1 μm and I, K=0.5 μm.

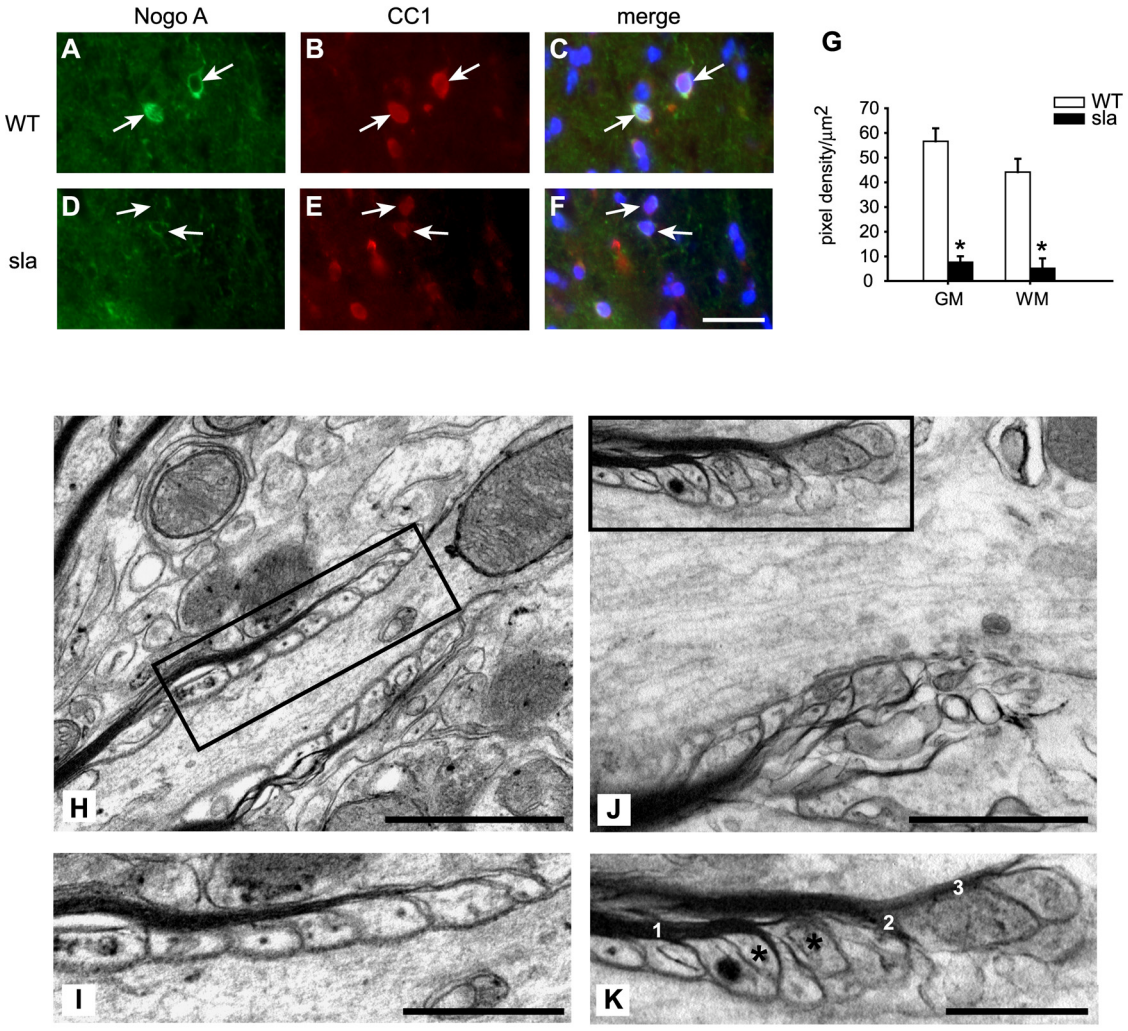
Nogo A
CC1
merge
WT
sla
A
B
C
D
E
F
G
pixel density/µm2
70
60
50
40
30
20
10
0
WT
sla
GM
WM
H
I
J
K
1
2
3

Figure 8

Expression of Cp is upregulated in white matter oligodendrocytes in sla mice. (**A**) RT-PCR analysis shows that cultured oligodendrocytes express mRNA for Heph, Fpn as well as Cp. In contrast, oligodendrocytes do not express Cp protein (data not shown). RNA isolated from the intestinal cell line Caco2 is included as a positive control for Heph and Fpn and a negative control for Cp. PPIA levels demonstrate that equal amounts of RNA were used. (**B**) Western blot shows that Cp expression is increased in the spinal cord of sla mice as compared to wildtype (WT) mice. Spinal cord protein extract of Cp KO ($Cp^{-/-}$) mice was used as a negative control. The blot was reprobed for β-actin to ensure equal protein loading. (**C**) Quantification of the Western blot data shows a significant increase of Cp expression in the spinal cord of sla mice. Results are shown as mean ± SEM; (n=3; *p≤0.05; Student's *t*-test). (**D** and **E**) *In situ* hybridization for Cp on spinal cord cross sections shows upregulation of Cp expression in the white matter of sla mice (E) as compared to wildtype mice (D). The dashed lines outline the boundary between grey (g) and white (w) matter. (**F**) Quantification of the number of Cp positive cells in the grey and white matter of sla spinal cord shows that Cp induction is markedly greater in the white matter as compared to the grey matter. Results are shown as mean ± SEM (n=3;*p≤0.05; Student's *t*-test). (**G-I**) Higher magnification of the sla spinal cord white matter showing *in situ* hybridization for Cp (**G**) combined with immunofluorescence labeling with anti-CC1 for oligodendrocytes (**H**), indicating that Cp expression is upregulated in white matter oligodendrocytes (arrows). (**J-L**) In contrast, there is no Cp expression (**J**) in CC1-positive oligodendrocytes (**K**) in wildtype (WT) mice. Panels **I** and **L** show merged images. Scale bars in E=100 μm; L=50 μm.

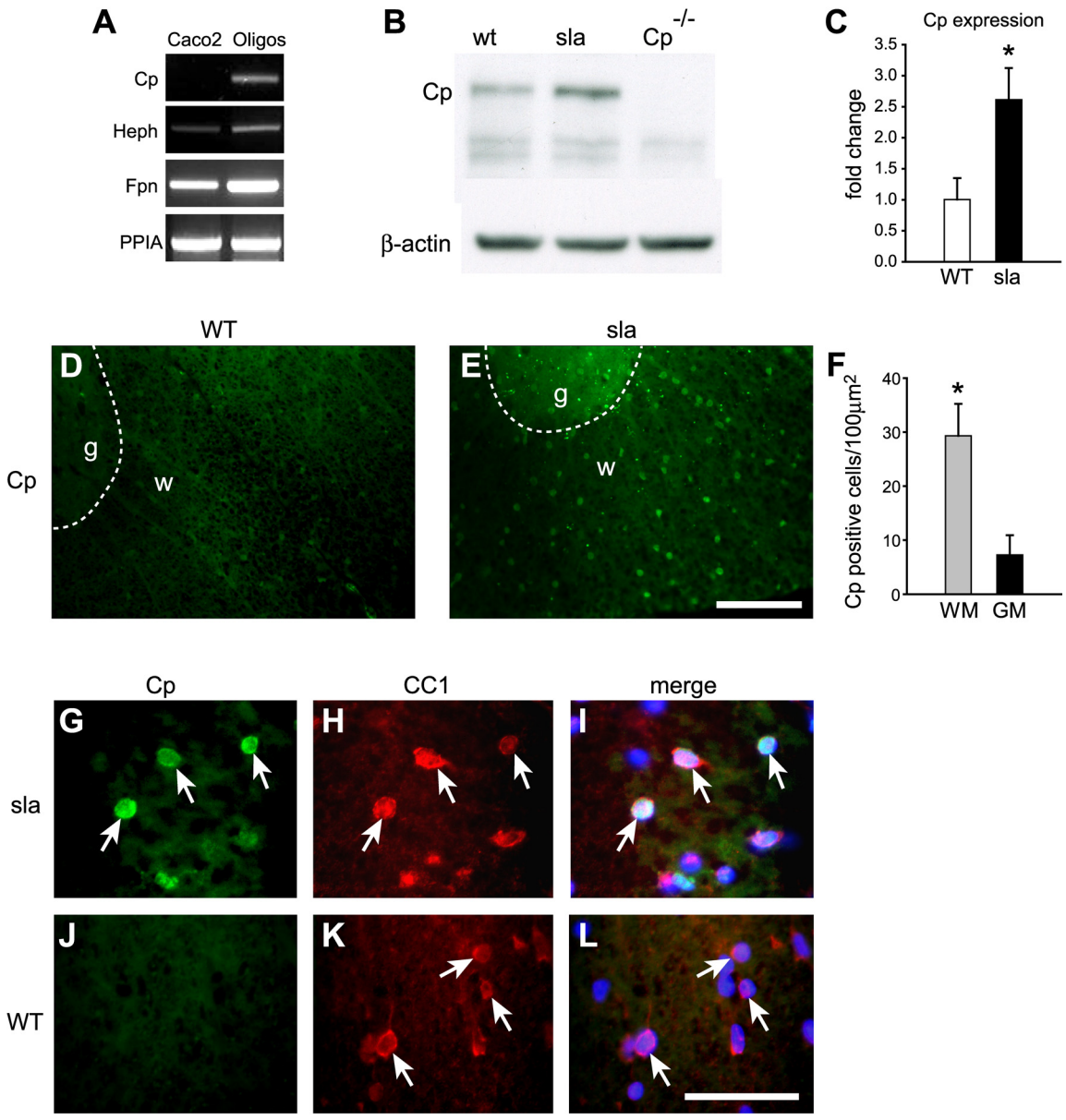
A
Caco2 Oligos
Cp
Heph
Fpn
PPIA
B
wt
sla
Cp -/-
Cp
β-actin
C
Cp expression
fold change
3.5
3.0
2.5
2.0
1.5
1.0
0.5
0.0
*
WT
sla
WT
sla
D
E
Cp
g
w
g
w
F
Cp positive cells/100μm2
40
30
20
10
0
*
WM
GM
Cp
CC1
merge
G
H
I
sla
J
K
L
WT

Figure 9

Iron accumulation occurs in spinal cord grey and white matter in *Heph^{sla}/Cp$^{-/-}$* double mutant mice. (**A, B**) Perl's histochemistry of spinal cord cross sections of 12 month-old wildtype (**A**) and *Heph^{sla}/Cp$^{-/-}$* (**B**) mice. Note the marked iron labeling in both the grey and white matter of the *Heph^{sla}/Cp$^{-/-}$* double mutant mouse in panel B. (**C, D**) Higher magnification micrographs showing Perl's staining of the ventral white matter region of wildtype (**C**) and *Heph^{sla}/Cp$^{-/-}$* (**D**) spinal cord. Note there is no iron labeling in the wildtype spinal cord (C) but marked iron accumulation in the white matter in the *Heph^{sla}/Cp$^{-/-}$* double mutant (D). The cell indicated in the rectangle in panel D is illustrated at higher magnification in the inset which shows an iron-loaded cell with the morphology of an oligodendrocyte that sends processes that appear to wrap around axons (arrows). (**E-G**) Immunofluorescence labeling of spinal cord cross sections with anti-ferritin used as a surrogate marker for iron shows very weak ferritin immunoreactivity in the wildtype mouse (**E**), strong ferritin immunoreactivity in the grey matter in sla mouse (**F**) and strong ferritin immunoreactivity in both the grey and white matter in the *Heph^{sla}/Cp$^{-/-}$* mouse (**G**). **(H-M)** Double immunofluorescence labeling with anti-ferritin (**H, K**) and the oligodendrocyte marker anti-CC1 (**I, L**) shows strong ferritin immunoreactivity in white matter oligodendrocytes in *Heph^{sla}/Cp$^{-/-}$* mouse spinal cord (arrows in K-M) but not in the wildtype mouse (H-J). The merged images that include DAPI stained nuclei are shown in panels **J** and **M**. Scale bars in B, G=500 μm and D, M=50 μm.

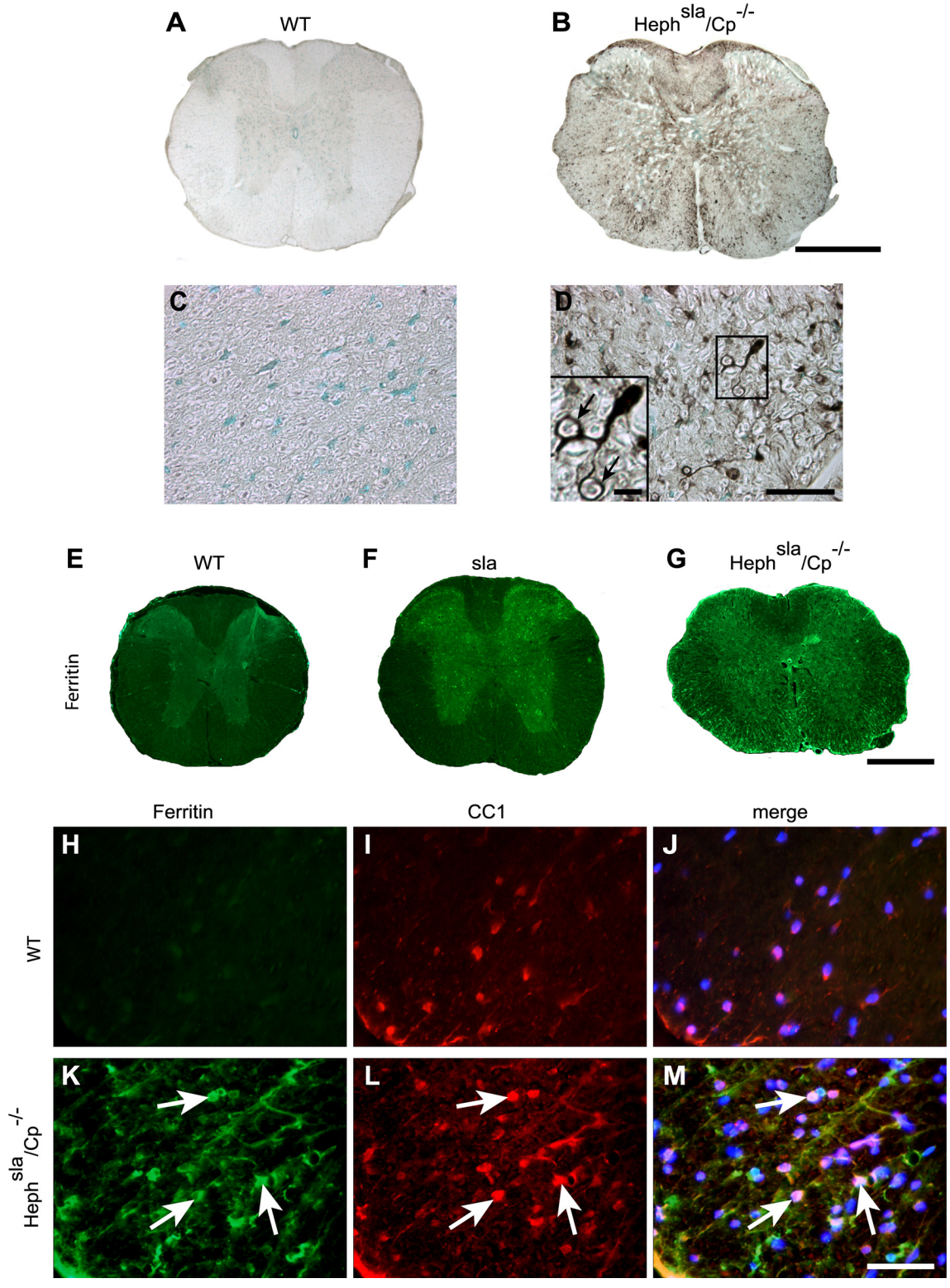
A
WT
B
Heph sla /Cp -/-
C
D
E
WT
F
sla
G
Heph sla /Cp -/-
Ferritin
Ferritin
CC1
merge
H
I
J
WT
K
L
M
Heph sla /Cp -/-

Chapter 3

Iron efflux from astrocytes is required for remyelination

Katrin Schulz, Nancy C. Andrews, Magdalena Götz and Samuel David

*The work presented in this chapter has been submitted for publication.

3.1 Preface

In the previous chapter, I showed that Heph is expressed by oligodendrocytes and plays a role in iron efflux from these glial cells. My findings also indicate that grey and white matter oligodendrocytes regulate iron efflux differentially by utilizing different ferroxidases. These results further demonstrate the importance of iron efflux mechanisms in maintaining stable intracellular iron levels. In the present chapter, I investigated the role of iron efflux in transporting iron between cells in the CNS. In particular, I focussed on how iron is delivered from the BBB to different cell types in the CNS. As part of the BBB, astrocytes are ideally located to take up iron from endothelial cells and export it to other CNS cells. Since this might be especially important in situations of high iron demand, I examined whether iron efflux from astrocytes is required for providing iron to OPCs and microglia during remyelination. To study this, I generated conditional deletion of Fpn in astrocytes *in vivo*.

3.2 Abstract

Iron plays a role in myelination as it is a cofactor for enzymes involved in lipid and cholesterol synthesis. Since astrocytic processes form endfeet around CNS capillaries, they are ideally located to take up iron from the circulation and distribute it to other CNS cells. Iron delivery by astrocytes might be especially important in a situation of high iron demand such as remyelination. To study this we generated a mouse with a conditional deletion of the iron efflux transporter ferroportin (Fpn) in astrocytes, and induced focal demyelination in the dorsal column white matter of the spinal cord by lysophosphatidylcholine (LPC) injections. Remyelination was analyzed by electron

microscopy 10 days after LPC injection. Quantification of the g-ratio revealed reduced remyelination in the astrocyte-specific Fpn knockout mice as compared to wildtype controls. Ki67 labeling revealed reduced proliferation of oligodendrocyte precursor cells in the Fpn knockout animals, which may contribute to the impaired remyelination. We further investigated whether lack of iron affects the ability of microglia to express cytokines involved in remyelination, such as TNF-α and IL-1β. Iron-deficient microglia in culture expressed reduced levels of these cytokines. This in turn could affect the ability of astrocytes to produce growth factors required for myelination, as astrocytes in culture were found to express high levels of FGF-2 in response to IL-1β, and IGF-1 in response to TNF-α stimulation. These data suggest that iron efflux from astrocytes is required for remyelination by either direct effects on oligodendrocyte precursor cells or indirectly by affecting glial activation.

3.3 Introduction

Remyelination can occur spontaneously in response to myelin damage in order to restore saltatory conduction of the action potential and to prevent axonal degeneration (Smith et al., 1979). However, the extent of remyelination that is observed in neurological conditions such as multiple sclerosis is limited (Franklin, 2002). In the central nervous system (CNS), remyelination is primarily carried out by oligodendrocyte precursor cells (OPCs) (Franklin and Ffrench-Constant, 2008). Following demyelination, OPCs proliferate and differentiate into myelinating oligodendrocytes. A number of growth factors have been identified that regulate the proliferation and differentiation phase of OPCs, such as fibroblast growth factor 2 (FGF-2) and insulin-like growth factor 1 (IGF-

1) (Frost et al., 2003; Wilson et al., 2003; Hsieh et al., 2004). In addition, cytokines such as tumor necrosis factor α (TNF-α) and interleukin-1β (IL-1β) have also been implicated in the remyelination process (Arnett et al., 2001; Mason et al., 2001).

An important metal ion required for myelination is iron. Iron is directly involved in the synthesis of myelin as an essential cofactor for enzymes involved in lipid and cholesterol synthesis (Connor and Menzies, 1996; Todorich et al., 2009). In addition, iron plays a role in proliferation and differentiation of cells because it is required for enzymes involved in the energy metabolism as well as DNA synthesis (Robbins and Pederson, 1970; Hoffbrand et al., 1976; Cazzola et al., 1990). However, not much is known about the role of iron in remyelination and how iron is made available to OPCs for proliferation and differentiation. Iron is thought to enter the CNS via capillary endothelial cells at the level of the blood brain barrier (Moos et al., 2007). Since about 95% of the capillary surface in the CNS is covered by astrocytic processes called endfeet, astrocytes are ideally located to take up iron from the circulation via endothelial cells and distribute it to other cell types in the CNS. Astrocytes possess the iron influx and efflux mechanisms that are required for cell-to-cell transport of iron. Iron import in astrocytes has been suggested to occur via the divalent metal transporter-1 (DMT1), which is especially high expressed in the astrocytic endfeet that contact the blood vessels (Burdo et al., 2001). Iron efflux from astrocytes is mediated by the ubiquitously expressed iron exporter ferroportin (Fpn) together with the ferroxidase ceruloplasmin (Cp), which oxidizes the ferrous iron (Fe^{2+}), that is transported through Fpn to the ferric form of iron (Fe^{3+}) (Jeong and David, 2003). Studies on Cp null mice that lack iron efflux from astrocytes showed that iron accumulates in astrocytes of Cp null mice with aging, and that this is

accompanied by neuronal death likely due to iron starvation of the neurons (Jeong and David, 2006). In the present study, we investigated whether astrocytes play a role in delivering iron to OPCs during remyelination, a situation that requires high amounts of iron. To study this, we generated mice that are deficient in astrocytic iron efflux by deleting the iron exporter Fpn specifically in astrocytes and induced chemically-induced demyelination in the spinal cord by injecting lysophosphatidylcholine (LPC) into the dorsal white matter of the spinal cord. Remyelination was assessed 10 days after LPC injection. We also examined OPC proliferation in the site of demyelination and remyelination. In addition, cell culture studies were carried out on astrocyte and macrophage cultures to assess the effects of iron retention and iron depletion on the expression of growth factors and cytokines that might contribute to remyelination *in vivo*. The data obtained support a role for astrocytes in providing iron for remyelination and underline the importance of iron in the remyelination process.

3.4 Materials and Methods

Animals. All animal procedures were approved by the Animal Care Committee of the Research Institute of the McGill University Health Centre and followed the guidelines set by the Canadian Council on Animal Care. Astrocyte-specific conditional deletion of Fpn, the iron efflux transporter was generated by crossing GLAST::CreERT2 mice (Mori et al., 2006) with $Fpn^{flox/flox}$ mice (Donovan et al., 2005) to generate GLAST::CreERT2; $Fpn^{flox/flox}$ mice. Tamoxifen was administered to 6-8 week old GLAST::CreERT2; $Fpn^{flox/flox}$ mice. Tamoxifen (Sigma) was dissolved in corn oil (sigma)/ethanol (9:1) at 10

mg/mL and 1 mg was injected intraperitoneally twice a day for 5 days. Control animals of the same genotype were injected with vehicle.

LPC injections. GLASTCre::ERT2;Fpn$^{flox/flox}$ mice between 8 and 10 weeks of age (two weeks after the last tamoxifen injection) were anaesthetized with ketamine/xylazine/acepromazine (100/10/3 mg/kg) and a laminectomy was performed to expose the spinal cord at the 11th thoracic vertebral level (T11). Using a glass micropipette with a tip diameter less than 50 μm, 1 μL of 1% LPC was injected into the dorsal column white matter immediately adjacent to the midline dorsal artery as previously described (Ousman and David, 2000).

PCR genotyping. DNA was extracted from brain, spinal cord and liver using the DNeasy blood & tissue kit (Qiagen) and PCR was performed using the Advantage® 2 PCR Kit (Clontech Laboratories inc). GLAST::CreERT2; Fpn$^{flox/flox}$ mice were genotyped with one PCR reaction that had one forward primer (5′-CTA CAC GTG CTC TCT TGA GAT-3′) and two reverse primers (5′-GGT TAA ACT GCT TCA AAG G-3′ and 5′-CCT CAT ATG TGA GTC AAA GTA TAG-3′). The Fpn wildtype allele generated a 355 bp band, and the Fpn floxed allele generated a 522 bp band. The band generated by full deletion of Fpn was 398 bp.

Electron microscopy. Animals were sacrificed 10 days after LPC injections by transcardiac perfusion with 0.5% paraformaldehyde and 2.5% glutaraldehyde in 0.1 M phosphate buffer (pH 7.4). Spinal cord segments containing the lesion site were removed

and post-fixed overnight in the same fixative. Segments were then cut transversely into 1 mm thick slices, which were further fixed in 2% osmium tetroxide for 2 hrs at room temperature and processed for embedding in Epon. One μm thick cross-sections of the spinal cord were cut, stained with 1% toluidine blue and examined by light microscopy. Ultrathin sections of the lesion site were cut and stained with lead citrate. Sections were viewed with a Philips CM 10 electron microscope.

G-ratio analysis. The ratio of the axon diameter over the fibre (axon + myelin) diameter (g-ratio) of axons located at the rostrocaudal mid-point of LPC injections was measured from electron micrographs. Briefly, EM images of cross-sections of the lesion site were taken at 1,550× magnification (10-15 images per animal). Digitized images were analyzed with the BioQuant Nova Prime image analysis system (BioQuant Image Analysis Corp., Nashville). Since the axons were not always circular, the diameters were calculated from measurements of the axonal circumference and the fiber circumference (i.e., outside the myelin sheath) based on the following formula: $d=p/\pi$ (where d=diameter; p=perimeter measurement). 100 axons per animal were analyzed (n=3 animals per group) and statistical significance was determined by two-way RM-ANOVA. Post-hoc Tukey tests were performed for comparisons between groups. The data are plotted as means ± SEM.

Immunofluorescence labeling. Animals were perfused with 4% paraformaldehyde in 0.1 M phosphate buffer (pH 7.4). Spinal cord segments containing the lesion site were removed, post-fixed for 2 hrs in the same fixative and cryoprotected in 30% sucrose. 14

μm cryostat sections were obtained and double immunofluorescence was performed using rat anti-GFAP (1:200; Invitrogen) and rabbit anti-Cre recombinase (1:400; Covance) or goat anti-olig2 (1:200; R&D Systems) and rabbit anti-Ki67 antibody (1:800; Abcam) as described previously (Jeong and David, 2006; Rathore et al., 2008).

Quantification of immunofluorescence labeling. Images were captured with a Retiga 1300 C digital camera (QImaging Corp., Burnaby, British Columbia) using a Zeiss AxioSkop II light microscope (Carl Zeiss Canada Ltd., Toronto), and analyzed with the BioQuant Nova Prime image analysis system (BioQuant Image Analysis Corp., Nashville). Olig2- and Ki67 double-labeled cells were counted at the rostrocaudal mid-point of the lesion and divided by the area of the respective lesion. Counts were obtained from three sections per animal and averaged (n=4 animals per group). Only animals with comparable lesion size were analyzed (mean lesion site: CTRL= 0.082 ± 0.001 mm^2; KO = 0.085 ± 0.005 mm^2).

Western blotting. Animals were sacrificed two weeks after the last tamoxifen injection and spinal cord, brain and liver tissue were removed. Protein was extracted, separated by SDS-PAGE and transferred onto a a polyvinylidene difluoride membrane (Bio-Rad). The blot was incubated with rabbit anti-Fpn IgG (1:1500; Alpha Diagnostics) overnight. Primary antibodies were visualized by incubation with horseradish peroxidase conjugated anti-rabbit antibody which was detected using the enhanced chemoluminescence Kit (Perkin Elmer). Blots were reprobed for β-actin to ensure equal protein loading.

Cell culture. Microglia cultures were prepared from neonatal mouse cerebral cortex as described previously (Saura et al., 2003). In brief, after dissection of cortices, meninges were removed and the tissue dissociated in 0.125% trypsin. Cells were plated onto poly-L-lysine coated tissue culture flasks in Dulbecco's modified eagle medium containing F12 (DMEM /F12) and 10 % fetal bovine serum (FBS). After 14 days in culture, mixed glia cultures were trypsinized with 0.0625% trypsin and 1 mM EDTA (pH 8.0) for 5-10 min to separate the upper layer of cells from the microglia attached to the bottom of the flask. Microglia were then washed and incubated with fresh DMEM/F12 containing 10% FBS and conditioned media from mixed glia cultures (50:50). Microglial purity examined using Mac-1 immunoreactivity was ~97%. Microglia were incubated with 10 ng/mL lipopolysaccharide (LPS from *E.coli* O111:B4) and 100 μM salicylaldehyde isonicotinoyl hydrazone (SIH) overnight. SIH is an analog of pyridoxal isonicotinoyl hydrazone that shows high affinity and selectivity for iron (Richardson and Ponka, 1998b). NaOH was used to dissolve SIH. Astrocyte cultures were prepared as described previously (Jeong and David, 2003). To load astrocytes with iron, cells were incubated overnight with 40 μM $FeCl_3$ together with L-ascorbate (molar ratio of $FeCl_3$ to L-ascorbate was 1:44). The next day, astrocytes were either incubated with 10 ng/mL TNF-α or 10 ng/mL IL-1β overnight.

RT-PCR. RNA was isolated from astrocyte and microglia cultures using the RNeasy Minikit (Qiagen) and reverse transcribed to cDNA with the Omniscript Reverse Transcriptase Kit (Qiagen). PCR was performed using the HotStarTaq PCR Kit (Qiagen) with the following primers: TGF-β_for: 5'-TGA TAC GCC TGA GTG GCT GTC TTT-

3'; TGF-β_rev: 5'-TGT ACT GTG TGT CCA GGC TCC AAA-3'; IGF-1_for: 5'-ACC TCA GAC AGG CAT TGT GGA TGA-3'; IGF-1_rev: 5'-CAG GTT GCT CAA GCA GCA AAG GAT-3'; FGF-2_for: 5'-AAC AGT ATG GCC TTC TGT CCA GGT-3'; FGF-2_rev: 5'-AAG AGC GAC CCA CAC GTC AAA CTA-3'; IL-1β_for: 5'-AAG TTT GTC ATG AAT GAT TCC CCT C-3'; IL-1β_rev: 5'-GTC TCA CTA CCT GTG ATG AGT-3'; TNF-α_for: 5'-ATG AGC ACA GAA AGC ATG-3'; TNF-α_rev: 5'-GAA GAC TCC TCC CAG GTA-3'.

3.5 Results

Generation of astrocyte-specific Fpn knockout mice. Since astrocytes are involved in forming and maintaining the blood brain barrier with their astrocytic endfeet tightly ensheathing the brain microvasculature, they are ideally located to take up iron from endothelial cells and deliver it to other cells in the CNS. To investigate the role of iron efflux from astrocytes in providing iron for remyelination, we first generated mice lacking the sole known iron exporter Fpn specifically in astrocytes by using the tamoxifen-inducible CreERT2/loxP system. We crossed mice that carry the homozygous floxed Fpn allele ($Fpn^{flox/flox}$ mice) to transgenic mice expressing the Cre recombinase under the control of the astrocyte specific L-glutamate/L-aspartate (GLAST) promoter (GLAST::CreERT2 mice). To ensure timed specific deletion of Fpn in adult astrocytes, we used the tamoxifen-inducible Cre system, which allows us to control the time point of Fpn inactivation. Therefore, we injected GLAST::CreERT2; $Fpn^{flox/flox}$ mice at 6-8 weeks of age with tamoxifen to ensure specific inactivation of Fpn in astrocytes. PCR analysis using primers that selectively recognize the recombined Fpn allele shows Fpn

deletion in DNA from brain and spinal cord but not in the liver of tamoxifen-treated animals, nor in vehicle-treated animals (Fig. 1A). The floxed allele is present in all tissues (Fig. 1A). The excision of Fpn was further confirmed at the protein level by western blotting. Fpn protein expression is reduced in the spinal cord and brain of tamoxifen-treated compared to vehicle-treated mice (Fig. 1B). Furthermore, double immunofluorescence labelling using an anti-Cre recombinase antibody and the astrocyte marker anti-GFAP shows expression of Cre recombinase in astrocytes in the spinal cord of GLAST::CreERT2; $Fpn^{flox/flox}$ mice (Figure 1C-H). Administration of tamoxifen results in the translocation of Cre recombinase from the cytosol into the nucleus, where it can then perform the recombination of the floxed Fpn allele. While the Cre recombinase is located in the cytosol of astrocytes in vehicle-treated animals (Fig. 1C-E), it is localized in the nucleus in tamoxifen-treated animals (Fig. 1F-H), indicating the activation of Cre with tamoxifen treatment. Together, these data confirm the excision of Fpn in astrocytes using the tamoxifen-inducible Cre/LoxP system.

Remyelination is impaired in astrocyte-specific Fpn knockout mice. In order to assess whether remyelination was altered in astrocyte-specific Fpn knockout (KO) mice, we used the LPC-induced demyelination/remyelination model. Injections of LPC into the spinal cord causes focal demyelination within 2-3 days followed by remyelination starting around 7 days after injections (Hall, 1972; Jeffery and Blakemore, 1995; Ousman and David, 2000). LPC was injected into the dorsal white matter of the spinal cord in astrocyte-specific Fpn KO mice and control mice 2 weeks after the last tamoxifen or vehicle injection. All control animals were GLAST::CreERT2; $Fpn^{flox/flox}$ littermates that

had been injected intraperitoneally with vehicle instead of tamoxifen 2 weeks before intraspinal LPC injections. From now on, we will refer to these vehicle-treated animals as control mice. Toluidine blue staining of epon-embedded spinal cord sections shows the lesion site in the dorsal white matter (Fig. 2A and B). To assess remyelination, ultrathin sections of the lesion site were analyzed by electron microscopy. Remyelinated axons can be identified by their thin myelin sheet in relation to the axon diameter. Several remyelinating axons with thin myelin sheaths can be seen in the LPC-injected control animals (Fig. 2C). In contrast, very few remyelinated axons are detected in the astrocyte-specific Fpn KO mice after LPC injection (Fig. 2D). The percentage of remyelinated axons present in the lesion area was determined by the analysis of the g-ratio; i.e. the axon diameter/fibre diameter (Foster et al., 1980). A g-ratio of 1 indicates demyelinated or unmyelinated axons, whereas a g-ratio $\geq$ 0.9 indicates remyelinated axons. Normal myelinated axons have a g-ratio between 0.7 and 0.8. Quantification shows that 51.03 ± 6.02% of counted axons within the lesion site of control animals have already started remyelination and only 33.76 ± 5.35% are still demyelinated (Fig. 2E). In contrast, in the astrocyte-specific Fpn KO mice, only 25.26 ± 3.53% of axons are remyelinated and 66.24 ± 4.22% are still demyelinated (Fig. 2E), indicating that remyelination is impaired in the astrocyte-specific Fpn KO mice. These results suggest that iron efflux from astrocytes via Fpn is required for remyelination.

Proliferation of oligodendrocyte precursor cells is impaired. The process of remyelination involves the proliferation and differentiation of OPCs into myelinating oligodendrocytes. Since iron is an essential cofactor for several enzymes involved in cell

proliferation, energy metabolism as well as in myelin synthesis in particular, iron is likely to play a role in the proliferation and differentiation of OPCs. Since in the astrocyte-specific Fpn KO mice, iron is retained within the astrocytes, OPCs might not receive enough iron for proliferation and differentiation. We therefore assessed whether the reduced remyelination seen in astrocyte-specific Fpn KO mice may be due to a decrease in OPC proliferation. Double immunofluorescence in the lesion site 10 days after LPC injection using the proliferation marker anti-Ki67 and the OPC marker anti-olig2 shows a reduction in proliferating OPCs in the astrocyte-specific Fpn KO mice (Fig. 3A-F) compared to control animals (Fig. 3G-L). Quantification of the immunostaining confirmed that there is a significant reduction in the number of proliferating OPCs in the lesion site in astrocyte-specific Fpn KO mice as compared to control animals (Fig. 3M). These results suggest that reduced OPC proliferation may contribute to the impaired remyelination seen in the astrocyte-specific Fpn KO mice. Thus, iron delivery from astrocytes to OPCs appears to be required for the proliferation of OPCs after LPC-induced demyelination.

The expression of TNF-α and IL-1β is reduced in iron-deficient microglia. Macrophages and microglia play a critical role in remyelination by clearing the myelin debris that is generated during demyelination and by secreting growth factors and cytokines that promote the proliferation and differentiation of OPCs (Kotter et al., 2005; Linker et al., 2009; Neumann et al., 2009). Since in our astrocyte-specific Fpn KO mice, the iron is held back in the astrocytes, not only OPCs but also microglia might be iron-deprived. We therefore investigated whether iron deficiency can alter microglia

activation and thus their ability to express cytokines. To address this, we used microglia cultures to assess the expression levels of TNF-α and IL-1β, two cytokines that have been implicated in remyelination, under iron deficient conditions. Purified microglia from mouse cerebral cortex were treated with the iron chelator SIH to render them iron-deficient and stimulated with LPS to activate them and to induce cytokine expression. RT-PCR analysis of LPS-activated microglia shows high mRNA expression levels of TNF-α and IL-1β which are reduced in the presence of the iron chelator SIH (Fig. 4), indicating that iron is required for the LPS-stimulated expression of TNF-α and IL-1β. These data suggest that microglia in the astrocyte-specific Fpn KO mice which may be iron-deficient might also express lower levels of TNF-α and IL-1β, and thus contribute to impaired remyelination in these mice. TNF-α and IL-1β could either directly affect OPC proliferation and differentiation or activate astrocytes to produce growth factors, which could in turn act on remyelinating OPCs.

The expression of growth factors by astrocytes under high iron conditions. Cytokine-activated astrocytes are known to secrete growth factors such as FGF-2 and IGF-1 that promote OPC proliferation and differentiation (Liberto et al., 2004; Moore et al., 2010). Since astrocytes in the astrocyte-specific Fpn KO mice are likely to accumulate iron, we investigated whether astrocytes change their ability to express growth factors under high iron conditions. We purified astrocytes from neonatal mouse cerebral cortex and loaded them with iron-ascorbate overnight. Astrocytes were then treated with either TNF-α or IL-1β to stimulate the production of growth factors involved in OPC proliferation and differentiation such as FGF-2 and IGF-1. RT-PCR analysis showed upregulation of FGF-

2 and IGF-1 mRNA levels by IL-1β and TNF-α, respectively (Fig. 5A and B). Iron loading did not affect the expression of these growth factors (Fig. 5A and B). However, the reduced expression of TNF-α and IL-1β by iron-deprived microglia might result in decreased astrocyte activation and thus in reduced expression of FGF-2 and IGF-1. We next looked at the astrocytic expression of transforming growth factor β (TGF-β) which has also been suggested to play a role in OPC differentiation (McKinnon et al., 1993). RT-PCR analysis demonstrates that TGF-β mRNA levels are upregulated with IL-1β stimulation. However, iron loaded astrocytes treated with IL-1β showed a significant reduction in TGF-β expression, indicating that iron may be involved in regulating TGF-β expression (Fig. 5C). In addition to a possible direct role in OPC differentiation (McKinnon et al., 1993), TGF-β has been also shown contribute to the polarization of microglia/macrophages towards an anti-inflammatory M2 phenotype which has been shown to mediate repair processes (Martinez et al., 2008). We therefore suggest that the reduced TGF-β levels by iron-loaded astrocytes might result in decreased macrophage M2 polarization and thus in less repair/remyelination.

The reduced remyelination seen in the astrocyte-specific Fpn KO mice might therefore be due to either the direct effects on OPCs through limited iron supply or to indirect effects via iron-deficient microglia which could in turn affect the ability of astrocytes to express growth factors involved in OPC proliferation and differentiation as summarized in Fig. 6. Another indirect effect on the remyelination process might also result from reduced M2 macrophage polarization and consequent reduction in repair and remyelination processes.

3.6 Discussion

The importance of iron for myelination during development has been demonstrated by several studies in animals as well as humans (Todorich et al., 2008b). As remyelination requires OPC proliferation and differentiation into myelin forming cells, it also requires increased iron levels. However, not much is known about the role of iron and iron delivery in remyelination in the adult CNS. Iron in the circulation is taken up by capillary endothelial cells as transferrin-bound iron via transferrin receptor 1 (Moos and Morgan, 2000; Moos et al., 2006). Since 95% of the capillary surface in the CNS is covered over by astrocytic processes called endfeet, they are suited to take up iron released from endothelial cells and deliver it to other cell types in the CNS. Astrocytes possess both iron uptake as well as iron efflux mechanisms that would aid in this process (Jeong and David, 2003). In this study, we investigated whether astrocytes deliver iron to OPCs for remyelination. To address this, we blocked iron efflux from astrocytes by specifically deleting Fpn in astrocytes. Fpn is the only known iron efflux transporter. Lack of Fpn results in iron retention in cells (Donovan et al., 2005). The astrocyte-specific Fpn KO mice in our study were generated by crossing a tamoxifen-inducible GLASTCre line to a line that carries the floxed Fpn allele. Cre-mediated Fpn excision was confirmed in the tamoxifen injected animals. Remyelination was examined in these animals after LPC-induced demyelination in the spinal cord. Our results revealed impaired remyelination in the astrocyte-Fpn KO mice suggesting that iron efflux from astrocytes is required for remyelination. Several mechanisms may underlie the reduced remyelination.

The defects in remyelination could be due to decreased proliferation and/or differentiation of OPCs. Iron is known to be required for proliferation and differentiation of cells, because it plays an important role in DNA synthesis as well as in oxidative

metabolism (Robbins and Pederson, 1970; Hoffbrand et al., 1976). Iron has also been shown before to be involved in proliferation and differentiation of OPCs *in vitro* (Morath and Mayer-Proschel, 2001) and in oligodendrogenesis after intraspinal lipopolysaccharide (LPS) injections *in vivo* (Schonberg and McTigue, 2009). Since iron is retained within astrocytes in the astrocyte-specific Fpn KO animals, OPCs might be iron deficient and might therefore possess only limited capacity to proliferate and differentiate. We found that proliferation of OPCs was reduced in the astrocyte-specific Fpn KO mice after LPC injection, which could account for the observed impairment of remyelination. These results suggest that astrocytes play a role in transporting iron to OPCs for proliferation. Microglia/macrophages have also been suggested to deliver iron to OPCs for oligodendrocyte genesis after intraspinal LPS injection (Schonberg and McTigue, 2009). However, in this model, increased local iron levels have been detected in the lesion site, whereas no iron accumulation was observed in the LPC-induced demyelination model (Schonberg and McTigue, 2009) that we have used in the current study. Therefore, in the LPS-injection model, microglia/ macrophages could react to the increased iron levels by storing the iron rapidly to prevent iron-mediated oxidative damage and then provide it to OPCs when needed. In contrast, in the LPC-induced demyelination model, it is likely that iron has to be taken up from the circulation to supply OPCs.

In addition to the direct effects of iron deprivation on OPCs, iron may also have indirect effects on remyelination such as by altering the levels of cytokines and growth factors that can influence OPC proliferation and differentiation. Iron retention in astrocytes in the astrocyte-specific Fpn KO mice could also render microglia iron-

deficient, which might affect their activation state and cytokine expression. Cytokines such as TNF-α and IL-1β have been shown to play a role in remyelination (Arnett et al., 2001; Mason et al., 2001). We found here that LPS-stimulated microglia in cell culture show decreased expression of TNF-α and IL-1β when treated with an iron chelator to render them iron-deficient. These data suggest a role of iron in the expression of TNF-α and IL-1β by microglia, which is consistent with a previous report showing decreased expression of these cytokines by microglia treated with the iron chelator deferoxamine (Zhang et al., 2006). TNF-α has been suggested to directly promote OPC proliferation and remyelination through its receptor TNFR2 (Arnett et al., 2001). In addition, TNF-α and IL-1β may also have indirect effects by activating other cells within the CNS to produce growth factors involved in OPC proliferation and differentiation (Mason et al., 2001). One of the factors known to induce OPC proliferation is FGF-2 (McKinnon et al., 1990; Wolswijk and Noble, 1992; Engel and Wolswijk, 1996). FGF-2 is predominantly expressed by astrocytes in response to myelin damage (Logan et al., 1992; Messersmith et al., 2000). Furthermore, it is also upregulated in reactive astrocytes after LPC-induced demyelination (Hinks and Franklin, 1999). We investigated whether iron loading of IL-1β stimulated astrocytes alters their ability to express FGF-2. We found that stimulation of astrocytes with IL-1β induced an increase in expression of FGF-2, and iron loading did not alter this upregulation. Iron status of the astrocytes therefore does not affect FGF-2 expression. Similar effects were seen with IGF-1 expression. IGF-1 not only promotes OPC differentiation and survival but also appears to affect OPC proliferation (Masters et al., 1991; Mozell and McMorris, 1991; Kuhl et al., 2002; Hsieh et al., 2004). IGF-1 is also expressed by astrocytes (Ballotti et al., 1987) and plays a protective and regenerative

role after experimentally induced demyelination (Mason et al., 2000b; Mason et al., 2000a). These results suggest that FGF-2 and IGF-1 can be upregulated by IL-1β and TNF-α, respectively, in astrocytes *in vitro* and that the intracellular iron status of astrocytes does not affect the expression of these growth factors. On the other hand, the reduced expression of IL-1β and TNF-α by iron-deficient microglia might indirectly result in decreased expression of FGF-2 and IGF-1 by astrocytes, which may contribute to impaired OPC proliferation and differentiation in our *in vivo* model.

TGF-β, has been suggested to play a role in differentiation of OPCs (McKinnon et al., 1993) and is also upregulated after LPC-induced demyelination (Hinks and Franklin, 1999). We show here that IL-1β stimulated astrocytes upregulate TGF-β expression, which is markedly reduced when astrocytes are iron loaded. Thus, reduced expression of TGF-β by astrocytes may either result from decreased IL-1β stimulation by iron-deficient microglia or directly from iron accumulation in astrocytes.

TGF-β can also influence the polarization of macrophages towards an M2 phenotype (Martinez et al., 2008). In contrast to 'classically activated', pro-inflammatory M1 macrophages, 'alternatively activated' M2 macrophages possess anti-inflammatory properties and have been shown to promote tissue repair processes after injury or disease (Popovich and Longbrake, 2008; Kigerl et al., 2009; David and Kroner, 2011). TGF-β contributes to the induction of a specific subtype of M2 macrophages called M2c which downregulates proinflammatory cytokines, upregulates anti-inflammatory cytokines such as IL-10 and in addition, appears to have high phagocytotic activity (Martinez et al., 2008). These processes may also be important for myelin repair following demyelination. Interestingly, in LPC-induced demyelination, TGF-β expression peaks at 10 days post

injection, an early time point of the remyelination phase (Hinks and Franklin, 1999). In addition, depletion of macrophages has been shown to impair remyelination, which was not only associated with reduced myelin removal but also with altered growth factor expression and reduced OPC proliferation (Kotter et al., 2005), emphasizing an important role for macrophages in remyelination.

In summary, our findings suggest that iron efflux from astrocytes through the iron exporter Fpn plays a role in providing iron for remyelination. As illustrated in Figure 6, astrocytes may acquire iron from brain capillary endothelial cells via their astrocytic endfeet and deliver it directly to OPCs, which can then utilize the iron for enzymatic processes involved in their proliferation and differentiation into myelin forming cells. In addition, astrocytes might also deliver iron to microglia, which require iron for the expression of IL-1β and TNF-α. These two cytokines could then act either directly on OPCs or stimulate astrocytes to produce growth factors involved in OPC proliferation and differentiation such as FGF-2 and IGF-1. IL-1β can also induce TGF-β expression by astrocytes which could either contribute directly to OPC differentiation or could promote the polarization of macrophages towards an M2 phenotype which may also play a role in the myelin repair process. These results suggest an important role for astrocytes in taking up iron from endothelial cells at the blood brain barrier and distributing it to other cell types in the CNS.

3.7 References

Arnett HA, Mason J, Marino M, Suzuki K, Matsushima GK, Ting JP (2001) TNF alpha promotes proliferation of oligodendrocyte progenitors and remyelination. Nat Neurosci 4:1116-1122.

Ballotti R, Nielsen FC, Pringle N, Kowalski A, Richardson WD, Van Obberghen E, Gammeltoft S (1987) Insulin-like growth factor I in cultured rat astrocytes: expression of the gene, and receptor tyrosine kinase. Embo J 6:3633-3639.

Burdo JR, Menzies SL, Simpson IA, Garrick LM, Garrick MD, Dolan KG, Haile DJ, Beard JL, Connor JR (2001) Distribution of divalent metal transporter 1 and metal transport protein 1 in the normal and Belgrade rat. J Neurosci Res 66:1198-1207.

Cazzola M, Bergamaschi G, Dezza L, Arosio P (1990) Manipulations of cellular iron metabolism for modulating normal and malignant cell proliferation: achievements and prospects. Blood 75:1903-1919.

Connor JR, Menzies SL (1996) Relationship of iron to oligodendrocytes and myelination. Glia 17:83-93.

David S, Kroner A (2011) Repertoire of microglial and macrophage responses after spinal cord injury. Nat Rev Neurosci 12:388-399.

Donovan A, Lima CA, Pinkus JL, Pinkus GS, Zon LI, Robine S, Andrews NC (2005) The iron exporter ferroportin/Slc40a1 is essential for iron homeostasis. Cell Metab 1:191-200.

Engel U, Wolswijk G (1996) Oligodendrocyte-type-2 astrocyte (O-2A) progenitor cells derived from adult rat spinal cord: in vitro characteristics and response to PDGF, bFGF and NT-3. Glia 16:16-26.

Foster RE, Kocsis JD, Malenka RC, Waxman SG (1980) Lysophosphatidyl choline-induced focal demyelination in the rabbit corpus callosum. Electron-microscopic observations. J Neurol Sci 48:221-231.

Franklin RJ (2002) Why does remyelination fail in multiple sclerosis? Nat Rev Neurosci 3:705-714.

Franklin RJ, Ffrench-Constant C (2008) Remyelination in the CNS: from biology to therapy. Nat Rev Neurosci 9:839-855.

Frost EE, Nielsen JA, Le TQ, Armstrong RC (2003) PDGF and FGF2 regulate oligodendrocyte progenitor responses to demyelination. J Neurobiol 54:457-472.

Hall SM (1972) The effect of injections of lysophosphatidyl choline into white matter of the adult mouse spinal cord. J Cell Sci 10:535-546.

Hinks GL, Franklin RJ (1999) Distinctive patterns of PDGF-A, FGF-2, IGF-I, and TGF-beta1 gene expression during remyelination of experimentally-induced spinal cord demyelination. Mol Cell Neurosci 14:153-168.

Hoffbrand AV, Ganeshaguru K, Hooton JW, Tattersall MH (1976) Effect of iron deficiency and desferrioxamine on DNA synthesis in human cells. Br J Haematol 33:517-526.

Hsieh J, Aimone JB, Kaspar BK, Kuwabara T, Nakashima K, Gage FH (2004) IGF-I instructs multipotent adult neural progenitor cells to become oligodendrocytes. J Cell Biol 164:111-122.

Jeffery ND, Blakemore WF (1995) Remyelination of mouse spinal cord axons demyelinated by local injection of lysolecithin. J Neurocytol 24:775-781.

Jeong SY, David S (2003) Glycosylphosphatidylinositol-anchored ceruloplasmin is required for iron efflux from cells in the central nervous system. J Biol Chem 278:27144-27148.

Jeong SY, David S (2006) Age-related changes in iron homeostasis and cell death in the cerebellum of ceruloplasmin-deficient mice. J Neurosci 26:9810-9819.

Kigerl KA, Gensel JC, Ankeny DP, Alexander JK, Donnelly DJ, Popovich PG (2009) Identification of two distinct macrophage subsets with divergent effects causing either neurotoxicity or regeneration in the injured mouse spinal cord. J Neurosci 29:13435-13444.

Kotter MR, Zhao C, van Rooijen N, Franklin RJ (2005) Macrophage-depletion induced impairment of experimental CNS remyelination is associated with a reduced oligodendrocyte progenitor cell response and altered growth factor expression. Neurobiol Dis 18:166-175.

Kuhl NM, De Keyser J, De Vries H, Hoekstra D (2002) Insulin-like growth factor binding proteins-1 and -2 differentially inhibit rat oligodendrocyte precursor cell survival and differentiation in vitro. J Neurosci Res 69:207-216.

Liberto CM, Albrecht PJ, Herx LM, Yong VW, Levison SW (2004) Pro-regenerative properties of cytokine-activated astrocytes. J Neurochem 89:1092-1100.

Linker R, Gold R, Luhder F (2009) Function of neurotrophic factors beyond the nervous system: inflammation and autoimmune demyelination. Crit Rev Immunol 29:43-68.

Logan A, Frautschy SA, Gonzalez AM, Baird A (1992) A time course for the focal elevation of synthesis of basic fibroblast growth factor and one of its high-affinity receptors (flg) following a localized cortical brain injury. J Neurosci 12:3828-3837.

Martinez FO, Sica A, Mantovani A, Locati M (2008) Macrophage activation and polarization. Front Biosci 13:453-461.

Mason JL, Suzuki K, Chaplin DD, Matsushima GK (2001) Interleukin-1beta promotes repair of the CNS. J Neurosci 21:7046-7052.

Mason JL, Ye P, Suzuki K, D'Ercole AJ, Matsushima GK (2000a) Insulin-like growth factor-1 inhibits mature oligodendrocyte apoptosis during primary demyelination. J Neurosci 20:5703-5708.

Mason JL, Jones JJ, Taniike M, Morell P, Suzuki K, Matsushima GK (2000b) Mature oligodendrocyte apoptosis precedes IGF-1 production and oligodendrocyte progenitor accumulation and differentiation during demyelination/remyelination. J Neurosci Res 61:251-262.

Masters BA, Werner H, Roberts CT, Jr., LeRoith D, Raizada MK (1991) Insulin-like growth factor I (IGF-I) receptors and IGF-I action in oligodendrocytes from rat brains. Regul Pept 33:117-131.

McKinnon RD, Matsui T, Dubois-Dalcq M, Aaronson SA (1990) FGF modulates the PDGF-driven pathway of oligodendrocyte development. Neuron 5:603-614.

McKinnon RD, Piras G, Ida JA, Jr., Dubois-Dalcq M (1993) A role for TGF-beta in oligodendrocyte differentiation. J Cell Biol 121:1397-1407.

Messersmith DJ, Murtie JC, Le TQ, Frost EE, Armstrong RC (2000) Fibroblast growth factor 2 (FGF2) and FGF receptor expression in an experimental demyelinating disease with extensive remyelination. J Neurosci Res 62:241-256.

Moore CS, Abdullah SL, Brown A, Arulpragasam A, Crocker SJ (2010) How factors secreted from astrocytes impact myelin repair. J Neurosci Res 89:13-21.

Moos T, Morgan EH (2000) Transferrin and transferrin receptor function in brain barrier systems. Cell Mol Neurobiol 20:77-95.

Moos T, Skjoerringe T, Gosk S, Morgan EH (2006) Brain capillary endothelial cells mediate iron transport into the brain by segregating iron from transferrin without the involvement of divalent metal transporter 1. J Neurochem 98:1946-1958.

Moos T, Rosengren Nielsen T, Skjorringe T, Morgan EH (2007) Iron trafficking inside the brain. J Neurochem 103:1730-1740.

Morath DJ, Mayer-Proschel M (2001) Iron modulates the differentiation of a distinct population of glial precursor cells into oligodendrocytes. Dev Biol 237:232-243.

Mori T, Tanaka K, Buffo A, Wurst W, Kuhn R, Gotz M (2006) Inducible gene deletion in astroglia and radial glia--a valuable tool for functional and lineage analysis. Glia 54:21-34.

Mozell RL, McMorris FA (1991) Insulin-like growth factor I stimulates oligodendrocyte development and myelination in rat brain aggregate cultures. J Neurosci Res 30:382-390.

Nave and Trapp (2008) Axon-glial signaling and the glial support of axon function. Annu Rev Neurosci 31:535–61.

Neumann H, Kotter MR, Franklin RJ (2009) Debris clearance by microglia: an essential link between degeneration and regeneration. Brain 132:288-295.

Ousman SS, David S (2000) Lysophosphatidylcholine induces rapid recruitment and activation of macrophages in the adult mouse spinal cord. Glia 30:92-104.

Popovich PG, Longbrake EE (2008) Can the immune system be harnessed to repair the CNS? Nat Rev Neurosci 9:481-493.

Rathore KI, Kerr BJ, Redensek A, Lopez-Vales R, Jeong SY, Ponka P, David S (2008) Ceruloplasmin protects injured spinal cord from iron-mediated oxidative damage. J Neurosci 28:12736-12747.

Richardson DR, Ponka P (1998) Pyridoxal isonicotinoyl hydrazone and its analogs: potential orally effective iron-chelating agents for the treatment of iron overload disease. J Lab Clin Med 131:306-315.

Robbins E, Pederson T (1970) Iron: its intracellular localization and possible role in cell division. Proc Natl Acad Sci U S A 66:1244-1251.

Saura J, Tusell JM, Serratosa J (2003) High-yield isolation of murine microglia by mild trypsinization. Glia 44:183-189.

Schonberg DL, McTigue DM (2009) Iron is essential for oligodendrocyte genesis following intraspinal macrophage activation. Exp Neurol 218:64-74.

Smith EJ, Blakemore WF, McDonald WI (1979) Central remyelination restores secure conduction. Nature 280:395-396.

Todorich B, Pasquini JM, Garcia CI, Paez PM, Connor JR (2009) Oligodendrocytes and myelination: the role of iron. Glia 57:467-478.

Wilson HC, Onischke C, Raine CS (2003) Human oligodendrocyte precursor cells in vitro: phenotypic analysis and differential response to growth factors. Glia 44:153-165.

Wolswijk G, Noble M (1992) Cooperation between PDGF and FGF converts slowly dividing O-2Aadult progenitor cells to rapidly dividing cells with characteristics of O-2Aperinatal progenitor cells. J Cell Biol 118:889-900.

Zhang X, Surguladze N, Slagle-Webb B, Cozzi A, Connor JR (2006) Cellular iron status influences the functional relationship between microglia and oligodendrocytes. Glia 54:795-804.

3.8 Figures

Figure 1

Conditional deletion of Fpn in astrocytes by GLASTCre::ERT2. (**A**) PCR analysis of tissue DNA from a GLASTCre::ERT2;Fpn$^{flox/flox}$ mouse that was injected with tamoxifen (TAM) or vehicle (veh). The Fpn deletion band (398 bp) is only seen in brain (Br) and spinal cord (Sc), but not in the liver (L) of the tamoxifen-treated mouse, nor in the vehicle-treated mouse. The floxed allele (522 bp) is present in all tissues. (**B**) Western blot of brain, spinal cord and liver of GLASTCre::ERT2;Fpn$^{flox/flox}$ mice shows reduced Fpn expression in brain and spinal cord but not liver of TAM-treated as compared to veh-treated mice. (**C-H**) Double immunofluorescence labelling for Cre and GFAP shows the expression of Cre recombinase (**C** and **F**) in GFAP-positive astrocytes (**D** and **G**) in TAM- and veh-treated GLASTCre::ERT2; Fpn$^{flox/flox}$ mice. Arrows indicate the localization of the Cre recombinase in the cytosol in veh-treated animals (**C-E**), as compared to its nuclear localization in TAM-treated animals (**F-H**). Merged images including a DAPI staining to label cell nuclei are shown in **E** and **H**. Scale bar in H=50 μm (inset=20 μm).

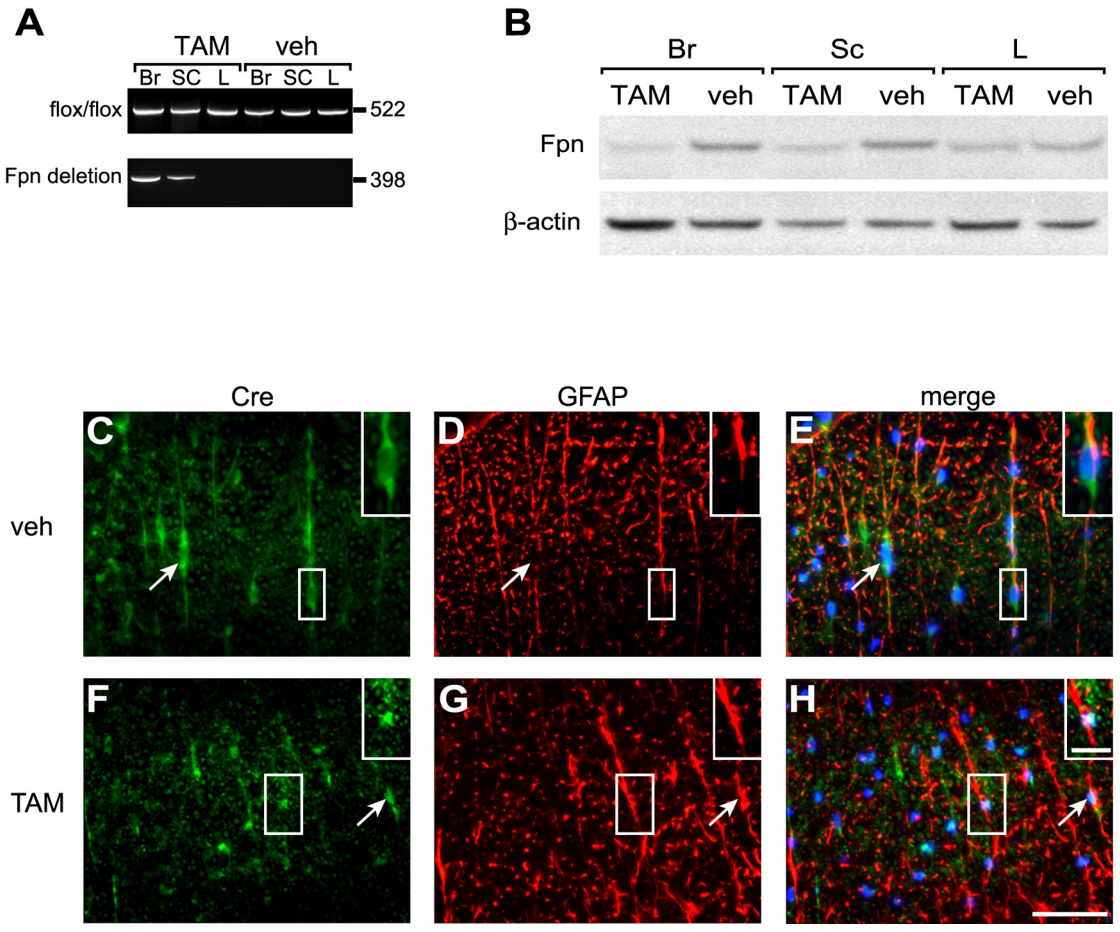
A
TAM
veh
Br SC L Br SC L
flox/flox
522
Fpn deletion
398
B
Br
Sc
L
TAM veh TAM veh TAM veh
Fpn
β-actin
Cre
GFAP
merge
veh
TAM
C
D
E
F
G
H

Figure 2

Remyelination after LPC-induced demyelination is impaired in astrocyte-specific Fpn knockout mice. (**A**) Epon-embedded cross-section of the spinal cord stained with toluidine blue demonstrates the LPC-induced demyelinating lesion (asterisk) in the dorsal white matter. (**B**) Higher magnification of the area outlined in the rectangle in panel A. The area of demyelination is indicated by the asterisk. Scale bars in A=300 μm, B=200 μm. (**C** and **D**) Electron micrograph illustrating the extent of remyelination 10 days after LPC-injection in control mice (**C**). In contrast, remyelination is markedly reduced in astrocyte-specific Fpn KO mice (**D**). Demyelinated axons are marked by asterisks, whereas thinly remyelinated axons are indicated by arrows. Scale bar in D=3 μm. (**E**) Quantification of the g-ratio shows that there is a significantly lower percentage of remyelinated axons (g-ratio=0.9) and a significant higher percentage demyelinated axons (g-ratio=1.0) in astrocyte-specific Fpn KO mice as compared to control mice. Data are shown as mean ± SEM (n=3; *p ≤0.05; Two-way RM ANOVA).

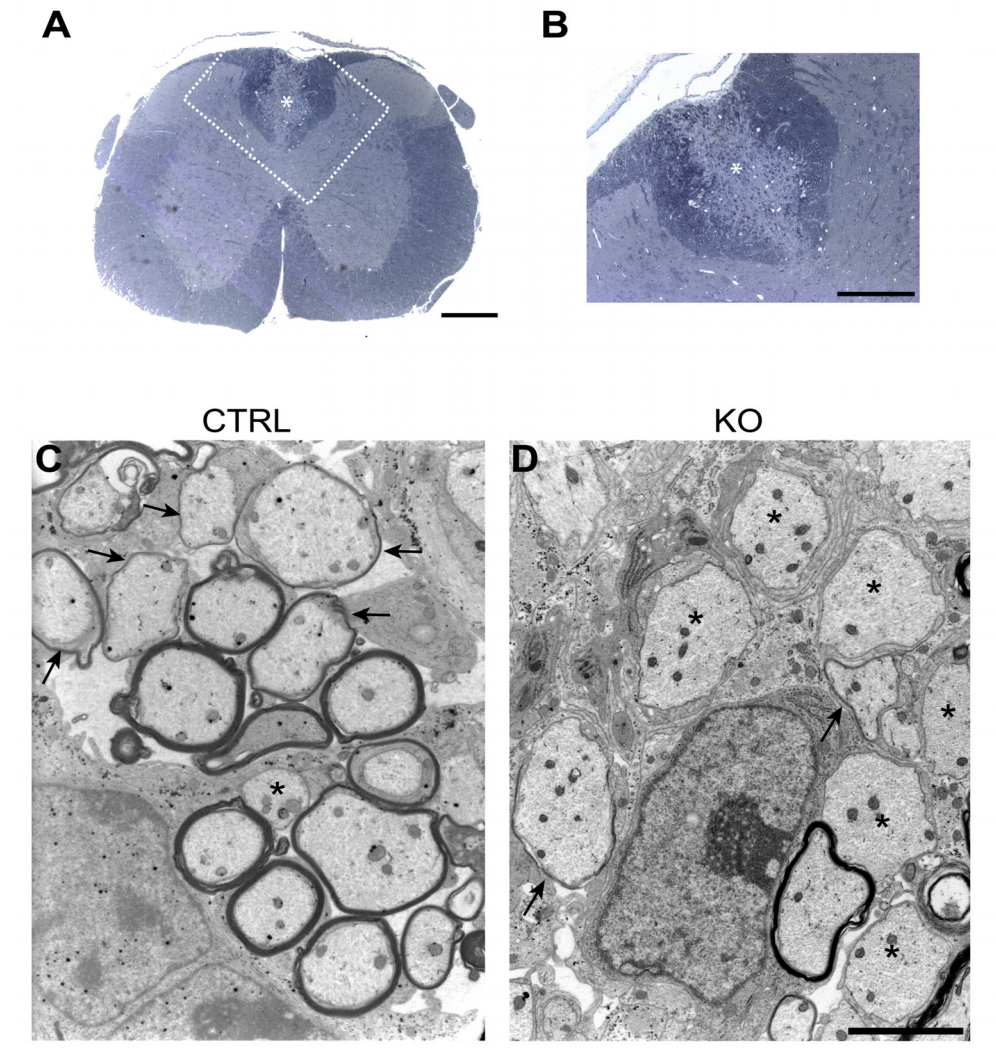
A
B
CTRL
KO
C
D
E
CTRL
KO
100
80
60
40
20
0
%
0.7
0.8
0.9
1.0
g-ratio

Figure 3

OPC proliferation after LPC-induced demyelination is reduced in astrocyte-specific Fpn knockout mice. Double immunofluorescence using the proliferation marker Ki67 (**A, D, G** and **J**) and the OPC marker olig2 (**B, E, H,** and **K**) shows a reduction in proliferating OPCs in astrocyte-specific Fpn KO mice (**G-L**) as compared to control mice (**A-F**). Cells double-labeled with Ki67 and olig2 are indicated by arrows. D-E and J-L represent higher magnification images of the areas outlined in A-C and G-I. Merged images including a nuclear DAPI stain are shown in panels, **C, F, I and L**. Scale bars in I=100 μm and L=50 μm. (**M**) Quantification of Ki67 and olig2 double labeled cells shows a significant reduction in the number of proliferating OPCs in the area of LPC-induced demyelination in astrocyte-specific Fpn KO mice as compared to control mice. Data are shown as mean ± SEM (n=4; *$p \leq 0.05$; Student's *t*-test).

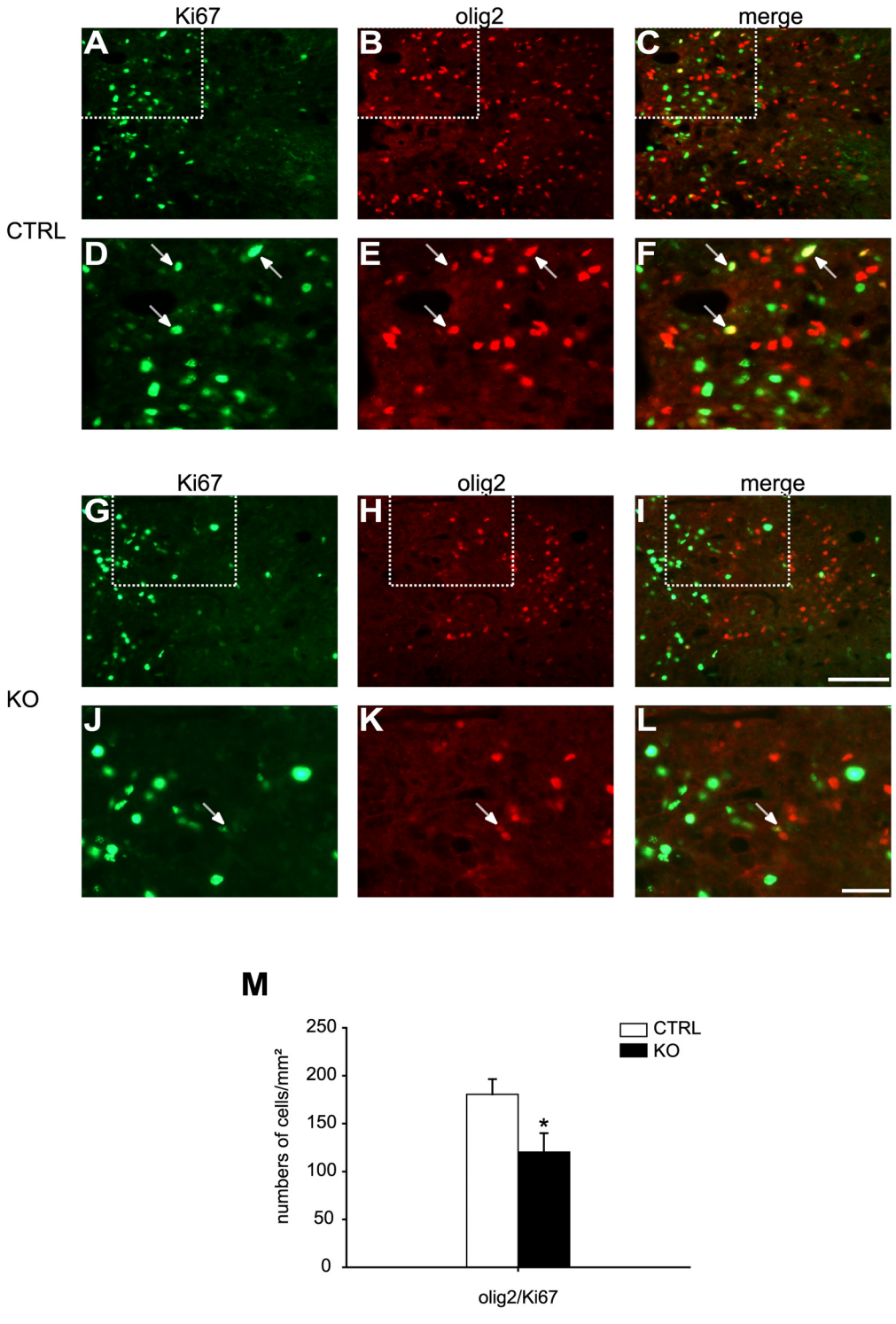
Ki67
olig2
merge
A
B
C
CTRL
D
E
F
Ki67
olig2
merge
G
H
I
KO
J
K
L
M
numbers of cells/mm²
250
200
150
100
50
0
CTRL
KO
*
olig2/Ki67

Figure 4

Expression of TNF-α and IL-1β are reduced in iron-deficient microglia. RT-PCR analysis demonstrates a significant reduction in IL-1β (**A**) and TNF-α (**B**) mRNA expression in LPS-stimulated microglia *in vitro* treated with the iron chelator SIH as compared to vehicle. Data are shown as mean ± SEM (n=3; *$p \leq 0.05$; Student's *t*-test).

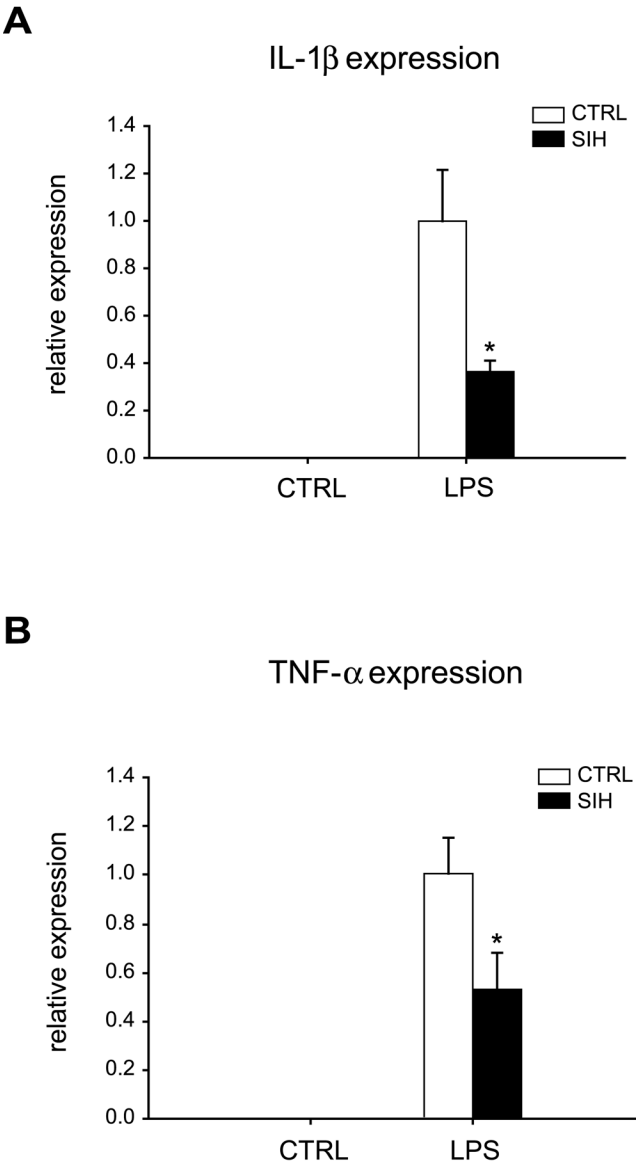
A
IL-1β expression
CTRL
SIH
relative expression
1.4
1.2
1.0
0.8
0.6
0.4
0.2
0.0
*
CTRL
LPS
B
TNF-α expression
CTRL
SIH
relative expression
1.4
1.2
1.0
0.8
0.6
0.4
0.2
0.0
*
CTRL
LPS

Figure 5

Expression of growth factors by astrocytes under high iron conditions. RT-PCR analysis showing increased mRNA expression of FGF-2 (**A**), IGF-1 (**B**) and TGF-β (**C**) by astrocytes in culture when treated with either IL-1β (**A** and **C**) or TNF-α (**B**). Loading astrocytes with iron did not change the expression levels of FGF-2 (**A**) and IGF-1 (**B**), but resulted in decreased TGF-β mRNA expression (**C**). Data are shown as mean ± SEM (n=3; *p≤0.05; Student's *t*-test).

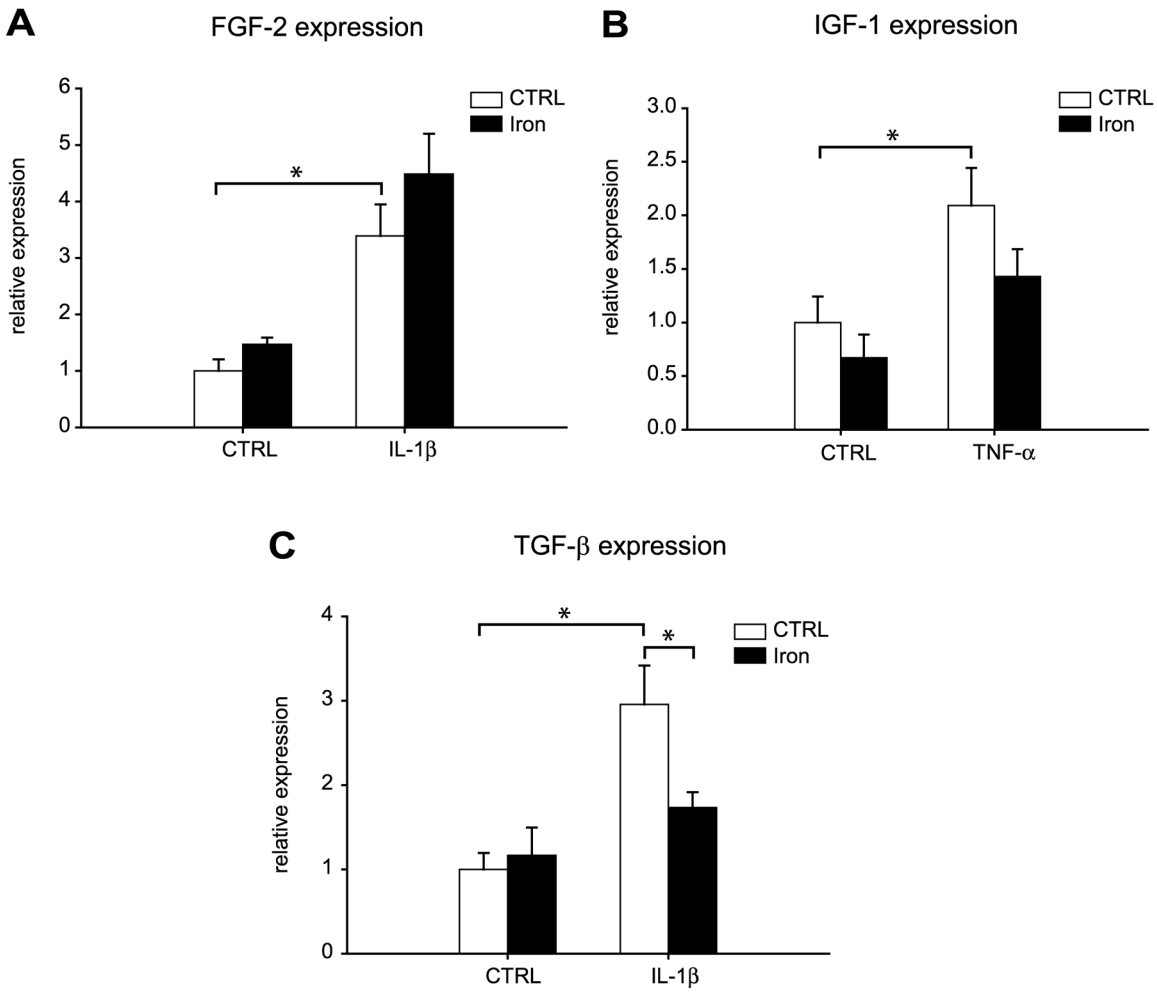
A
FGF-2 expression
relative expression
CTRL
Iron
CTRL
IL-1β
B
IGF-1 expression
relative expression
CTRL
Iron
CTRL
TNF-α
C
TGF-β expression
relative expression
CTRL
Iron
CTRL
IL-1β

Figure 6

Direct and indirect effects of blocking iron efflux from astrocytes on remyelination. Astrocytes in the Fpn-conditional null mouse retained iron due to deletion of the iron exporter Fpn. Iron from astrocytes thus cannot be delivered to other cells in the CNS. This might directly affect the proliferation (**a**) and differentiation (**b**) of OPCs which may not receive enough iron required for these processes. In addition, microglia might also be iron-deficient in the astrocyte-specific Fpn null mice which might impair their ability to express cytokines such as TNF-α and IL-1β (**c**). These cytokines are directly and indirectly implicated in the process of remyelination by stimulating astrocytes to produce growth factors involved in OPC proliferation (FGF-2, **d**) and differentiation (IGF-1, **e**). In addition, the reduced expression of TGF-β (**f**) by astrocytes may result in less polarization of macrophages towards an anti-inflammatory and regeneration-promoting M2 phenotype, which might also contribute to reduced remyelination.

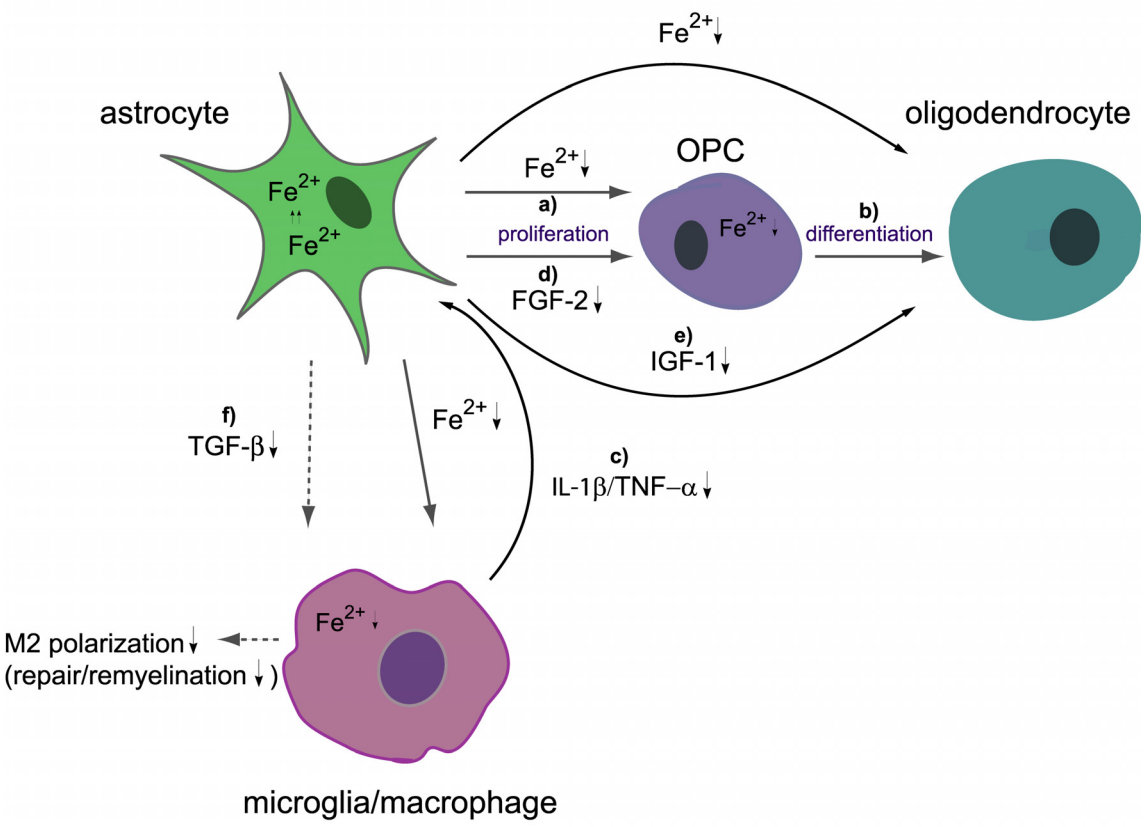
Fe2+↓
astrocyte
oligodendrocyte
OPC
Fe2+
Fe2+
Fe2+↓
a)
proliferation
Fe2+↓
b)
differentiation
d)
FGF-2↓
e)
IGF-1↓
f)
TGF-β↓
Fe2+↓
c)
IL-1β/TNF−α↓
Fe2+↓
M2 polarization↓
(repair/remyelination↓)
microglia/macrophage

Chapter 4

Iron plays a role in neurite growth in vitro and axon regeneration in peripheral nerve

Katrin Schulz and Samuel David

*The work presented in this chapter is being prepared for submission.

4.1 Preface

The results presented in the previous chapter indicate that iron efflux from astrocytes plays a role in remyelination, likely by delivering iron to OPCs for proliferation and differentiation and to microglia in which it regulates expression of cytokines involved in remyelination. These results contribute to the understanding of iron transport between cells within the CNS. In chapter 4, I studied the role of iron efflux from Schwann cells in the PNS in delivering iron to peripheral nerve axons for axon growth and regeneration. I first assessed whether iron is required for axonal growth *in vitro* and then examined whether Cp-mediated iron efflux from Schwann cells is involved in peripheral axonal regeneration after sciatic nerve injury.

4.2 Abstract

The metabolic requirements of axons are met by mitochondria that travel anterogradely and retrogradely along axons. Mitochondria require iron for their function, which they might acquire along the length of the axons rather than just at the region of the cell body. We hypothesize that Schwann cells are an important source of iron for peripheral axons because of their close association with axons. Moreover, Schwann cells express the iron exporter ferroportin and the ferroxidase ceruloplasmin, which partner together to export iron. Schwann cells are therefore equipped with the machinery required for iron efflux, and might play a role in delivering iron to axons in peripheral nerve under physiological conditions, as well as after nerve injury when the metabolic demands are higher. We show here that treatment of DRG cultures with an iron chelator results in reduction of neurite growth and causes mitochondria cluster formation. Since growth cones at the

growing tips of regenerating axons have a high-energy requirement, local iron supply from Schwann cells might be especially important for axonal regeneration after peripheral nerve injury. We show here that sciatic nerve crush injury in Cp knockout mice in which iron efflux from Schwann cells is likely to be defective, results in impairment of axon regeneration and motor recovery. These findings suggest that iron delivery from Schwann cells to axons might be important for axon regeneration, likely to maintain proper mitochondrial function.

4.3 Introduction

Axonal mitochondria are important for the maintenance of neuronal function by providing the axon with ATP. These organelles are not evenly distributed along the length of the axon, but concentrate at regions of high energy demand such as nodes of Ranvier, synapses and axonal growth cones (Bogan and Cabot, 1991; Fabricius et al., 1993; Morris and Hollenbeck, 1993). Mitochondrial function is highly dependent on iron, because iron is an essential cofactor for enzymes involved in oxidative phosphorylation. The mitochondrial respiratory complexes I-IV are heme- and/or iron-sulfur cluster-containing enzymes that require iron for their conformation and activity (Gille and Reichmann, 2011). Since axonal mitochondria are in some cases, especially in the peripheral nervous system (PNS), located far away from the cell body, they might acquire iron locally from Schwann cells which are in close association with the axon. Interactions between Schwann cells and axons are known to play a key role in the development, function and maintenance of peripheral axons (Bunge, 1993; Reynolds and Woolf, 1993; Corfas et al., 2004). For example, Schwann cells have been shown to provide axons with

neurotrophic factors (Reynolds and Woolf, 1993). Schwann cells may also be an important source of iron for peripheral axons. Furthermore, Schwann cells express a glycosylphosphatidylinositol-anchored (GPI)-anchored form of the ferroxidase ceruloplasmin (Cp) (Salzer et al., 1998), a protein which has been shown to mediate iron efflux from various cell types (Harris et al., 1999; Patel et al., 2002; Jeong and David, 2006). In the central nervous system (CNS), Cp mediates iron export from astrocytes by interacting with the iron exporter ferroportin (Fpn) (Jeong and David, 2003). The ferroxidase activity of Cp appears to be necessary for the iron efflux to occur, as astrocytes from Cp knockout ($Cp^{-/-}$) mice are unable to export iron *in vitro* (Jeong and David, 2003). Iron efflux from Schwann cells via Fpn and Cp may therefore play a role in delivering iron to mitochondria within peripheral nerve axons. Since axonal mitochondria are enriched in axonal growth cones, this glia-derived iron supply might be especially important for axonal regeneration after peripheral nerve injury.

In the present study, we first investigated in dorsal root ganglia (DRG) neuronal cultures whether reduced iron levels affect neurite growth. We also studied whether axon regeneration in the sciatic nerve is impaired after crush injury in Cp null mice in which iron efflux from Schwann cells would be impaired. Our findings suggest that iron is essential for neurite growth *in vitro*, and that iron efflux from Schwann cells appears to be required for effective axon regeneration in injured peripheral nerve likely by ensuring proper axonal mitochondrial function.

4.4 Materials and Methods

Sciatic nerve injury. Female $Cp^{-/-}$ and $Cp^{+/+}$ mice on a C57BL/6 background at 8-10 weeks of age were used for sciatic nerve crush injuries. $Cp^{-/-}$ mice were generated in our laboratory as previously described (Patel et al., 2002). Mice were anesthetized with ketamine:xylazine:acepromazine (100:10:3 mg/kg), the right sciatic nerve was exposed and crushed with fine forceps (Dumont no 5) for 30 s. The crush site was labelled with a 10-0 suture through the epineurium of the peroneal branch. All procedures were approved by the McGill University Animal Care committee and followed the guidelines of the Canadian Council on Animal Care.

Footprint analysis. Prior to lesion and at 7, 11, 14, 17, 21 and 28 days following sciatic nerve crush injury, mice were allowed to walk down a 40 cm long track after inking their hind paws. The sciatic functional index (SFI) was calculated from the footprints using a formula developed by de Medinaceli and co-workers (de Medinaceli et al., 1982) and modified for mice by Inserra and co-workers (Inserra et al., 1998). The analysis was carried out blind. Data are plotted as mean ± SEM. Two-way RM-ANOVA was used to determine statistical significance.

Assessment of axonal regeneration. Four days after nerve crush injury, animals were transcardially perfused with 4% paraformaldehyde (PFA) in 0.1 M phosphate buffer, pH 7.4. A segment of the sciatic nerve distal to the lesion site was taken out and prepared for cryostat sectioning. Longitudinal sections (10 μm) were incubated in 0.1% Triton-X 100, 2% normal goat serum and 2% ovalbumin in phosphate buffered saline containing goat

anti-mouse IgG (1:100) for 5 hrs to block non-specific binding. The tissue sections were then incubated overnight at 4 °C with a polyclonal rabbit antibody against growth associated protein 43 (GAP-43) (1:500, Chemicon) and a monoclonal mouse anti-S100β (1:600, Sigma; for Schwann cells). Primary antibodies were visualized by incubation with rhodamine-conjugated goat anti-mouse IgG (1:400, Jackson ImmunoResearch) and Alexa 488-conjugated goat anti-rabbit IgG (1:400; Invitrogen) for 2 hrs at room temperature. Sections were coverslipped with mounting medium containing 100 ng/mL 4'-6-diamidino-2-phenylindole (DAPI) (Vector Laboratories) to visualize cell nuclei, and viewed with a Zeiss Axioskop 2 plus microscope. Axonal regeneration was assessed by counting the numbers of GAP-43 positive and S100β negative fibres at 3, 4 and 5 mm distal to the crush site (3 sections per animal, 3 mice per group; n=3). The diameter of the fibre was measured at the respective site of the axonal counts and the numbers of axons was divided by the fibre diameter. Results are shown as mean ± SEM. Two-way RM-ANOVA was used to determine statistical significance.

RT-PCR. Total RNA was isolated from sciatic nerves distal to the crush injury site at 1, 7 and 14 days post injury and from uninjured nerves using RNeasy Mini Lipid Tissue Kit (Qiagen). RT-PCR was performed using the Omniscript RT Kit (Qiagen) The PCR step was carried out with the Hotstart MasterMix (Qiagen) and the following primers: Cp_forward: 5′-TGG GAC TAT GCT TCT GGC AGT GAA-3’; Cp_reverse: 5′-TTG GCA CGC AGA ACG TAC AAA TAC-3’ ; DMT1_forward: 5′-ACA AAT ATG GCT TGC GGA AGC TGG -3′ ; DMT1_reverse: 5′-ACA TGT TGT GCG GCA TGA TCA CAG -3′; Fpn_forward: 5′-TCA GGA CTG GCT CAG CTT TCT TGT-3′ ; Fpn_reverse:

5′-CAG CAA TGA CTC CTG CAA ACA GCA-3′; TfR1_forward: 5′-AGC AGC ATC TGC TAA TGA GAC CCA-3′; TfR1_reverse: 5′-TGC AAG CTT TGT CTT CCC AAC AAC -3′. 18S rRNA was included as a housekeeping gene.

Neuronal cultures from DRG. Neuronal cultures were prepared from postnatal mouse DRGs (P1-P2) as follows. DRGs were dissected and incubated in 0.25% trypsin (Invitrogen) for 30 min at 37 °C. DRGs were then mechanically dissociated by triturating 5-10 times with a 22½ G needle followed by a 25½ G needle. The resulting cell suspension was passed through a 70 μm mesh and centrifuged at 500 x g for 10 min. Cells were resuspended in Dulbecco's Modified Eagle Medium containing F12 (DMEM/F12, Invitrogen) with 10% fetal bovine serum (FBS, Invitrogen) and 100 ng/mL nerve growth factor (NGF, Sigma) and plated onto glass coverslips coated with laminin (5 μg/mL, Sigma). Cells were treated either 5 hrs or 10 hrs after plating with the iron chelator salicylaldehyde isonicotinoyl hydrazone (SIH, 100 μM) or vehicle only and incubated overnight. SIH is an analog of pyridoxal isonicotinoyl hydrazone that shows high affinity and selectivity for iron (Richardson and Ponka, 1998a).

Schwann cell cultures. Schwann cells were isolated from postnatal mouse sciatic nerve (P5-P7) as follows. Sciatic nerves were taken out and digested first with 1% collagenase at 37 °C for 45 min and then with 0.25% trypsin at 37 °C for 15 min. Nerves were mechanically dissociated by triturating them first with a 21G needle and then with a 23G needle. The cell suspension was passed through a 70 μm mesh and centrifuged for 10 min

at 500 x g. Cells were resuspended in DMEM/F12 with 10% FBS and plated onto poly-L-lysine-coated glass coverslips.

Double immunofluorescence. DRG neurons on coverslips were fixed and permeabilized in 4% PFA at 4 °C for 20 min and then incubated with monoclonal mouse anti-SMI32 and anti-SMI312 (both 1:200; Covance) and polyclonal rabbit anti-COXIV antibodies in MEM/HEPES containing 2% normal goat serum and 2% ovalbumin for 30 min. Schwann cells on coverslips were first incubated with IgG-purified polyclonal rabbit anti-Fpn antibody (1:200, Alpha Diagnostics) for 30 min at room temperature, then permeabilized and incubated with monoclonal mouse anti-S100β antibody (1:200, Sigma). Primary antibodies were visualized with rhodamine-conjugated goat anti-mouse IgG (1:400, Jackson ImmunoResearch) and Alexa 488-conjugated goat anti-rabbit IgG (1:400; Invitrogen) for 30 min at room temperature. Cells were coverslipped with DAPI-containing mounting medium (Vector Laboratories) and viewed with a Zeiss Axioskop 2 plus microscope.

Sholl analysis. To quantify axon growth, a semi-automated Sholl analysis (Sholl, 1953) was carried out using ImageJ software with Sholl analysis plugin. First, the cell bodies and neurites were outlined to exclude adjacent cells. In order to remove background labelling and to better identify detailed neurites, densitometric thresholds were set for each neuron. Using ImageJ, templates of concentric circles increasing in radii by 20 μm were overlaid onto the center of a cell body. The total number of neurites intersecting each circle was counted using the automated Sholl analysis plugin. The maximal ring

with an intersecting process (maximal neurite length) and the sum of the number of intersections (branching complexity) for all rings were generated for each cell. The analysis was carried out for 15 cells per coverslip (2 coverslips per trial, 3 experimental trials; n=3). Data are shown as mean ± SEM. Two-way RM-ANOVA and student's *t*-test were used to determine statistical significance.

4.5 Results

Iron is involved in neurite growth initiation. We first assessed *in vitro* whether iron plays a role in neurite outgrowth. We isolated neurons from postnatal mouse DRGs and plated them on laminin-coated coverslips in the presence of NGF and allowed them to attach to the substrate for 5hrs (Fig. 1A). Immunofluorescence labeling for neurofilaments (SMI) after 5 hrs of plating showed that DRG neurons have not yet started to grow neurites (Fig. 1B). To render cells iron deficient, the iron chelator salicylaldehyde isonicotinoyl hydrazone (SIH) was added after 5 hrs of plating and left overnight. Immunofluorescence labeling for neurofilaments revealed impaired neurite outgrowth in the presence of the iron chelator (Fig. 1D) as compared to vehicle treated controls (Fig. 1C). Sholl analysis was used to quantify neurite outgrowth. This analysis makes use of a template of concentric rings of 20 μm distance that was overlaid onto the neuronal cell body. The intersections of the numbers of neurites with each ring were counted and plotted as a function of the distance from the cell body (Fig. 1E). This analysis revealed a significant reduction in neurite outgrowth in the SIH-treated group as compared to the vehicle-treated control (Fig. 1E). To further analyze neurite outgrowth, the branching complexity (sum of all intersections) and maximal neurite length (maximal

ring) were quantified revealing reduced branching complexity (Fig. 1F) and reduced maximal neurite length (Fig. 1G) in the SIH-treated as compared to the vehicle-treated group. These data suggest that iron is required for the initiation of neurite outgrowth from DRG neurons in culture.

Iron is involved in neurite growth elongation. We next assessed whether iron is also required for the elongation of neurites once growth has been initiated. DRG neurons were plated for 10 hrs before iron chelation to allow them not only to attach but also to start extending neurites (Fig. 2A). Immunofluorescence labeling for neurofilaments 10 hrs after plating shows that neurite outgrowth had started by that time (Fig. 2B). Cells were then treated with the iron chelator SIH or vehicle overnight. Immunofluorescence labeling for neurofilaments demonstrates reduced neurite outgrowth in the presence of SIH (Fig. 2D) compared to vehicle-treated control (Fig. 2C). Sholl analysis of these cultures showed a significant difference in neurite outgrowth elongation between the SIH- and vehicle-treated groups (Fig. 2E). Also the total branching complexity and the maximal neurite length were significantly reduced in the SIH-treated compared to the vehicle-treated group (Fig. 2F and G) suggesting that iron is involved in the elongation of neurites from DRG neurons in culture.

Changes in mitochondria under iron-deficient conditions. Axonal growth is a highly metabolic process that requires high-level ATP production by mitochondria. Since mitochondrial function is dependent on iron, we reasoned that impaired mitochondrial function might underlie the reduced neurite outgrowth observed under iron-deficient

conditions. We therefore assessed whether mitochondrial morphology is affected in our neurite outgrowth assay, as changes in morphology have previously been associated with mitochondrial dysfunction (Yoon et al., 2004; Yoon et al., 2006). DRG neurons were plated onto coverslips for 10 hrs and then incubated with the iron chelator SIH overnight. Double immunofluorescence labeling was performed using anti-SMI for neurofilaments and anti-cytochrome C oxidase subunit VI (COXVI) antibodies as a marker for mitochondria. Fine labeling for COXVI-positive mitochondria was detected in the vehicle-treated neurons (Fig. 3A-C). In contrast, SIH-treated neurons showed larger aggregates of COXVI-positive immunoreactivity (Fig. 3D-F), suggesting that iron deficiency affects the morphology and/or distribution of mitochondria. The increased mitochondrial cluster formation under iron-deficient conditions may suggest mitochondrial dysfunction.

Expression of Ceruloplasmin and Ferroportin in Schwann cells. Schwann cells are in close association with peripheral axons and might therefore be a primary source of iron for peripheral axons. To determine whether Schwann cells are able to export iron, we assessed the expression of the iron efflux proteins Fpn and Cp in Schwann cells. Fpn and a GPI-anchored form of Cp have been shown to be required for iron export from astrocytes (Jeong and David, 2003). Double immunofluorescence labeling of Schwann cells isolated from postnatal mouse sciatic nerve revealed expression of Cp (Fig. 4A-C) and Fpn (Fig. 4D-F) in S100β-positive Schwann cells suggesting that Schwann cells have the ability to export iron via these two proteins. The ferroxidase Hephaestin is not expressed in the sciatic nerve (data not shown).

Expression of iron influx and efflux proteins after sciatic nerve crush injury. Since iron appears to play a role in neurite outgrowth, iron supply from Schwann cells to peripheral axons may be especially important for axonal regeneration after peripheral nerve injury. To determine whether increased import and export of iron occur in the peripheral nerve distal to the site of injury, we assessed the expression of proteins known to be involved in iron uptake and release. Transferrin receptor 1 (TfR1) and divalent metal transporter 1 (DMT1) are implicated in two different iron import mechanisms: while TfR1 takes up transferrin-bound iron, DMT1 imports non-transferrin bound iron. RT-PCR analysis using RNA isolated from the nerve segment distal to the lesion site showed a small but significant induction of TfR1 mRNA expression at 1 day after injury, whereas mRNA levels for DMT1 did not change (Fig. 5A). An increase was also seen at a later time point but was not statistically significant because of the large variance in the control group (Fig. 5A). The increased TfR1 expression may reflect an increased iron need after injury. The mRNA expression of the iron exporter Fpn was highly upregulated at day 1, 7 and 14 (~5-6-fold at day 7 and 14) after nerve crush (Fig. 5B). The mRNA levels for Cp, which is normally high did not increase (Fig. 5B). The induction of Fpn levels suggest that increased iron efflux, likely from Schwann cells, may be required for axon regeneration after sciatic nerve crush injury.

Recovery of motor function and axonal regeneration after sciatic nerve injury are impaired in $Cp^{-/-}$ mice. Previous work has shown that iron efflux requires the presence of GPI-Cp. Its absence in Schwann cells in $Cp^{-/-}$ mice is likely to impair iron efflux from these glia in peripheral nerve. We therefore performed sciatic nerve crush injuries in $Cp^{-/-}$

mice and assessed axon regeneration and motor recovery. The rate of motor recovery after sciatic nerve crush was evaluated using the sciatic nerve functional index (SFI) prior to injury and at days 7, 11, 14, 17, 21 and 28 post injury. The SFI is calculated by measuring the distance between the first and the fifth toes and the length of the footprint. Following sciatic nerve injury, the SFI drops to a value of about -80, indicating a marked motor dysfunction of the injured hind paw (Fig. 6A). The recovery of the disability towards a normal SFI value of 0 reflects axonal regeneration and target reinnervation. $Cp^{-/-}$ mice exhibited significant lower SFI values at day 7, 11, 17 and 21 post-injury as compared to wildtype mice indicating a delay in motor recovery (Fig. 6A).

We further assessed directly whether axonal regeneration after sciatic nerve injury is impaired in $Cp^{-/-}$ mice by double immunofluorescence labelling for GAP-43, a protein expressed in growing axons. This analysis showed decreased GAP-43 immunoreactivity distal to the lesion site in $Cp^{-/-}$ mice (Fig. 6D and E) as compared to wildtype mice (Fig. 6B and C) at 4 days after injury. To quantify these results, we counted the numbers of GAP-43 positive profiles that were S100β negative, as S100β-positive non-myelinating Schwann cells may also express GAP-43 (Curtis et al., 1992). The numbers of GAP-43 positive axons were significantly decreased in longitudinal sections of the nerve at distances of 3 and 4 mm distal to the crush site at 4 days after injury (Fig. 6F), suggesting that axonal regeneration is impaired in $Cp^{-/-}$ mice.

4.6 Discussion

The importance of iron for metabolic processes is well known. However, the involvement of iron in specific highly energetic processes in the nervous system such as axonal growth

has not been studied in much detail. Here we show that neurite outgrowth initiation and extension in DRG neurons in culture is impaired in the presence of the iron chelator SIH suggesting that iron is required for both the initiation phase of neurite outgrowth and the elongation of an already existing neurite. This finding is in agreement with a previous study demonstrating that iron promotes NGF-induced neurite outgrowth in PC12 cells (Yoo et al., 2004). In the latter study, the addition of iron was shown to enhance neuronal differentiation by stimulating the extracellular signal-regulated kinase (ERK), a signaling molecule known to be involved in NGF-induced neurite outgrowth (Klesse et al., 1999; Perron and Bixby, 1999). Others have reported that the iron-containing porphyrin heme enhances neuronal differentiation (Ishii and Maniatis, 1978; Shinjyo and Kita, 2006). In addition, a recent study demonstrated a neurite growth-promoting effect of iron oxide nanoparticles in PC12 cells through the activation of signaling pathways involved in neuronal differentiation (Kim et al., 2011). We argue here that the impaired neurite outgrowth in our iron-deficient DRG neurons may be due to reduced iron supply to mitochondria which could affect mitochondrial function, and thus the production of ATP required for axonal growth. In support of this, we found increased mitochondrial aggregation in iron-deficient DRG neurons which might indicate mitochondrial dysfunction. Iron deficiency has been shown before to result in changes in mitochondrial morphology that have been associated with defects in mitochondrial function (Yoon et al., 2004; Yoon et al., 2006). These studies demonstrated the formation of highly elongated mitochondria in Chang cells in the presence of the iron chelator desferrioxamine, which was accompanied by increased levels of reactive oxygen species (ROS), decreased mitochondrial DNA content and a decrease in the iron-dependent

enzymatic activity of the respiratory chain complex II, indicating mitochondrial dysfunction (Yoon et al., 2004; Yoon et al., 2006). Changes in mitochondrial morphology due to mitochondrial dysfunction have also been reported in several pathological conditions (DiMauro et al., 1985; Chow and Thorburn, 2000; Duvezin-Caubet et al., 2006).

Axonal mitochondria are enriched in regions of high metabolic needs such as active axonal growth cones, nodes of Ranvier and synapses (Bogan and Cabot, 1991; Fabricius et al., 1993; Morris and Hollenbeck, 1993). Therefore, proper mitochondrial function is important for both, axonal growth and maintaining axonal function. Impairment of either axonal transport of mitochondria or mitochondrial function per se has been also associated with a number of neurological diseases (Baloh, 2008; Mahad et al., 2008; Chen and Chan, 2009; Magrane and Manfredi, 2009), further underlining the importance of axonal mitochondria. Since axons in the PNS can be very long, mitochondria are often located far away from the neuronal cell body, the major site where they are produced. It is therefore conceivable that mitochondria receive iron along the length of the axon from Schwann cells to ensure their proper functioning rather than having to return to the cell body to acquire iron. We show here that Schwann cells express the iron efflux proteins Fpn and Cp, and are therefore equipped to export iron. In the CNS, GPI-Cp mediates iron efflux from astrocytes in the CNS by interacting with the iron exporter Fpn (Jeong and David, 2003). The action of the ferroxidase Cp is essential for the iron efflux to occur, as astrocytes from $Cp^{-/-}$ mice are unable to efflux iron *in vitro* (Jeong and David, 2003). In addition, iron accumulation occurs in different tissues of $Cp^{-/-}$ mice including liver, spleen and CNS (Harris et al., 1999; Patel et al., 2002; Jeong and

David, 2006), indicating the importance of Cp in iron efflux from different tissues. The expression of the GPI-anchored form of Cp in Schwann cells has been also previously reported (Salzer et al., 1998). Thus, iron efflux from Schwann cells is likely to be mediated by Cp and Fpn. We investigated here the role of iron efflux from Schwann cells in providing peripheral axons with iron during axonal regeneration after peripheral nerve injury, a situation that might require high amounts of iron. We found increased Fpn mRNA expression at 1, 7 and 14 days after sciatic nerve crush injury distal to the lesion site indicating the need of increased iron export for axonal regeneration. Since our *in vitro* data demonstrate that iron is required for neurite growth, the increased iron export might be important for supporting axonal regrowth. The observed Fpn upregulation after sciatic nerve injury is likely to occur in Schwann cells which have been shown to play a key role in promoting axonal regeneration after peripheral nerve injury. Following injury-induced axonal degeneration, Schwann cells dedifferentiate and start proliferating within the basal lamina tubes in a longitudinal fashion to form the so called "bands of Büngner" (Liu et al., 1995). This alignment of cells together with the extracellular matrix components secreted by Schwann cells provides structural guidance and growth-promoting substrates to the regenerating axons. In addition, Schwann cells secrete neurotrophic factors such as NGF, CNTF and BDNF which have been shown to support axon regeneration (Heumann et al., 1987; Sahenk et al., 1994; Zhang et al., 2000). Our results suggest that Schwann cells may also supply iron to mitochondria within growing axons and in growth cones. Although we cannot rule out the possibility that the increased Fpn expression seen occurs in invading macrophages, in general, macrophages in tissues (except the spleen) retain iron.

We also observed increased mRNA expression of the iron importer TfR1 after sciatic nerve crush injury at 1 day after injury. TfR1which is known to mediate the endocytosis of transferrin-bound iron plays an important role in iron uptake in many cells. An increase in TfR1 expression after sciatic nerve injury has also been reported by others (Raivich et al., 1991), which also included the demonstration of increased TfR1 expression in Schwann cells that paralleled an increase in endoneural iron uptake. These lines of evidence confirm the increased need for iron after peripheral nerve injury. The early upregulation of TfR1 at 1 day post injury is likely to be attributed to Schwann cells, as macrophages only invade the injured nerve at a later time point. Schwann cells might have high iron requirements at this time, due to their increased metabolic activity following injury such as the degradation and phagocytosis of myelin, and their proliferation which starts around 3 days after injury. Schwann cells might also accumulate iron for providing it to the newly formed axonal growth cones. Schwann cells have also been shown to increase the synthesis of TF after peripheral nerve injury (Salis et al., 2007), which could serve to support their own iron uptake as well as axonal iron import. Thus, Schwann cells appear to upregulate their iron uptake and iron export after sciatic nerve injury, possibly to provide iron for axonal regeneration. We show here that axonal regeneration and recovery of motor function in $Cp^{-/-}$ mice is impaired. This impairment of axon regeneration may be due to the loss of iron export from Schwann cells in mice lacking Cp.

Taken together, our data indicate that iron is required for neurite outgrowth *in vitro*, likely being required for proper mitochondrial function. Our data further suggest that iron efflux from Schwann cells, which might play a role in delivering iron to axons,

is involved in axon regeneration after peripheral nerve injury. These results provide insight into a novel aspect of Schwann cell contribution to peripheral axon regeneration.

4.7 References

Baloh RH (2008) Mitochondrial dynamics and peripheral neuropathy. Neuroscientist 14:12-18.

Bogan N, Cabot JB (1991) Light and electron microscopic analyses of intraspinal axon collaterals of sympathetic preganglionic neurons. Brain Res 541:241-251.

Bunge RP (1993) Expanding roles for the Schwann cell: ensheathment, myelination, trophism and regeneration. Curr Opin Neurobiol 3:805-809.

Chen H, Chan DC (2009) Mitochondrial dynamics--fusion, fission, movement, and mitophagy--in neurodegenerative diseases. Hum Mol Genet 18:R169-176.

Chow CW, Thorburn DR (2000) Morphological correlates of mitochondrial dysfunction in children. Hum Reprod 15 Suppl 2:68-78.

Corfas G, Velardez MO, Ko CP, Ratner N, Peles E (2004) Mechanisms and roles of axon-Schwann cell interactions. J Neurosci 24:9250-9260.

Curtis R, Stewart HJ, Hall SM, Wilkin GP, Mirsky R, Jessen KR (1992) GAP-43 is expressed by nonmyelin-forming Schwann cells of the peripheral nervous system. J Cell Biol 116:1455-1464.

de Medinaceli L, Freed WJ, Wyatt RJ (1982) An index of the functional condition of rat sciatic nerve based on measurements made from walking tracks. Exp Neurol 77:634-643.

DiMauro S, Bonilla E, Zeviani M, Nakagawa M, DeVivo DC (1985) Mitochondrial myopathies. Ann Neurol 17:521-538.

Duvezin-Caubet S, Jagasia R, Wagener J, Hofmann S, Trifunovic A, Hansson A, Chomyn A, Bauer MF, Attardi G, Larsson NG, Neupert W, Reichert AS (2006) Proteolytic processing of OPA1 links mitochondrial dysfunction to alterations in mitochondrial morphology. J Biol Chem 281:37972-37979.

Fabricius C, Berthold CH, Rydmark M (1993) Axoplasmic organelles at nodes of Ranvier. II. Occurrence and distribution in large myelinated spinal cord axons of the adult cat. J Neurocytol 22:941-954.

Gille G, Reichmann H (2011) Iron-dependent functions of mitochondria--relation to neurodegeneration. J Neural Transm 118:349-359.

Harris ZL, Durley AP, Man TK, Gitlin JD (1999) Targeted gene disruption reveals an essential role for ceruloplasmin in cellular iron efflux. Proc Natl Acad Sci U S A 96:10812-10817.

Heumann R, Korsching S, Bandtlow C, Thoenen H (1987) Changes of nerve growth factor synthesis in nonneuronal cells in response to sciatic nerve transection. J Cell Biol 104:1623-1631.

Inserra MM, Bloch DA, Terris DJ (1998) Functional indices for sciatic, peroneal, and posterior tibial nerve lesions in the mouse. Microsurgery 18:119-124.

Ishii DN, Maniatis GM (1978) Haemin promotes rapid neurite outgrowth in cultured mouse neuroblastoma cells. Nature 274:372-374.

Jeong SY, David S (2003) Glycosylphosphatidylinositol-anchored ceruloplasmin is required for iron efflux from cells in the central nervous system. J Biol Chem 278:27144-27148.

Jeong SY, David S (2006) Age-related changes in iron homeostasis and cell death in the cerebellum of ceruloplasmin-deficient mice. J Neurosci 26:9810-9819.

Kim JA, Lee N, Kim BH, Rhee WJ, Yoon S, Hyeon T, Park TH (2011) Enhancement of neurite outgrowth in PC12 cells by iron oxide nanoparticles. Biomaterials 32:2871-2877.

Klesse LJ, Meyers KA, Marshall CJ, Parada LF (1999) Nerve growth factor induces survival and differentiation through two distinct signaling cascades in PC12 cells. Oncogene 18:2055-2068.

Levi S, Rovida E (2009) The role of iron in mitochondrial function. Biochim Biophys Acta 1790:629-636.

Liu HM, Yang LH, Yang YJ (1995) Schwann cell properties: 3. C-fos expression, bFGF production, phagocytosis and proliferation during Wallerian degeneration. J Neuropathol Exp Neurol 54:487-496.

Magrane J, Manfredi G (2009) Mitochondrial function, morphology, and axonal transport in amyotrophic lateral sclerosis. Antioxid Redox Signal 11:1615-1626.

Mahad D, Lassmann H, Turnbull D (2008) Review: Mitochondria and disease progression in multiple sclerosis. Neuropathol Appl Neurobiol 34:577-589.

Morris RL, Hollenbeck PJ (1993) The regulation of bidirectional mitochondrial transport is coordinated with axonal outgrowth. J Cell Sci 104 (Pt 3):917-927.

Patel BN, Dunn RJ, Jeong SY, Zhu Q, Julien JP, David S (2002) Ceruloplasmin regulates iron levels in the CNS and prevents free radical injury. J Neurosci 22:6578-6586.

Perron JC, Bixby JL (1999) Distinct neurite outgrowth signaling pathways converge on ERK activation. Mol Cell Neurosci 13:362-378.

Raivich G, Graeber MB, Gehrmann J, Kreutzberg GW (1991) Transferrin Receptor Expression and Iron Uptake in the Injured and Regenerating Rat Sciatic Nerve. Eur J Neurosci 3:919-927.

Reynolds ML, Woolf CJ (1993) Reciprocal Schwann cell-axon interactions. Curr Opin Neurobiol 3:683-693.

Richardson DR, Ponka P (1998) Orally effective iron chelators for the treatment of iron overload disease: the case for a further look at pyridoxal isonicotinoyl hydrazone and its analogs. J Lab Clin Med 132:351-352.

Sahenk Z, Seharaseyon J, Mendell JR (1994) CNTF potentiates peripheral nerve regeneration. Brain Res 655:246-250.

Salis C, Setton CP, Soto EF, Pasquini JM (2007) The mRNA of transferrin is expressed in Schwann cells during their maturation and after nerve injury. Exp Neurol 207:85-94.

Salzer JL, Lovejoy L, Linder MC, Rosen C (1998) Ran-2, a glial lineage marker, is a GPI-anchored form of ceruloplasmin. J Neurosci Res 54:147-157.

Shinjyo N, Kita K (2006) Up-regulation of heme biosynthesis during differentiation of Neuro2a cells. J Biochem 139:373-381.

Sholl DA (1953) Dendritic organization in the neurons of the visual and motor cortices of the cat. J Anat 87:387-406.

Yoo YE, Hong JH, Hur KC, Oh ES, Chung JM (2004) Iron enhances NGF-induced neurite outgrowth in PC12 cells. Mol Cells 17:340-346.

Yoon YS, Cho H, Lee JH, Yoon G (2004) Mitochondrial dysfunction via disruption of complex II activity during iron chelation-induced senescence-like growth arrest of Chang cells. Ann N Y Acad Sci 1011:123-132.

Yoon YS, Yoon DS, Lim IK, Yoon SH, Chung HY, Rojo M, Malka F, Jou MJ, Martinou JC, Yoon G (2006) Formation of elongated giant mitochondria in DFO-induced cellular senescence: involvement of enhanced fusion process through modulation of Fis1. J Cell Physiol 209:468-480.

Zhang JY, Luo XG, Xian CJ, Liu ZH, Zhou XF (2000) Endogenous BDNF is required for myelination and regeneration of injured sciatic nerve in rodents. Eur J Neurosci 12:4171-4180.

4.8 Figures

Figure 1

Initiation of neurite outgrowth is impaired in DRG neurons under iron-deficient conditions. DRG neurons were isolated from P1-P2 day old postnatal mouse, plated onto coverslips for 5 hrs to allow cells to attach, and then treated overnight with the iron chelator SIH or vehicle. (**A**) illustrates the experimental timeline. (**B**) Immunofluorescence labelling with anti-SMI antibody for neurofilaments shows no neurite outgrowth in the first 5 hrs after plating. After overnight incubation, vehicle-treated control cultures showed neurite growth (**C**). In contrast, there was impaired neurite outgrowth initiation in the SIH-treated group (**D**). Scale bar in D=100 μm. Sholl analysis revealed a significant difference in neurite branching complexity (**E** and **F**) and maximal neurite length (**E** and **G**) between the SIH- and vehicle-treated groups. Results are shown as mean ± SEM (n=3; *$p \leq 0.05$; Two-way RM-ANOVA or Student's *t* test).

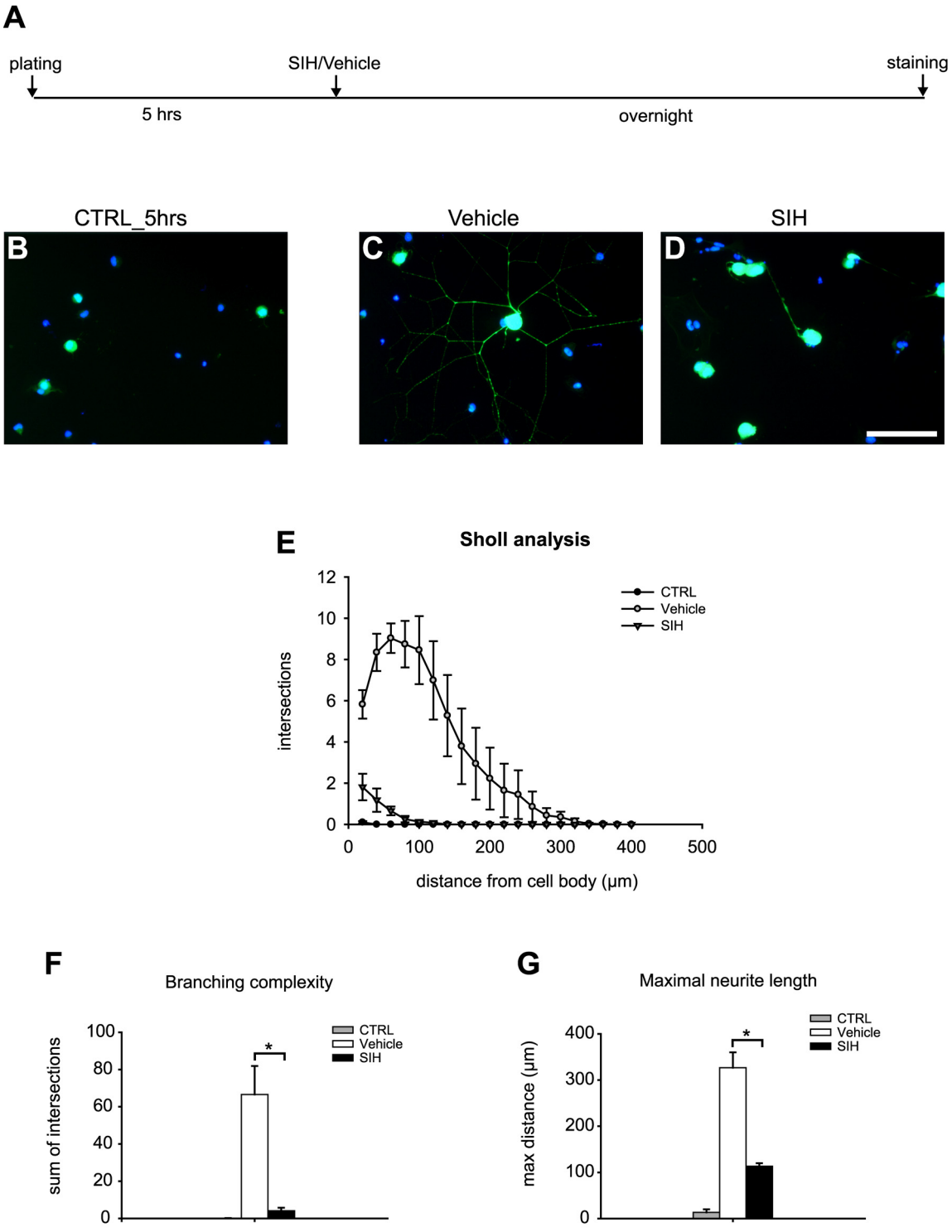
A
plating
SIH/Vehicle
staining
5 hrs
overnight
CTRL_5hrs
Vehicle
SIH
B
C
D
E
Sholl analysis
intersections
distance from cell body (μm)
CTRL
Vehicle
SIH
F
Branching complexity
sum of intersections
G
Maximal neurite length
max distance (μm)

Figure 2

Extension of neurite outgrowth is impaired in DRG neurons under iron-deficient conditions. DRG neuronal cultures were plated onto coverslips for 10 hrs to allow neurite outgrowth to start, and then treated overnight with the iron chelator SIH or vehicle. (**A**) illustrates the experimental timeline. (**B**) Immunofluorescence labelling with anti-SMI antibody for neurofilaments shows that neurite outgrowth has already started in the first 10 hrs after plating. (**C**) After overnight incubation, vehicle-treated control cultures show extensive neurite growth. (**D**) In contrast, SIH-treated cultures show marked impairment of neurite extension. Scale bar in D=100 μm. Sholl analysis revealed a significant difference in neurite branching complexity (**E** and **F**) and maximal neurite length (**E** and **G**) between the SIH- and vehicle-treated groups. Results are shown as mean ± SEM (n=3; *$p \leq 0.05$; Two-way RM-ANOVA or Student's *t* test).

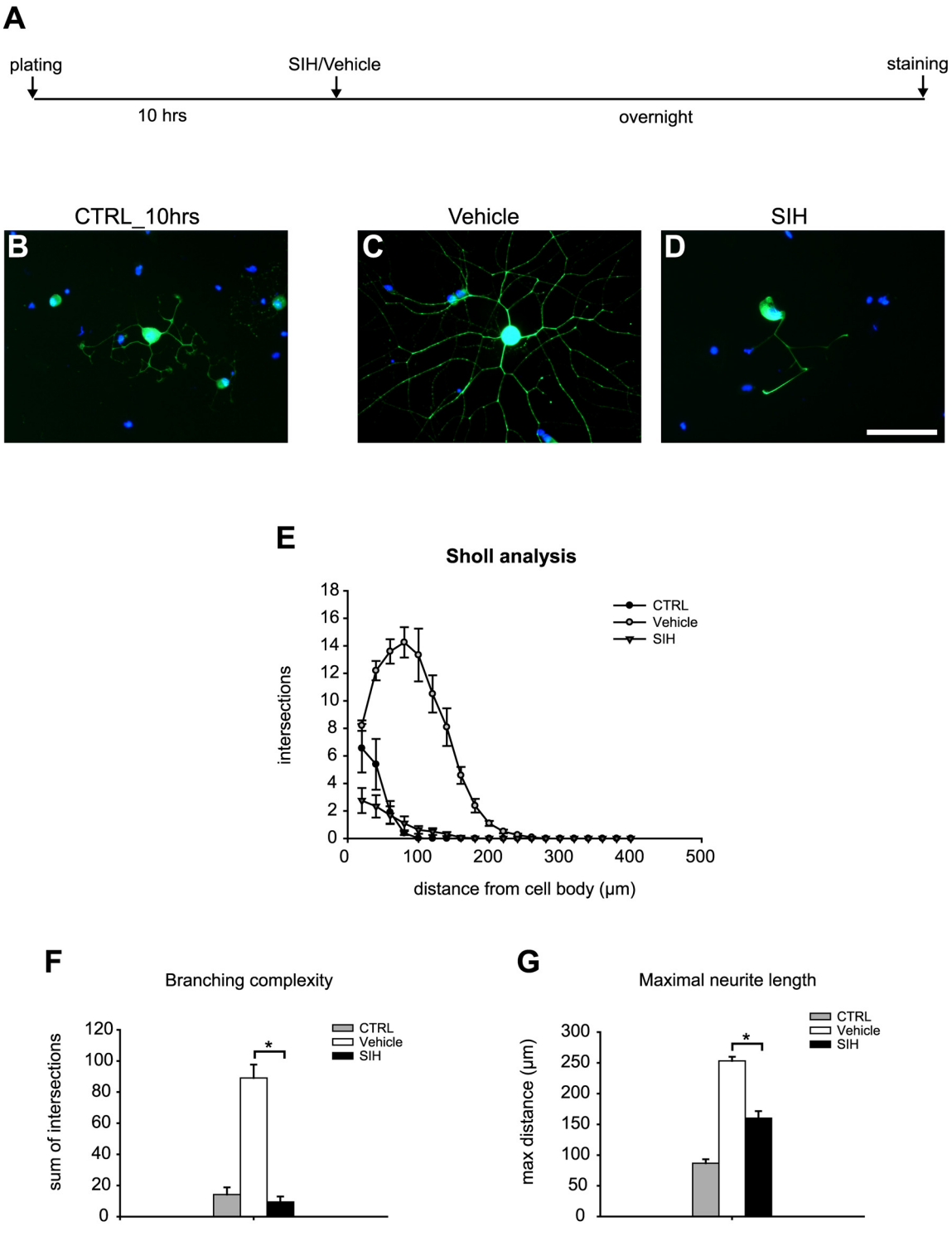
A
plating
SIH/Vehicle
staining
10 hrs
overnight
CTRL_10hrs
Vehicle
SIH
B
C
D
E
Sholl analysis
CTRL
Vehicle
SIH
intersections
distance from cell body (μm)
F
Branching complexity
sum of intersections
G
Maximal neurite length
max distance (μm)

Figure 3

Mitochondrial aggregation under iron-deficient conditions. DRG neurons were plated for 10 hrs on coverslips, and then treated with the iron chelator SIH overnight. Double immunofluorescence labelling using the mitochondrial marker anti-COXIV (**A** and **D**) and the neuronal marker anti-SMI (**B** and **E**) demonstrates mitochondrial cluster formation (as indicated by arrows) in the SIH-treated DRG neurons as compared to the fine labeling for mitochondria in the vehicle (VEH) -treated control group. Merged images including DAPI staining to visualize cell nuclei are shown in **C** and **F**. Scale bar in F=20 μm.

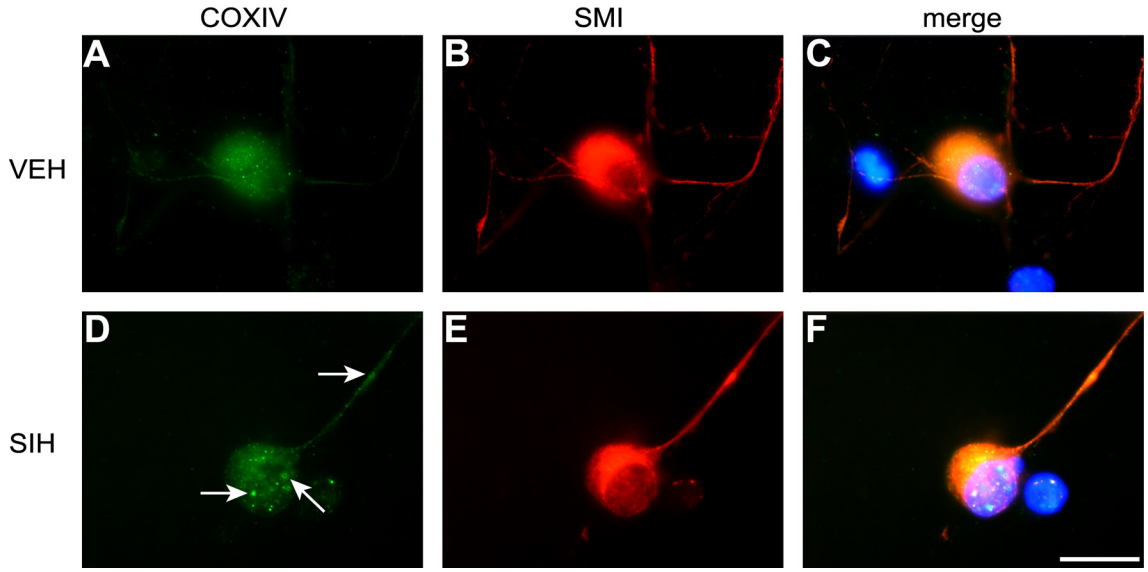
COXIV
SMI
merge
A
B
C
VEH
D
E
F
SIH

Figure 4

Expression of Fpn and Cp in Schwann cells. Schwann cells were isolated from P5-P7 day old postnatal mouse sciatic nerve. Double immunofluorescence labelling with anti-Cp (**A**) or anti-Fpn (**D**) and the Schwann cell marker anti-S100β (**B** and **E**) antibodies demonstrates expression of Cp and Fpn in Schwann cells. Merged images including DAPI staining to visualize cell nuclei are shown in **C** and **F**. Scale bar in F=50 μm.

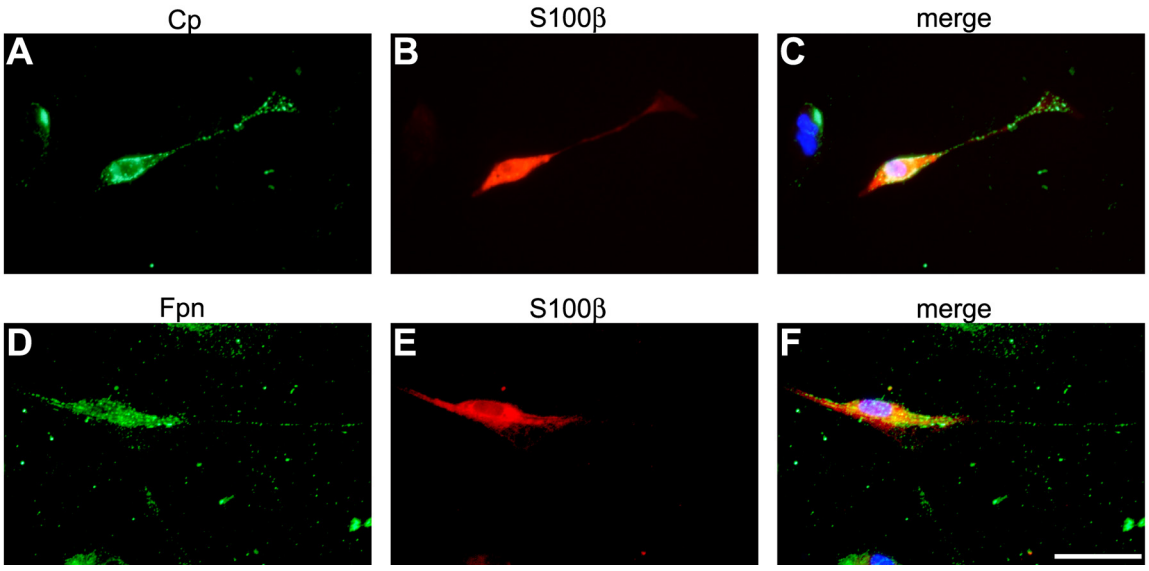
Cp
S100β
merge
A
B
C
Fpn
S100β
merge
D
E
F

Figure 5

The mRNA expression of iron import and export proteins after sciatic nerve injury. (**A**) RT-PCR analysis for the iron import proteins TfR1 and DMT1 was performed after sciatic nerve crush injury using RNA from the nerve segment distal to the lesion site. The results show that mRNA expression levels of TfR1 were upregulated 1-day post injury, whereas DMT1 levels did not change. (**B**) RT-PCR analysis for the iron export proteins Fpn and Cp showed a significant upregulation of Fpn, but not Cp, mRNA expression levels at 1, 7 and 14 days post injury. Results are shown as mean ± SEM (n=3; *$p \leq 0.05$; Student's *t* test).

A

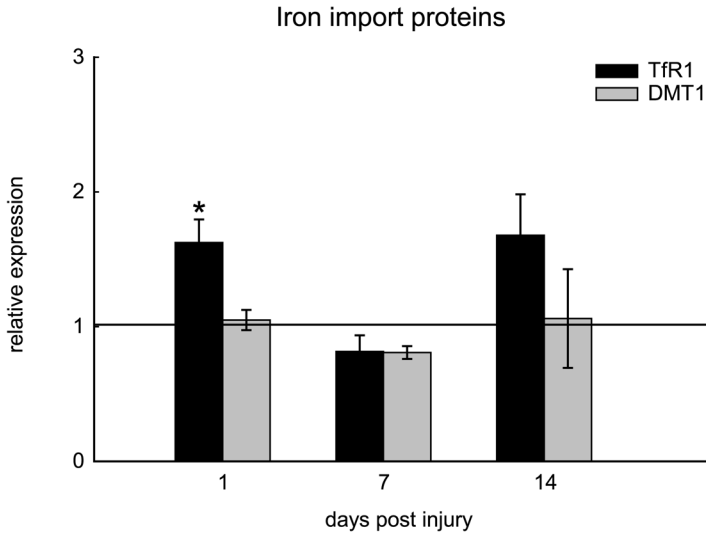
Iron import proteins
TfR1
DMT1
relative expression
0
1
2
3
*
1
7
14
days post injury

B

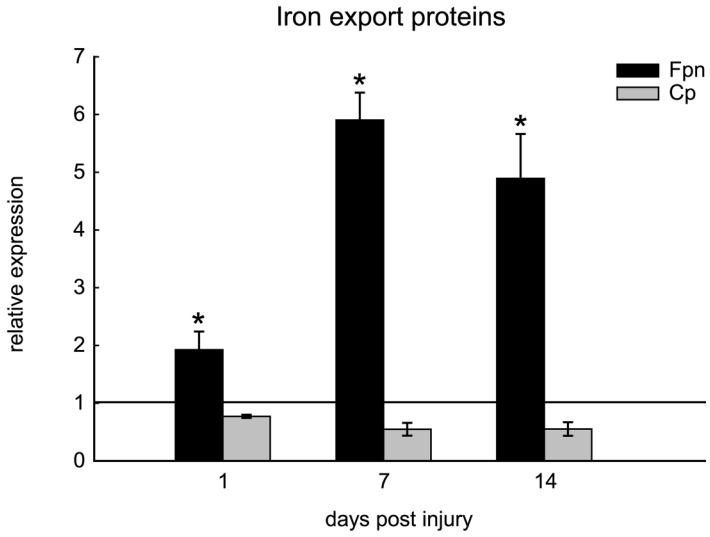
Iron export proteins
Fpn
Cp
relative expression
0
1
2
3
4
5
6
7
*
*
*
1
7
14
days post injury

Figure 6

Axonal regeneration and motor recovery after sciatic nerve injury are impaired in Cp KO mice. (**A**) Footprint analysis in Cp KO and WT mice was performed at 0, 7, 10, 14, 17, 21 and 28 days following sciatic nerve crush. Recovery of motor function as determined by the sciatic functional index (SFI, calculated from footprints) was significantly delayed in Cp KO compared to WT mice. Immunofluorescence analysis in longitudinal sections of crushed sciatic nerves using anti-GAP43 (**B** and **D**) antibody, a marker for regenerating axons, shows less regenerating axons at 4 mm distal to the lesion site in Cp KO compared to WT mice 4 days after injury. Images with DAPI staining to label cell nuclei are shown in **C** and **E**. Scale bar in E=200 μm. (**F**) Quantification of the numbers of GAP43-positive axons 3, 4 and 5 mm distal to the lesion site revealed a significant decrease of regenerating axons in Cp KO compared to WT mice. Results are shown as mean ± SEM (n=3; *$p \leq 0.05$; Two-way RM-ANOVA).

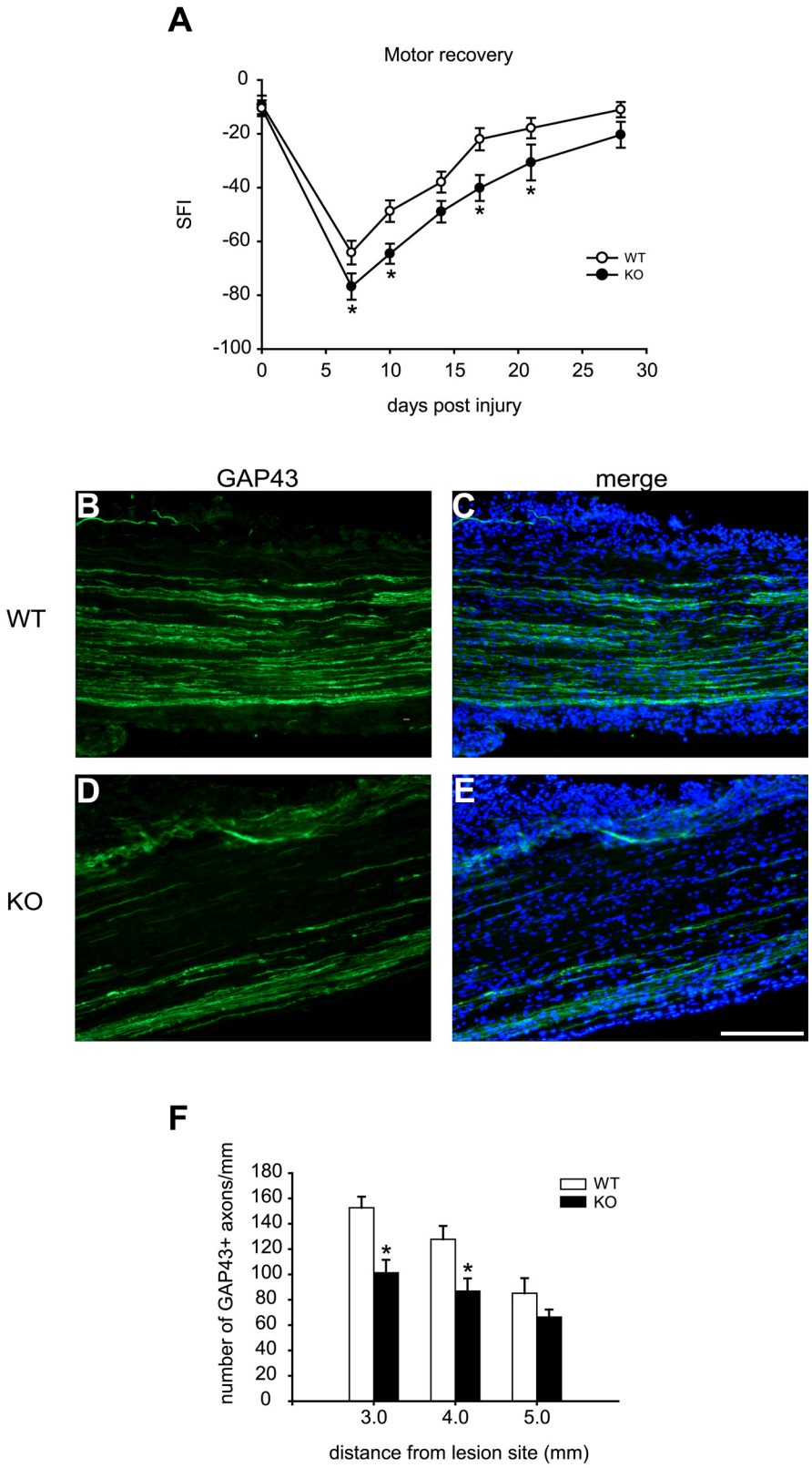
A
Motor recovery
SFI
0
-20
-40
-60
-80
-100
0
5
10
15
20
25
30
days post injury
WT
KO
GAP43
merge
B
C
D
E
WT
KO
F
number of GAP43+ axons/mm
180
160
140
120
100
80
60
40
20
0
3.0
4.0
5.0
distance from lesion site (mm)
WT
KO

Chapter 5

Summary and General Discussion

Iron is required for various metabolic functions including mitochondrial oxidation and DNA synthesis (Andrews and Schmidt, 2007). Since the CNS is a highly metabolic active organ, consuming about 20% of the body's total energy, its proper functioning is dependent on iron. Besides its role in general metabolism, iron is also involved in CNS-specific function such as myelination and neurotransmitter synthesis (Beard et al., 1993). However, excessive, unshielded iron can be toxic due to its ability to promote the production of free radicals. Several neurodegenerative diseases have been associated with iron accumulation and oxidative damage, which may be either due to primary defects in iron homeostatic proteins or to secondary dysregulation of iron homeostasis. Thus, the regulation of iron homeostasis in the CNS is essential on the one hand to prevent iron-induced cytotoxicity, and on the other hand to ensure sufficient iron supply for proper CNS function. To maintain cellular iron balance, iron homeostatic mechanisms have evolved that control the uptake, storage and export of iron. Despite the importance of iron homeostasis in the CNS, it is still not well understood. In my Ph.D. thesis work, I therefore sought to investigate the control of iron homeostasis in the nervous system with a focus on iron efflux mechanisms. I specifically assessed how iron is exported by glial cells and how iron efflux serves to provide neighbouring cells with iron.

5.1 The ferroxidase Hephaestin is involved in mediating iron efflux from oligodendrocytes.

Previously, our laboratory has identified a GPI-anchored form of the ferroxidase Cp that is only expressed by astrocytes in the CNS (Patel and David, 1997). It was further demonstrated that GPI-Cp plays a role in iron efflux from astrocytes by interacting with the iron exporter Fpn (Jeong and David, 2003). In my work, I showed that

oligodendrocytes express the Cp homologue Heph and that it is involved in iron efflux from these cells. Like Cp, Heph is a ferroxidase that converts the ferrous iron into the ferric form, and thus cannot transport iron by itself, but needs to interact with an iron exporter. I showed that the only known iron exporter Fpn is also expressed in oligodendrocytes. Heph has been previously shown to interact with Fpn in HEK293 cells (Yeh et al., 2009) and thus, is likely to mediate iron efflux via Fpn in a similar way than Cp. The immediate oxidation of ferrous iron that is transported by Fpn appears to be required for iron efflux to occur, as astrocytes from $Cp^{-/-}$ mice (Jeong and David, 2003) and oligodendrocytes from sla mice that are deficient in Heph are unable to release iron in culture. My results also show that iron accumulates in oligodendrocytes in sla mice *in vivo*, further confirming the role of Heph in iron export from oligodendrocytes. Interestingly, iron accumulation in the sla mice occurred only in grey but not white matter oligodendrocytes, suggesting differences in the regulation of iron homeostasis between grey and white matter oligodendrocytes. In support of this idea, I found upregulation of Cp in white matter oligodendrocytes in the sla mice as a compensation for the loss of Heph function. In addition, mice deficient in both ferroxidases ($Cp^{-/-}$ /$Heph^{sla}$ double mutants) demonstrated iron accumulation in both, grey and white matter oligodendrocytes, further supporting a protective role of Cp in white matter oligodendrocytes in the sla mice. These results suggest that grey and white matter oligodendrocytes utilize different ferroxidases to efflux iron. Given the important function of myelinating long fibre tracts, white matter oligodendrocytes may possess this additional fail-safe mechanism to prevent iron overload and potential damage to these white matter tracts. As mentioned earlier, accumulation of free, unshielded iron can

promote oxidative damage, and thus affect cellular function. My results revealed impaired motor function in the sla mice which appeared to be even more pronounced in the $Cp^{-/-}/Heph^{sla}$ double mutants, consistent with the extent of iron accumulation. I did not observe oligodendrocyte loss nor defects in gross myelination that could underlie the motor deficits in sla mice. However, subtle changes in myelination occurred at the paranodal regions of myelinated fibres in the spinal cord of sla mice. I found a decrease in the expression of the axonal protein Caspr, which is involved in establishing and maintaining the paranodal junctions (Einheber et al., 1997). Paranodal junctions form between the terminal myelin loops and the axon, and present a critical barrier between the voltage-gated Na^+ channels at the node of Ranvier and the delayed rectifier K^+ channels in the juxtaparanodal region (Denisenko-Nehrbass et al., 2002). These barriers are therefore crucial for the propagation of action potentials via saltatory conduction. Consequently, disruptions of paranodal junctions, e.g. due to loss of Caspr, can result in motor deficits, which has been also reported by others (Bhat et al., 2001; Boyle et al., 2001). In addition, oligodendrocytes in the sla spinal cord showed reduced expression levels of Nogo-A which has been shown to form a complex with Caspr at the paranodal myelin loops (Nie et al., 2003). At present, it is not clear how iron accumulation in oligodendrocytes causes the decrease in Nogo-A and Caspr, but may be associated with iron-related oxidative stress. Free radical stress has been previously reported to result in a reduction of protein expression (Singh and Wangemann, 2008). In addition, reactive oxygen species have been implicated in the regulation of the transcription of various genes, e.g. by modulating the activity of redox-sensitive transcription factors such as NFκB or AP-1 (Sen and Packer, 1996; Shlomai, 2010). Therefore, iron-promoted free

radical formation may also affect the expression of Nogo-A by oligodendrocytes. The reduction of Nogo-A at the myelin loops could then in turn cause a decrease in its axonal binding partner Caspr due to loss of complex formation. Electron microscopic analysis revealed abnormalities in the paranodal structure in sla mice, likely due to reduced Nogo-A and Caspr expression/interaction. It would be interesting to further assess, whether the disruption of the paranodal structure actually results in disorganization of ion channels at the nodes of Ranvier and whether the conduction velocity of action potentials is reduced in the spinal cord of sla mice. Such disturbances in saltatory conduction are likely to underlie the motor deficits observed in the sla mice. These results emphasize the importance of proper functioning iron export from oligodendrocytes, and further suggest that dysregulation of iron efflux mechanisms may also contribute to the iron accumulation and iron-associated damage seen in neurodegenerative diseases.

5.2 Iron efflux from astrocytes is required for remyelination

In chapter 3, I addressed the question of whether iron efflux plays a role in the delivery of iron from one cell to another. I specifically focussed on iron efflux from astrocytes, since astrocytes might be the first cells in the CNS to acquire iron from the circulation due to their close proximity to brain endothelial cells. In addition, astrocytes are equipped with iron influx and efflux mechanisms that enable them to take up iron at the blood-brain barrier (BBB) and distribute it to other cell types in the CNS. As mentioned earlier, iron efflux from astrocytes is mediated by Fpn and GPI-Cp. To study the role of iron efflux from astrocytes in delivering iron to other CNS cells, Fpn was specifically deleted in astrocytes. In addition, this idea was examined in a situation that requires high amounts of iron, such as remyelination. I showed that LPC-induced demyelination which is

normally followed by rapid remyelination resulted in reduced remyelination in astrocyte-specific Fpn KO mice. In the CNS, remyelination is carried out by OPCs which first proliferate and then differentiate into mature oligodendrocytes (Franklin and Ffrench-Constant, 2008). Both phases of remyelination are iron-dependent. Iron is involved in the proliferation of cells, because it is an essential cofactor for many metabolic enzymes and the ribonucleotide reductase which is required for DNA synthesis (Cazzola et al., 1990). In addition, iron plays a role in myelin formation as a cofactor for enzymes involved in cholesterol and lipid synthesis (Todorich et al., 2009). Thus, during the process of remyelination, OPCs have a high iron demand that might be met by iron delivered from astrocytes, which may be able to upregulate iron uptake into the CNS at the level of the BBB. I showed that the proliferation of OPCs after LPC injections was reduced in the astrocyte-specific Fpn KO mice, further supporting the idea of iron transport from astrocytes to OPCs. Whether the differentiation of OPCs is also affected as a primary result of iron deficiency in OPCs in these animals, is currently not known. However, consistent with previous reports, a decrease in the pool of OPCs after experimentally-induced demyelination is likely to result in lower numbers of mature oligodendrocytes, and consequently in reduced remyelination (Arnett et al., 2001). Although OPCs are the key players in remyelination, astrocytes and microglia/macrophages also contribute to remyelination by secreting growth factors and cytokines that promote OPC proliferation and differentiation (Franklin et al., 2002; Moore et al., 2010). Thus, iron delivery from astrocytes during remyelination might not only be important for OPCs but also for microglia/macrophages. Using cell culture, I addressed whether iron plays a role in the secretion of cytokines by microglia. My results show that rendering LPS-activated

microglia iron-deficient leads to reduced expression of the cytokines TNF-α and IL-1β. Both cytokines promote remyelination following chemically-induced demyelination (Arnett et al., 2001; Mason et al., 2001). My findings indicate that iron plays a role in the expression of IL-1β and TNF-α by activated microglia, and thus suggest that iron-deprived microglia may also contribute to reduced remyelination in the astrocyte-specific Fpn KO mice. Although it is possible that microglia receive iron from astrocytes, it is not clear at present whether microglia in our *in vivo* model are indeed iron-deficient and whether a reduction in cytokines occurs in these animals. One way in which IL-1β and TNF-α could be influencing remyelination is by stimulating astrocytes to produce growth factors involved in OPC proliferation and differentiation. Stimulating astrocytes in culture with IL-1β and TNF-α resulted in increased expression of FGF-2 and IGF-1, respectively. While FGF-2 has been implicated in enhancing the proliferation of OPCs (McKinnon et al., 1990), IGF-1 is thought to promote primarily the differentiation of OPCs (Mozell and McMorris, 1991). Thus, the reduced expression of IL-1β and TNF-α by iron-deficient microglia might result in decreased expression of FGF-2 and IGF-1 by astrocytes, which may also contribute to the impaired OPC proliferation and differentiation in our *in vivo* model. Another growth factor that was found to be upregulated in astrocytes when stimulated with IL-1β was TGF-β. Besides a potential role in OPC differentiation (McKinnon et al., 1993), TGF-β has been implicated in the polarization of macrophages towards an anti-inflammatory M2 phenotype. M2 macrophages have been shown to promote regeneration and repair processes (David and Kroner, 2011), and may therefore also play a role in promoting remyelination. Reduced TGF-β levels as a result of decreased IL-1β expression by iron-deficient microglia may

therefore also contribute to the reduced remyelination observed in the astrocyte-specific Fpn KO mice. Thus, iron retention in astrocytes may affect remyelination by either directly depriving OPCs of iron required for their proliferation and differentiation, or by depriving microglia of iron, which in turn could result in a reduction of cytokines and growth factors involved in OPC proliferation and differentiation. Further investigations are needed to assess whether these cytokines and growth factors are actually downregulated in the LPC lesion site in the astrocyte-specific Fpn KO mice. This is technically difficult because of the very small demyelinating lesions produced by LPC injection. A model with more widespread demyelination and remyelination such as that induced by cuprizone in the corpus callosum might be more suitable. It would be also interesting to examine whether less M2 macrophages are present in the spinal cord after LPC injections. Together, these results indicate a role of iron efflux from astrocytes in remyelination, and suggest different ways in which iron may be implicated in OPC proliferation and differentiation. Given the low concentration of iron in the CSF, iron uptake by astrocytes at the BBB and subsequent iron delivery to CNS cells which have an increased demand for iron might be essential to ensure adequate iron supply to these cells. In support of this, a previous study from our laboratory has also suggested a role for astrocytes in providing iron to neurons (Jeong and David, 2006). Such a rather cell-to-cell transport of iron may be particularly important in the CNS considering the toxicity of free iron and the high vulnerability of the CNS to oxidative stress. Thus, iron efflux from astrocytes may be crucial in supplying other CNS cells safely with iron, especially in situations of high iron demand.

5.3 Iron efflux from Schwann cells plays a role in peripheral axon regeneration

Not much is known so far about iron homeostatic mechanisms in the PNS. However, the GPI-anchored form of Cp is expressed by Schwann cells (Salzer et al., 1998). My results show that in addition to Cp, Fpn is also expressed by Schwann cells, indicating that Schwann cells have the equipment required for iron efflux. In chapter 4 of my thesis, I addressed whether iron efflux from Schwann cells via Fpn and Cp is involved in providing peripheral axons with iron. To meet their metabolic needs, axons contain an abundant number of mitochondria that are particularly concentrated in regions of high-energy consumption such as synapses, nodes of Ranvier and growth cones. As mentioned earlier, mitochondria require iron for their function due to several iron-dependent enzymes involved in mitochondrial oxidation. Since mitochondria within peripheral axons can be located far away from the cell body (in some cases several meters), acquiring iron along the length of the axons may be more efficient for mitochondria than travelling all the way back to the cell body. Therefore, iron efflux from Schwann cells that are closely associated with peripheral axons might play a role in ensuring adequate iron supply to mitochondria within axons. This might be especially important during axonal growth, as mitochondria are highly enriched in growth cones. My results show that the initiation and elongation of neurite growth from DRG neurons in culture is impaired under iron-deficient conditions. In the initial phase of neurite growth, mitochondria have been shown to accumulate in axonal hillocks of outgrowing axons, suggesting that they play a role in the polarization of neurons and in regulating neurite outgrowth (Dedov et al., 2000). Once neurite outgrowth has been initiated, a high density of mitochondria in axonal growth cones is required for further elongation of the axon. Thus, mitochondrial function plays an important role in the initiation and elongation of

neurites. My results show increased mitochondrial cluster formation in the region of the neuronal cell body in iron-deficient DRG neurons, possibly indicating mitochondrial dysfunction. Iron-deprivation has previously been shown to result in mitochondrial enlargement accompanied by defects in mitochondrial function (Yoon et al., 2004; Yoon et al., 2006). Whether mitochondrial function in the DRG neuronal cultures is indeed reduced under iron-deficient conditions needs to be further investigated. The results obtained from these cell culture experiments indicate that iron is involved in neurite growth, possibly by ensuring proper mitochondrial function. *In vivo*, iron required for axonal growth might be locally delivered to axonal mitochondria by Schwann cells. I therefore carried out experiments to determine whether iron efflux from Schwann cells via Fpn/Cp is required for axonal regeneration after sciatic nerve crush injury. My results demonstrate increased Fpn expression levels in the sciatic nerve distal to the lesion site, suggesting that increased iron efflux may be required for axonal regeneration after injury. At 1-day post injury, the upregulation of Fpn expression likely occurs in Schwann cells which are the predominant cells in the distal nerve segment at that time point. The increased Fpn expression at 7 and 14 days post injury may be attributed to Schwann cells as well as hematogenous macrophages that begin to infiltrate the distal segment around 4 days after injury. Surprisingly, Cp expression was not upregulated after sciatic nerve crush injury. However, the stoichiometry between Cp and Fpn interaction is unknown. It is therefore possible that an upregulation of Fpn but only moderate levels of Cp may be sufficient to increase iron export. This is further supported by studies showing that high intracellular iron levels increase Fpn expression mainly via the 5'IRE binding motif in its mRNA (Yang et al., 2002; Delaby et al., 2005), whereas expression of Cp which does not

contain an IRE motif is unaffected by iron levels (Chang et al., 2007). Increased iron efflux after peripheral nerve injury may be important to meet increased iron needs required for axonal regeneration. In agreement with this idea, a previous study reported increased endoneural iron uptake following sciatic nerve injury (Raivich et al., 1991). In addition, sciatic nerve crush injury in $Cp^{-/-}$ mice resulted in impaired axonal regeneration and delayed recovery of motor function. These findings suggest a role for Cp in peripheral axon regeneration, likely by mediating iron efflux from Schwann cells. However, whether the impaired axonal regeneration in $Cp^{-/-}$ mice is indeed due to decreased iron supply to axonal growth cones and subsequent mitochondrial dysfunction is currently not known. Taken together, these results indicate that iron is involved in neurite growth, and further suggest a role for Cp/Fpn-mediated iron efflux from Schwann cells in providing iron to peripheral axons for axonal regeneration.

5.4 Conclusions

In summary, my thesis demonstrates the importance of iron efflux mechanisms in the central and peripheral nervous system. My results reveal a novel role for Heph in iron efflux from oligodendrocytes in the CNS, and suggest that oligodendrocytes in the grey and white matter regulate iron efflux differentially by utilizing different ferroxidases. They also highlight an important role of iron export in oligodendrocytes in regulating intracellular iron homeostasis, as impaired iron efflux from these cells can have pathological consequences. Disturbances of iron efflux mechanisms in oligodendrocytes may also contribute to neurodegenerative diseases in which iron accumulation has been observed. In addition, my thesis work provides insights into the role of iron in remyelination, and suggests that iron efflux from astrocytes is involved in providing other

cells in the CNS with iron. Thus, these results help in understanding iron transport in the CNS, specifically, how iron may be safely delivered from the BBB to different cell types in the parenchyma. Moreover, my work indicates a role of iron in peripheral axon growth, and suggests that iron efflux from Schwann cells is involved in delivering iron to peripheral axons for axonal regeneration. Taken together, these results contribute to the knowledge of iron homeostatic mechanisms in the central and peripheral nervous system and in particular, emphasize the role of iron efflux mechanisms in maintaining stable intracellular iron levels as well as in delivering iron between cells of the nervous system.

5.5 References

Andrews NC, Schmidt PJ (2007) Iron homeostasis. Annu Rev Physiol 69:69-85.

Arnett HA, Mason J, Marino M, Suzuki K, Matsushima GK, Ting JP (2001) TNF alpha promotes proliferation of oligodendrocyte progenitors and remyelination. Nat Neurosci 4:1116-1122.

Beard JL, Connor JR, Jones BC (1993) Iron in the brain. Nutr Rev 51:157-170.

Bhat MA, Rios JC, Lu Y, Garcia-Fresco GP, Ching W, St Martin M, Li J, Einheber S, Chesler M, Rosenbluth J, Salzer JL, Bellen HJ (2001) Axon-glia interactions and the domain organization of myelinated axons requires neurexin IV/Caspr/Paranodin. Neuron 30:369-383.

Boyle ME, Berglund EO, Murai KK, Weber L, Peles E, Ranscht B (2001) Contactin orchestrates assembly of the septate-like junctions at the paranode in myelinated peripheral nerve. Neuron 30:385-397.

Cazzola M, Bergamaschi G, Dezza L, Arosio P (1990) Manipulations of cellular iron metabolism for modulating normal and malignant cell proliferation: achievements and prospects. Blood 75:1903-1919.

Chang YZ, Qian ZM, Du JR, Zhu L, Xu Y, Li LZ, Wang CY, Wang Q, Ge XH, Ho KP, Niu L, Ke Y (2007) Ceruloplasmin expression and its role in iron transport in C6 cells. Neurochem Int 50:726-733.

David S, Kroner A (2011) Repertoire of microglial and macrophage responses after spinal cord injury. Nat Rev Neurosci 12:388-399.

Dedov VN, Armati PJ, Roufogalis BD (2000) Three-dimensional organisation of mitochondrial clusters in regenerating dorsal root ganglion (DRG) neurons from neonatal rats: evidence for mobile mitochondrial pools. J Peripher Nerv Syst 5:3-10.

Delaby C, Pilard N, Goncalves AS, Beaumont C, Canonne-Hergaux F (2005) Presence of the iron exporter ferroportin at the plasma membrane of macrophages is enhanced by iron loading and down-regulated by hepcidin. Blood 106:3979-3984.

Denisenko-Nehrbass N, Faivre-Sarrailh C, Goutebroze L, Girault JA (2002) A molecular view on paranodal junctions of myelinated fibers. J Physiol Paris 96:99-103.

Einheber S, Zanazzi G, Ching W, Scherer S, Milner TA, Peles E, Salzer JL (1997) The axonal membrane protein Caspr, a homologue of neurexin IV, is a component of the septate-like paranodal junctions that assemble during myelination. J Cell Biol 139:1495-1506.

Franklin RJ, Ffrench-Constant C (2008) Remyelination in the CNS: from biology to therapy. Nat Rev Neurosci 9:839-855.

Franklin RJM, Zhao C, Sim FJ (2002) Astrocyte and macrophage interactions in promoting oligodendrocyte remyelination of the CNS. In: Aldskogius, H, Fraher, J (Eds), Glial Interfaces in the Nervous System IOS Press, Amsterdam, pp 95–104.

Jeong SY, David S (2003) Glycosylphosphatidylinositol-anchored ceruloplasmin is required for iron efflux from cells in the central nervous system. J Biol Chem 278:27144-27148.

Jeong SY, David S (2006) Age-related changes in iron homeostasis and cell death in the cerebellum of ceruloplasmin-deficient mice. J Neurosci 26:9810-9819.

Mason JL, Suzuki K, Chaplin DD, Matsushima GK (2001) Interleukin-1beta promotes repair of the CNS. J Neurosci 21:7046-7052.

McKinnon RD, Matsui T, Dubois-Dalcq M, Aaronson SA (1990) FGF modulates the PDGF-driven pathway of oligodendrocyte development. Neuron 5:603-614.

McKinnon RD, Piras G, Ida JA, Jr., Dubois-Dalcq M (1993) A role for TGF-beta in oligodendrocyte differentiation. J Cell Biol 121:1397-1407.

Moore CS, Abdullah SL, Brown A, Arulpragasam A, Crocker SJ (2010) How factors secreted from astrocytes impact myelin repair. J Neurosci Res 89:13-21.

Mozell RL, McMorris FA (1991) Insulin-like growth factor I stimulates oligodendrocyte development and myelination in rat brain aggregate cultures. J Neurosci Res 30:382-390.

Nie DY, Zhou ZH, Ang BT, Teng FY, Xu G, Xiang T, Wang CY, Zeng L, Takeda Y, Xu TL, Ng YK, Faivre-Sarrailh C, Popko B, Ling EA, Schachner M, Watanabe K, Pallen CJ, Tang BL, Xiao ZC (2003) Nogo-A at CNS paranodes is a ligand of Caspr: possible regulation of K(+) channel localization. Embo J 22:5666-5678.

Patel BN, David S (1997) A novel glycosylphosphatidylinositol-anchored form of ceruloplasmin is expressed by mammalian astrocytes. J Biol Chem 272:20185-20190.

Raivich G, Graeber MB, Gehrmann J, Kreutzberg GW (1991) Transferrin Receptor Expression and Iron Uptake in the Injured and Regenerating Rat Sciatic Nerve. Eur J Neurosci 3:919-927.

Salzer JL, Lovejoy L, Linder MC, Rosen C (1998) Ran-2, a glial lineage marker, is a GPI-anchored form of ceruloplasmin. J Neurosci Res 54:147-157.

Sen CK, Packer L (1996) Antioxidant and redox regulation of gene transcription. Faseb J 10:709-720.

Shlomai J (2010) Redox control of protein-DNA interactions: from molecular mechanisms to significance in signal transduction, gene expression, and DNA replication. Antioxid Redox Signal 13:1429-1476.

Singh R, Wangemann P (2008) Free radical stress-mediated loss of Kcnj10 protein expression in stria vascularis contributes to deafness in Pendred syndrome mouse model. Am J Physiol Renal Physiol 294:F139-148.

Todorich B, Pasquini JM, Garcia CI, Paez PM, Connor JR (2009) Oligodendrocytes and myelination: the role of iron. Glia 57:467-478.

Yang F, Wang X, Haile DJ, Piantadosi CA, Ghio AJ (2002) Iron increases expression of iron-export protein MTP1 in lung cells. Am J Physiol Lung Cell Mol Physiol 283:L932-939.

Yeh KY, Yeh M, Mims L, Glass J (2009) Iron feeding induces ferroportin 1 and hephaestin migration and interaction in rat duodenal epithelium. Am J Physiol Gastrointest Liver Physiol 296:G55-65.

Yoon YS, Cho H, Lee JH, Yoon G (2004) Mitochondrial dysfunction via disruption of complex II activity during iron chelation-induced senescence-like growth arrest of Chang cells. Ann N Y Acad Sci 1011:123-132.

Yoon YS, Yoon DS, Lim IK, Yoon SH, Chung HY, Rojo M, Malka F, Jou MJ, Martinou JC, Yoon G (2006) Formation of elongated giant mitochondria in DFO-induced cellular senescence: involvement of enhanced fusion process through modulation of Fis1. J Cell Physiol 209:468-480.